

DISSERTATION

THE EFFECTS OF SALT ON THE LOWER CRITICAL SOLUTION
TEMPERATURES OF POLY (N-ISOPROPYLACRYLAMIDE) AND ITS
COPOLYMER STUDIED FROM MOLECULAR DYNAMICS SIMULATIONS

Submitted by

Hongbo Du

Department of Mechanical Engineering

In partial fulfillment of the requirements

For the Degree of Doctor of Philosophy

Colorado State University

Fort Collins, Colorado

Spring 2011

Doctoral Committee:

Advisor: Xianghong Qian

Susan P. James

Ketul C. Papat

S. Ranil Wickramasinghe

ABSTRACT

THE EFFECTS OF SALT ON THE LOWER CRITICAL SOLUTION TEMPERATURES OF POLY (N-ISOPROPYLACRYLAMIDE) AND ITS COPOLYMER STUDIED FROM MOLECULAR DYNAMICS SIMULATIONS

Classical molecular dynamics (MD) simulations were performed to investigate the effects of salt on the lower critical solution temperature (LCST) of Poly (N-isopropylacrylamide) (PNIPAM). PNIPAM is often studied as a protein proxy due to the presence of a peptide bond in its monomer unit. PNIPAM is a temperature sensitive polymer which exhibits hydrophobic-hydrophilic phase transition at its LCST. The presence of salt in the solution will shift its LCST, typically to a lower temperature. This LCST shift follows the so-called Hofmeister series. MD simulations of PNIPAM in 1 M NaCl, NaBr, NaI and KCl solutions were carried out to elucidate the effects of different salts on the LCST and protein stability. The simulation results suggest that direct interactions between the salt cations and the polymer play a critical role in the shift of LCST and subsequently on protein stability. Further, cations have a much stronger affinity with the polymer, whereas anions bind weakly with the polymer. Moreover, the cation-polymer binding affinity is inversely correlated with the cation-anion contact pairassociation constant in solution. MD simulations were also carried out for PNIPAM in 1 M mixed salt solution containing 0.5 M Na^+ , K^+ , Cl^- and Br^- each.

The simulation results further confirmed the conclusions. Additional MD simulations were conducted for PNIPAM-co-PEGMA copolymer in 1 M NaCl solution. Interestingly, Na^+ was found to form a complex with multiple O atoms on the PNIPAM-co-PEGMA chain thus greatly enhancing the cationic binding with the copolymer. These results provide significant insight into the effects of salt on protein stability.

ACKNOWLEDGEMENTS

I would like to first acknowledge my advisor, Professor Xianghong Qian for her guidance and assistance throughout the course of this project. I am also very grateful to my other committee members, Professor Susan P. James, Professor Ketul C. Popat, and Professor S. Ranil Wickramasinghe for their insightful comments and recommendations for this work. I also thank Professor David Wang for his helpful recommendation on the analysis of the caged Na^+ in the simulation of the copolymer at higher temperature.

I would like to thank Dr. Haitao Dong, Dr. Jilai Li, Dr. Xinhua Zhang for their advice on *ab initio* calculations with CPMD and Gaussian 03, suggested methods to build simulation systems and helpful suggestions on data analysis. I also thank my colleague Manish Sharma to explore PNIPAM-co-PEGMA simulations in water at lower and higher temperatures below and above the LCST. The advice and help from my colleagues including Xinying Wang, Dajiang liu and Yu Cao is also greatly appreciated. I thank my family and friends for their invaluable support and encouragement.

This work was supported by the US National Science Foundation (CBET 0651646) and computing resources are from Colorado State University and TeraGrid.

TABLE OF CONTENTS

ABSTRACT.....	ii
ACKNOWLEDGEMENTS	iv
TABLE OF CONTENTS.....	v
LIST OF FIGURES	viii
CHAPTER 1 INTRODUCTION	1
1.1. POLY (N-ISOPROPYLACRYLAMIDE) — A SMART POLYMER	1
1.2. APPLICATIONS OF PNIPAM	3
1.3. THE LCST OF PNIPAM.....	6
1.4. THE EFFECTS OF SALT ON THE LCST OF PNIPAM.....	6
1.5. MOTIVATIONS	9
1.6. MOLECULAR DYNAMICS SIMULATION METHOD.....	12
1.7. THE PROCEDURE TO GENERATE A SIMULATION CELL	18
1.8. SUMMARY	22
CHAPTER 2 THE EFFECTS OF SALT ON THE LOWER CRITICAL SOLUTION TEMPERATURE OF POLY (N-ISOPROPYLACRYLAMIDE)	23
2.1. INTRODUCTION	23
2.2. COMPUTATIONAL METHODOLOGY AND SIMULATION DETAILS	25
2.3. RESULTS AND DISCUSSION	30
2.4. CONCLUSION.....	59
CHAPTER 3 MOLECULAR DYNAMICS SIMULATIONS OF PNIPAM IN MIXED SALT SOLUTION	60
3.1. INTRODUCTION	60
3.2. COMPUTATIONAL METHODOLOGY AND SIMULATION DETAILS	61
3.3. RESULTS AND DISCUSSION	62
3.4. CONCLUSION.....	82
CHAPTER 4 MOLECULAR DYNAMICS SIMULATIONS OF THE LCST PHASE TRANSITION OF PNIPAM-CO-PEGMA IN NA₂CO₃ SOLUTION.....	83
4.1. INTRODUCTION	83

4.2. SIMULATION DETAILS	90
4.3. RESULTS AND DISCUSSION	91
4.4. CONCLUSION.....	108
CHAPTER 5 MOLECULAR DYNAMICS STUDY OF THE VOLUME PHASE TRANSITION OF PNIPAM IN HCL SOLUTION	110
5.1. INTRODUCTION	110
5.2. COMPUTATIONAL METHODOLOGY AND SIMULATION DETAILS	112
5.3. RESULTS AND DISCUSSION	114
5.4. CONCLUSION.....	126
CHAPTER 6 CONCLUSIONS AND FUTURE WORK.....	127
6.1. CONCLUSIONS.....	127
6.2. LIMITATIONS OF CURRENT WORK.....	130
6.3. RECOMMENDATIONS FOR FUTURE WORK.....	131
REFERENCES	133
APPENDIX A - PERL PROGRAM 1	139
APPENDIX B - PERL PROGRAM 2	141
APPENDIX C - PERL PROGRAM 3	144
APPENDIX D - PERL PROGRAM 4	147
APPENDIX E - PERL PROGRAM 5.....	148
APPENDIX F - PERL PROGRAM 6.....	150
APPENDIX G - PERL PROGRAM 7	152
APPENDIX H - PERL PROGRAM 8	153
APPENDIX I - PERL PROGRAM 9.....	155
APPENDIX J - PERL PROGRAM 10	156
APPENDIX K - PERL PROGRAM 11	157
APPENDIX L - PERL PROGRAM 12.....	158
APPENDIX M - PERL PROGRAM 13	160
APPENDIX N - PERL PROGRAM 14	163
APPENDIX O - PERL PROGRAM 15	165
APPENDIX P - PERL PROGRAM 16.....	166
APPENDIX Q - PERL PROGRAM 17	168
APPENDIX R - PERL PROGRAM 18	169

APPENDIX S - PERL PROGRAM 19	170
APPENDIX T - PUBLICATIONS	171

LIST OF FIGURES

Figure 1-1 Chemical structure of PNIPAM	2
Figure 1-2 Schematics of PNIPAM-grafted capsule membrane for drug release.....	3
Figure 1-3 Schematics of the association of the copolymer PEG-PNIPAM grafted on a lysine core	4
Figure 1-4 The shrinkage of comb-type grafted thermo-responsive hydrogels with the increase of temperature	5
Figure 1-5 Influences of the anion types and concentrations of sodium salts on the LCST of PNIPAM	8
Figure 1-6 Suggested mechanisms for the effects of salt on the LCST of PNIPAM by Cremer et al	8
Figure 1-7 Periodic boundary conditions.....	15
Figure 1-8 Relations of cut-off, switching distance and pair list distance	17
Figure 2-1 The structure of PNIPAM monomer unit. The atoms are numbered for easy discussion in the text.....	26
Figure 2-2 Radii of gyration of PNIPAM in water at 310 K (red line) and 295 K (black line) respectively during the 46 ns MD simulation.	30
Figure 2-3 The numbers of water molecules within the PNIPAM's first hydration shell in pure water at 310 K (red line) and 295 K (black line) respectively during the 46 ns MD simulations.	31
Figure 2-4 PNIPAM conformations after 46 ns MD simulations in water at 295 K (the extended structure shown in 2-4a) and at 310 K (the folded structure shown in 2-4b). Molecular graphics images of PNIPAM and PNIPAM-co-PEGMA in the text were produced using the UCSF Chimera package from the Computer Graphics Laboratory, University of California, San Francisco (supported by NIH P41 RR-01081).	32
Figure 2-5 The numbers of H-bonds during the course of MD simulations for PNIPAM in water at 295 K (left) and 310 K (right)	33
Figure 2-6 Radii of gyration (left) and the numbers of water molecules in the first hydration shell of PNIPAM (right) in 1 M NaCl, NaBr and NaI solutions above and below their respective LCSTs.	36
Figure 2-7 Radii of gyration (left) and the numbers of water molecules in the first hydration shell of PNIPAM (right) in 1 M KCl solution above and below its LCST.	37
Figure 2-8 End-to-end distances of PNIPAM in 1 M NaCl, KCl, NaBr and NaI solutions above and below their respective LCST during MD simulations.....	37
Figure 2-9 Conformations of PNIPAM at the ends of simulations in different salt solutions	38
Figure 2-10 The number of H-bonds during the course of MD simulations for PNIPAM in 1 M NaCl solution at 288 K (left) and 300 K (right).....	40

Figure 2-11	The number of H-bonds during the course of MD simulations for PNIPAM in 1 M NaBr solution at 278 K (left) and 318 K (right).....	41
Figure 2-12	The number of H-bonds during the course of MD simulations for PNIPAM in 1 M NaI solution at 288 K (left) and 328 K (right)	42
Figure 2-13	The number of H-bonds during the course of MD simulations for PNIPAM in 1 M KCl solution at 277 K (left) and 307 K (right).....	43
Figure 2-14	The internal energies for polymer-polymer (left) and polymer-water interactions (right)	44
Figure 2-15	Pair correlation functions between the O, C atoms on the amide groups and the cations, anions of the salt solutions containing PNIPAM.....	46
Figure 2-16	Pair correlation functions between the amide N and O (H ₂ O)	47
Figure 2-17	Pair correlation functions between the amide N, backbone C and the cations, anions of the salt solutions containing PNIPAM.....	48
Figure 2-18	Pair correlation functions between amide N and H(water)	49
Figure 2-19	Pair correlation functions between C1, C2 and O(water)	50
Figure 2-20	Pair correlation functions between the C atoms on the isopropyl groups of PNIPAM and the cations (left), anions (right) of the salt solutions	52
Figure 2-21	Cation-anion pair correlation functions for 1 M NaCl, NaBr, NaI and KCl solution with (upper left) and without (lower left) PNIPAM. The pair correlation functions between the O of water and salt cation (upper right), anion (lower right).	54
Figure 2-22	The pair correlation functions between cation and O (H ₂ O) in 1 M NaCl, NaBr and NaI solutions with (left panel) and without (middle panel) PNIPAM determined above and below their respective LCSTs. The pair correlation functions were also determined for the three systems at constant temperature of 300 K (right panel). Only the first peaks are shown in order to show the temperature and ionic effects more clearly.	56
Figure 2-23	Contact ion pair correlation functions in 1 M KCl, NaCl, NaBr and NaI solutions at 300 K (left). The pair correlation functions between anion and O (H ₂ O) are also shown (right).....	57
Figure 3-1	Radii of gyration (a) and the number of water molecules in the first hydration shell of PNIPAM (b) in the mixed salt solution above and below its estimated LCST value.	63
Figure 3-2	The end-to-end distances of PNIPAM along MD simulations in 1 M mixed salt solution at 278 K and 318 K respectively.	64
Figure 3-3	The conformations of PNIPAM after the 75 ns simulations in 1 M mixed salt solution at 278 K (a) and 318 K (b) respectively	65
Figure 3-4	The number of H-bonds during the course of MD simulations for PNIPAM in 1 M mixed salt solution at 278 K (left) and 318 K (right).....	66
Figure 3-5	Pair correlation functions between the O, N, C atoms on the amide group and the cations, anions of the salt solutions with PNIPAM.....	69
Figure 3-6	Pair correlation functions between the C, N atoms on the amide groups and O atoms on water molecules.....	72

Figure 3-7 Pair correlation functions between the N atoms on the amide groups and H atoms on water molecules.....	72
Figure 3-8 Pair correlation functions between the C atoms on the isopropyl group of PNIPAM and the salt ions (cations on left panel and anions on right panel) in the 1 M mixed salt solution.	74
Figure 3-9 Pair correlation functions between the backbone C atoms (C1 and C2) in PNIPAM and the salt ions in the mixed salt solution (upper panel); the pair correlation functions between the backbone C1, C2 and the O atom in H ₂ O (lower panel).	76
Figure 3-10 The Na ⁺ binds simultaneously to two amide O atoms on PNIPAM after it goes through LCST phase transition at the higher temperature of 318 K. Only part of the PNIPAM chain is shown. The Na ⁺ ion is shown in green, O atoms in red, N atoms in blue, C atoms in gray and H atoms in light white.	78
Figure 3-11 Pair correlation functions between cation and anion, between anion and O(water) and between cation and O(water) with and without PNIPAM at both temperatures in the mixed salt solution.	80
Figure 4-1 The structures of monomer unit NIPAM (a) and PEGMA side chain (b), and the starting structure (c) of the copolymer for the simulations. The atoms are numbered for easy discussion in the text.	88
Figure 4-2 The conformations of the PNIPAM -co-PEGMA copolymer after 65 ns of simulations at 278 K (a) and 318 K (b)	92
Figure 4-3 Radii of gyration of the PNIPAM -co-PEGMA copolymer (a) and the number of water molecules (b) associated with the first hydration shell of the copolymer in 1 M NaCl solution at 318 K (red line) and 278 K (black line) respectively during the 65 ns MD simulations.	92
Figure 4-4 End-to-end distances of the PNIPAM-co-PEGMA copolymer at 318 K (red line) and 278 K (black line) during the 65 ns MD simulations.....	93
Figure 4-5 Intra-chain hydrogen bonds and intermolecular hydrogen bonds between the copolymer and water during the course of simulations.....	94
Figure 4-6 Pair correlation functions between amide O, N, C on NIPAM and salt cation (left panel), anion (right panel).....	96
Figure 4-7 Pair correlation functions between isopropyl C5, C6, C7, backbone C on PNIPAM and the salt cation (left panel), salt anion (right panel).....	99
Figure 4-8 The pair correlation functions between salt ions (Na ⁺ or Cl ⁻) and various O atoms on PEGMA chain 1 and 2.	101
Figure 4-9 The complex formed between the Na ⁺ ion and the PNIPAM-co-PEGMA copolymer. The center atom in blue is the Na ⁺ ion. The other blue atoms on the copolymer represent N atoms. The O, C and H atoms are red, gray and white in color respectively. The letters a, c, d, e, f and g indicate the bindings between the various O atoms and the Na ⁺	105
Figure 4-10 The pair correlation functions between the amide O on PNIPAM and Na ⁺ with and without caged Na ⁺ at 318K. The corresponding g(r) at 278 K was also shown for comparison.	107
Figure 5-1 The structures of Eigen and Zundel models.....	112

Figure 5-2	The conformations of the PNIPAM chain at the end of 42 ns simulations at 282 K (a) and 322 K (b) respectively.	115
Figure 5-3	Radii of gyration of PNIPAM (a) and the numbers of water molecules (b) associated with the first hydration shell of PNIPAM in 1 M HCl solution at 322 K (red line) and 282 K (black line) respectively during the 42 ns MD simulations.	115
Figure 5-4	End-to-end distances of PNIPAM at 322 K (red line) and 282 K (black line) during the 42 ns MD simulations.	116
Figure 5-5	PNIPAM's intra-chain hydrogen bonds (top panel) and intermolecular hydrogen bonds between PNIPAM and water (middle and lower panels) during the course of simulations at higher and lower temperatures respectively.	118
Figure 5-6	Pair correlation functions between the amide C, N or O on PNIPAM and the H atoms of the H_3O^+ or Cl^- ions	120
Figure 5-7	Pair correlation functions between the isopropyl C5, C6, C7 or backbone C on PNIPAM and the H(H_3O^+) or Cl^-	121
Figure 5-8	Pair correlation functions between the amide O or N and water H.....	123
Figure 5-9	Pair correlation functions between $\text{O}(\text{H}_3\text{O}^+)$ and $\text{O}(\text{H}_3\text{O}^+)$ and between Cl^- and Cl^-	124
Figure 5-10	Pair correlation functions between $\text{H}(\text{H}_3\text{O}^+)$ and Cl^- at 282 and 322 K	125

CHAPTER 1 INTRODUCTION

1.1. POLY (N-ISOPROPYLACRYLAMIDE) – A SMART POLYMER

Smart polymers, also called stimulus-responsive materials, are polymeric materials that can reversibly change their conformations and associated properties in response to an external stimulus such as temperature, pH, ionic strength, electric field or light.¹⁻⁸ Because of their stimulus-responsive behaviors, smart polymers are popularly being applied to fabricate smart devices, e.g., biosensors, actuators, triggers and drug release systems in various forms such as permanent cross-linked hydrogels, reversible hydrogels, micelles, modified interfaces like typical grafted membranes and conjugated solutions.

Thermo-responsive polymers are the most common smart polymers applied to responsive systems both *in vitro* and *in vivo* in biomedical applications. Thermo-responsive polymers in solution possess a unique critical solution temperature. If a thermo-responsive polymer solution is miscible below the critical temperature and is phase-separated above the critical temperature, the critical temperature is called a lower critical solution temperature (LCST) of the polymer. On the other hand, if a miscible solution exists above the critical temperature and the solution is phase-separated below the critical temperature, it is an upper critical solution temperature (UCST).⁹

Since poly (N-isopropylacrylamide) (PNIPAM) was first synthesized in the 1950s, it has been studied and utilized as the most common intelligent polymer. PNIPAM exhibits a volume phase transition at the LCST.^{6,10-14} Below its LCST, this thermo-responsive polymer is hydrated and represents a swollen coil-like conformation. Above the LCST, it becomes dehydrated and adopts a folded structure. The structure of PNIPAM is shown in Figure 1-1. Its thermo-responsiveness is thought to be resulting from the presence of the hydrophobic carbon backbone, a hydrophobic isopropyl group and a hydrophilic amide group along the side chain in each monomer unit.

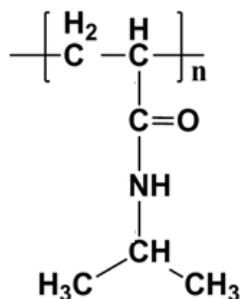


Figure 1-1 Chemical structure of PNIPAM

The research on temperature-dependent interactions between PNIPAM and water revealed the possible mechanisms for the PNIPAM's LCST phase transition or the hydrophobic-hydrophilic transition. It is generally thought that entropy is the driving force for the LCST phase transition in aqueous solution.¹⁵⁻²¹ When the temperature is below its LCST, the enthalpic contribution including hydrogen-bonding interactions between the amide groups on PNIPAM and water dominates so that PNIPAM possesses a hydrophilic coil-like conformation. However, when the temperature is above its LCST, the solvation entropy of the hydrophobic isopropyl groups and the carbon backbone dominates and PNIPAM exhibits a hydrophobic folded structure in aqueous solution.

1.2. APPLICATIONS OF PNIPAM

Because of its unique thermo-responsive property, PNIPAM and its copolymers are widely applied to drug delivery systems, tissue engineering and membrane technology for water treatment.^{1,2,5-8} Due to the fact that PNIPAM can change its conformation from a hydrophilic coil to a hydrophobic globule around its LCST, PNIPAM can be used as a temperature sensitive drug delivery carrier in various forms such as capsule, micelle and hydrogel. PNIPAM and its copolymers with enhanced hydrophilicity may also be potentially used as anti-fouling surface coatings for water treatment²².

The work of Okahata et al. has demonstrated thermo-selective permeation of drug through PNIPAM grafted membrane in capsules.²³ PNIPAM chains were grafted on surfaces of large nylon capsule membranes as shown in Figure 1-2. The grafted PNIPAM chains on capsules could collapse or extend to close or open the pores in the membrane for drug release at its transition temperature.

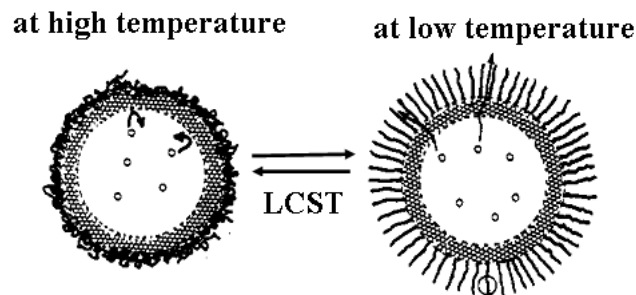


Figure 1-2 Schematics of PNIPAM-grafted capsule membrane for drug release²³

Oupicky and coworkers grafted a Y-shaped copolymer of polyethylene glycol (PEG) and PNIPAM on a lysine core as shown in Figure 1-3 by radical addition

fragmentation transfer (RAFT).^{24,25} The terminal of the PNIPAM chain was connected to biotin. The copolymer exhibits a LCST phase transition at approximately 32 °C in aqueous solution. The copolymer is able to turn on and off the biotin signal in response to temperature. When the temperature increases above the copolymer's LCST, PNIPAM units collapse, but the copolymer chains are not capable of precipitating fully due to the higher hydrophilicity of PEG and subsequently develop into aggregated micelles. So the biotin ligands remain in the central cores of micelles at a temperature above the LCST of PEG-PNIPAM. When the temperature is reduced to a temperature below the LCST, biotin ligands are exposed and subsequently able to bind to organic drug compounds.

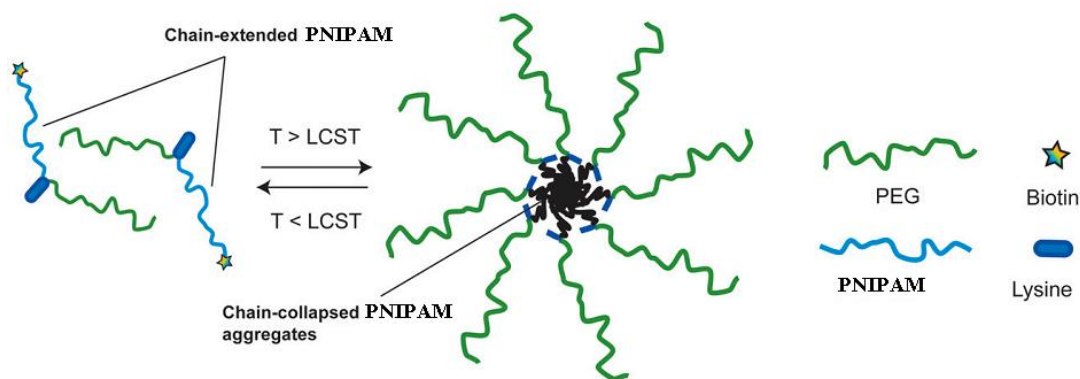


Figure 1-3 Schematics of the association of the copolymer PEG-PNIPAM grafted on a lysine core^{24,25}

Cross-linked PNIPAM hydrogels can also be used as drug carrier in drug delivery. Conventional cross-linked PNIPAM gels usually experience a sharp phase transition between swollen and shrunken structures around the LCST of PNIPAM.^{26,27} The gels release drug through diffusion when the temperature reaches below its LCST. When temperature increases above its LCST, a dense and shrunken layer quickly develops on

the surface of the cross-linked hydrogel, preventing water and drug permeation from inside to outside. Opposite to the conventional gels, a specific elaboration method was proposed to enhance the drug release rate at temperatures above the LCST by grafting linear PNIPAM chains to the conventional hydrogels as shown in Figure 1-4.²⁸ Comb-type grafted thermo-responsive hydrogels were created by terminally grafting PNIPAM chains onto the cross-linked hydrogels and leaving the opposite ends of the chains free. When the temperature increases above its LCST, the one-end-free PNIPAM chains quickly collapse before hydrogels shrink. The collapsed PNIPAM chains dehydrate to generate hydrophobic nuclei, which speed up the shrinkage of the cross-linked hydrogels.

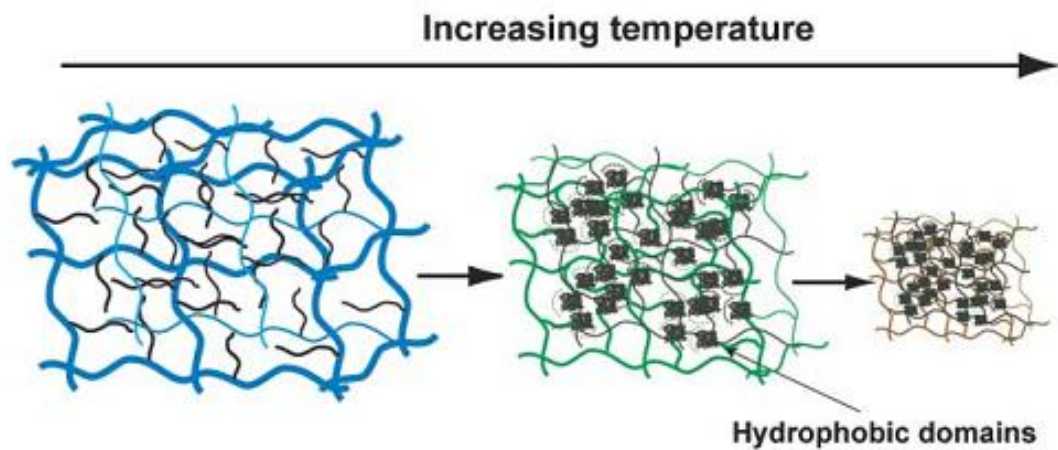


Figure 1-4 The shrinkage of comb-type grafted thermo-responsive hydrogels with the increase of temperature²⁸

1.3. THE LCST OF PNIPAM

The LCST of PNIPAM is influenced by some factors including molecular weight, polymer concentration, solution pH, the presence of salt, salt type and salt concentration.^{10,29-31} The observed LCST of PNIPAM is about 305 K (32 °C) in water, Schild and Tirrell found that the LCST is slightly dependent on molecular weight, increasing by about 2 K when the molecular weight is decreased from 1.6×10^5 to 5.4×10^3 .²⁹ Fujishige and coworkers argued that the LCST of PNIPAM is independent of either the molecular weight (5×10^4 to 840×10^4) or the polymer concentration (0.01 to 1 wt %).³⁰ Furyk and coworkers reported based on their experimental results that the LCSTs of high molecular weight PNIPAMs are not influenced by molecular weight and end group functionality, but the LCSTs of low molecular weight PNIPAMs are slightly affected by molecular weight and terminal hydrophobic groups.¹² PNIPAM's LCSTs decrease with the increase of alkyl chain length if the terminals are propyl, hexyl, and octyl groups. Yong Pei et al. studied the pH-sensitivity of PNIPAM and the shift of the LCST due to pH change in acrylic acid buffer solutions.³¹ They found that the LCST increases from 297.25 K (24.1 °C) to 301.85 K (28.7 °C) when pH decreases from 7 to 1 in acrylic acid buffer solutions.

1.4. THE EFFECTS OF SALT ON THE LCST OF PNIPAM

Earlier experiments found that salt ions have significant impacts on the LCST of PNIPAM^{10,11,32,33}, subsequently affecting the behavior of PNIPAM in drug delivery. The experimental results obtained by Eeckman et al. showed that the addition of salts leads to a significant decrease of PNIPAM's LCST.^{33,34} A 1 M NaCl solution leads to a decrease

of the PNIPAM's LCST by about 12 K from approximate 305 K in pure water to about 293 K, while a 0.2 M Na₂SO₄ solution decreases its LCST by about 10 K. It appears that the salt type, concentration, valence and size of the anions play important roles in influencing the LCST of PNIPAM. However, the effects of the cations on LCST are not obvious. They proposed that the reason for the decrease of the LCST in salt solutions is that the addition of electrolytes changes the water structure and water molecule's orientation in the hydration shell surrounding PNIPAM. As a result, the hydrophobicity of PNIPAM increases, causing a reduction in its LCST.

Cremer et al. investigated the effects of sodium salts of CO₃²⁻, SO₄²⁻, H₂PO₄⁻, F⁻, Cl⁻, Br⁻, NO₃⁻, I⁻, ClO₄⁻ and SCN⁻ on the LCST of PNIPAM as shown in Figure 1-5 and discovered that the LCST is affected by the concentration of salts as well as the molecular weight and polymer concentration using a novel temperature gradient device.^{11,12} Further there exists a two-step phase transition as a function of molecular weight at certain salt concentrations. The first step is related to the salting out of the amide groups, and the second is the dehydration of the hydrophobic parts of PNIPAM. The PNIPAM's LCST was also measured at different salt concentrations. At each salt concentration, the LCST shift from its LCST value in water was found to follow the anionic order in Hofmeister series as Na₂CO₃ > Na₂SO₄ > Na₂S₂O₃ > NaH₂PO₄ > NaF > NaCl > NaClO₄ > NaBr > NaNO₃ > NaI > NaSCN. They suggested three possible mechanisms for the LCST shift induced by the presence of salt anions as shown in Figure 1-6. First, salt anions around PNIPAM could polarize its neighboring water molecules to affect water's hydrogen bonding interactions to the amide groups (Figure 1-6a). Second, salt anions might influence the hydrophobic hydration of PNIPAM by increasing surface

tension of the cavity around the PNIPAM's backbone and isopropyl groups (Figure 1-6b). Third, the anionic effect on LCST could possibly arise from the anion's direct binding to the amide group on PNIPAM (Figure 1-6c).

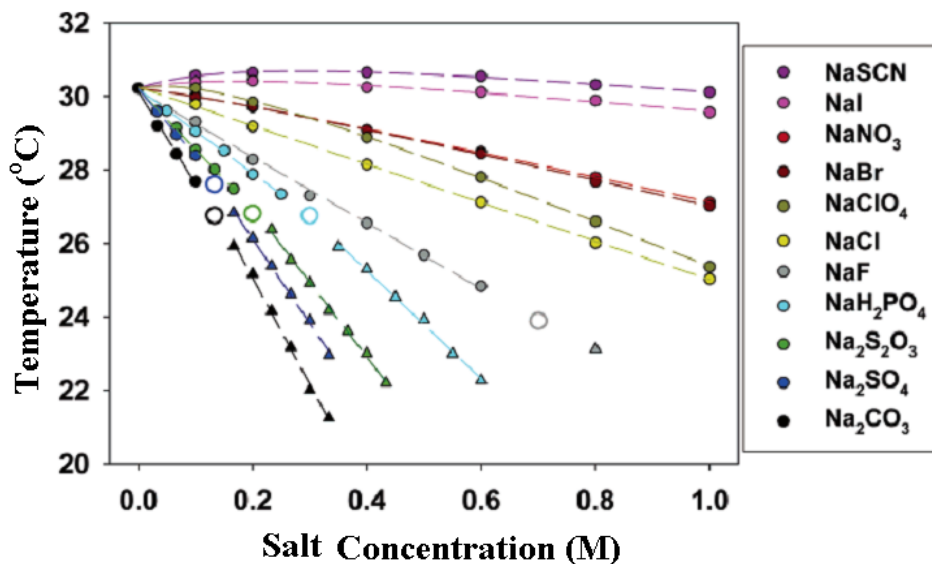


Figure 1-5 Influences of the anion types and concentrations of sodium salts on the LCST of PNIPAM^{11,12}

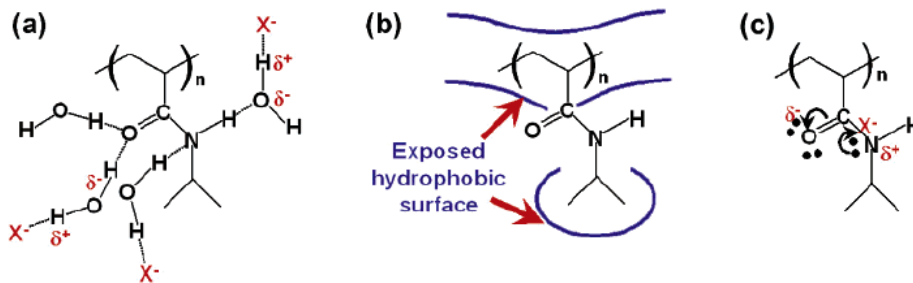


Figure 1-6 Suggested mechanisms for the effects of salt on the LCST of PNIPAM by Cremer et al.^{11,12}

1.5. MOTIVATIONS

The majority of salt ions tend to reduce the LCST of PNIPAM. Further experimentally, it appears that salt anions have significant impacts on the LCST of PNIPAM. The goal of this work is to elucidate the true nature of the effects of salt ions on the LCST of PNIPAM using classical molecular dynamics simulations. Salt ions play a critical role in many biological processes including protein solubility, stability, denaturation and aggregation. Understanding ion–protein interaction is crucial for elucidating the fundamental underlying mechanisms. The Hofmeister series refers to the ability of salt ions to precipitate proteins from an aqueous solution based on empirical observations. However, till now, the fundamental mechanisms remain elusive. Previously it was thought that ions in solution can affect the bulk water structure thus affecting the hydrophobic-hydrophilic transition of proteins in aqueous solution.^{34,35} Ions are considered chaotropic (structure breaking) or kosmotropic (structure making). Recently spectroscopic and calorimetric studies show that ions only affect the closest hydration shells and the bulk water structure is not altered by the presence of the salt ions.³⁶⁻³⁸ In addition, attempts have been made to correlate the Hofmeister series with surface tension, the solvation entropy of the ions and other physical and thermodynamics properties of the ions.³⁹⁻⁴¹ However, all these correlations have failed to explain the entire series and the inverse Hofmeister series sometimes observed. A fundamental molecular level understanding is also lacking. Since the monomer unit in PNIPAM contains an amide group along the side chain, it often serves as a protein proxy for investigating ionic effect of protein denaturation.

It was suggested by Cremer and coworkers that anions play a critical role in the LCST conformational transition of PNIPAM.^{10,11,42-44} It appears that the difference in reduction of LCST is due to the presence of different anionic species. In particular, they suggested that this anionic effect arises most likely from the direct bonding between the anions and the amide groups on the polymer side chains. The anions could further destabilize the hydrogen bonding interaction between the amide group and water through polarization, thus affecting the LCST of PNIPAM. On the other hand, Jungwirth and coworkers carried out MD simulations of some proteins, actin, bovine pancreatic trypsin inhibitor (BPTI), ubiquitin, hyperthermophilic rubredoxin and ribonuclease (RNase) A in NaCl and KCl solutions, as well as monomeric N-methylacetamide (NMA) in 1 M NaCl, KCl, KBr and NaBr solutions.⁴⁵⁻⁴⁷ These simulations showed that cations prefer to bind to the O atoms on amide groups, and the affinity of Na⁺ to the amide O is much higher than that of K⁺, whereas the halide anions exhibit no or very weak binding to the peptide bond. Previously, Collins and other researchers suggested that ion pairing via “matching water affinity”^{39,48,49} is the major mechanism of interaction of ions with the proteins in salt solutions^{46,47,50}.

We can see that the direct binding of anions to the amide groups of PNIPAM proposed by Cremer et al. is in conflict with the findings of the direct cation–protein interactions from MD simulations. Since PNIPAM exhibits hydrophobic–hydrophilic phase transition at its LCST and the presence of salt presents a significant impact on the LCST value, it would be necessary to understand the fundamental mechanisms for the effects of salt on LCST due to many potential applications of PNIPAM in drug delivery and as antifouling surfaces. In order to elucidate the true nature of the ionic effect on the

LCST transition of PNIPAM and on protein stability, MD simulations of PNIPAM in pure water, 1 M different salt solutions were carried out above and below their respective LCSTs in our current work.

Our hypothesis is that the LCST reduction of PNIPAM in salt solution may be caused by the direct binding of salt cations to the amide groups of PNIPAM, and more importantly, the interaction is modulated by the interactions between salt cations and anions in solution. In order to test this hypothesis, MD simulations of PNIPAM were performed in two types of salt solutions. One type is to keep the same cation of Na^+ and change the anions with Cl^- , Br^- and I^- . The other type is to keep the same anion of Cl^- and change the cations with Na^+ and K^+ . MD simulations of PNIPAM were also performed in a mixed NaCl-KBr salt solution to investigate the competition of different salt ions in such a mixed salt solution. In order to improve the property of PNIPAM in biomedical and membrane applications, some copolymers based on PNIPAM are often used. For example, PNIPAM-co-poly (ethylene glycol) methacrylate (PEGMA) (PNIPAM-co-PEGMA) increases the hydrophilicity of the polymer for improved applications as anti-fouling surface materials. MD simulations of PNIPAM-co-PEGMA in 1 M NaCl solution were also conducted above and below its LCST to investigate salt ion interactions with PNIPAM and PEGMA units. Further, the effects of pH on the LCST of PNIPAM are also perplexing. MD simulations of PNIPAM in 1 M HCl solution were also conducted in order to elucidate the pH effects.

Longhi et al. simulated a dilute aqueous solution of a 50-unit PNIPAM at 300 and 310 K below and above the LCST of water at 305 K (32 °C).⁵¹ In order to obtain the parameters for MD simulations, they performed *ab initio* calculations on a saturated

monomer N-isopropylacrylamide (NIPAM) at RHF/6-31G* level using GAUSSIAN 98 and evaluated the atomic charges for atoms in PNIPAM according to the RESP protocol⁵². MD simulations for about 4 nanoseconds (ns) in water were performed under the constant pressure and temperature (NPT) using Amber 6⁵³. The simulation results showed that the equilibrated PNIPAM configurations are more compact at 310 K than at 300 K, in good agreement with experimental results. In 2008, Longhi et al. also presented 75-ns MD simulations of 26-unit PNIPAM and its copolymers in water and demonstrated the similar LCST transition for PNIPAM and its copolymers around their LCSTs.⁵⁴ Recently, molecular modeling of a PNIPAM hydrogel was conducted in water below, above and at the LSCT to understand the fundamental mechanisms of the hydrogel swelling behavior using another MD simulation package of Gromacs.⁵⁵ However, all these calculations were performed in water without the presence of salts. Our work mainly focuses on the effects of salt on the LCST of PNIPAM and on elucidating the salt ion–PNIPAM interactions.

1.6. MOLECULAR DYNAMICS SIMULATION METHOD

Molecular Dynamics simulation is a powerful tool to investigate the fundamental mechanisms for protein folding/unfolding and polymer structure and/or conformation. Force fields which describe interatomic interactions in MD simulations have already been developed for proteins and polymeric materials including PNIPAM^{51,54-58}. These force fields include Amber, Charmm, OPLS, Gromos and etc. Classical MD simulations provide potential energy changes and atomic trajectories of the system. Besides the dynamic properties, it is also possible to obtain thermodynamics properties including free energy changes using an appropriate sampling method⁵⁹.

NAMD⁶⁰ is an excellent parallelized molecular dynamics program designed for efficient MD simulations of soft condensed materials, particularly for research in structural biology. NAMD easily interfaces with the popular molecular graphics program VMD for simulation setup and trajectory analysis⁶¹, and is also compatible with Amber, Charmm, and X-Plor force fields. Amber force fields in conjunction with NAMD are adopted in all the current MD simulations of PNIPAM and the PNIPAM-co-PEGMA copolymer.

Amber force fields

Amber force fields^{52,53} are broadly applied to MD simulations of proteins, nucleic acids and other organic molecules. In addition, the bonding, angle, dihedral, improper torsion parameters for interatomic interactions of PNIPAM and PEGMA are available in the Amber force fields. The Amber 94 force field was successfully applied to simulate the PNIPAM's LCST transition in pure water by Longhi et al⁵¹. In the Amber force fields, Equation (1-1) was used to express the bonding, bending, torsional, *van der Waals*, and electrostatic interactions.

$$E_{total} = \sum_{bonds} K_r (r - r_{eq})^2 + \sum_{angles} K_\theta (\theta - \theta_{eq})^2 + \sum_{dihedrals} [1 + \cos(n\phi - \gamma)] + \sum_{i < j} \left[\frac{A_{ij}}{R_{ij}^{12}} - \frac{B_{ij}}{R_{ij}^6} + \frac{q_i q_j}{\epsilon R_{ij}} \right] \quad (1-1)$$

Here r_{eq} is the equilibrium distance between two bonded atoms, θ_{eq} is the equilibrium angle of three bonded atoms, K_r , K_θ , V_n are the force constants, n is the multiplicity, γ is the dihedral angle, A_{ij} and B_{ij} are the Lennard-Jones parameters for *van der Waals* interactions, and q_i and q_j are the atomic partial charges on the atoms i and j .

Verlet's algorithm

The simplest and widely used algorithm in MD simulation is a third-order Störmer algorithm (Verlet's method). The algorithm is a combination of two Taylor expansions. The Taylor expansion of position from time t towards $t+\Delta t$ is described in Equation (1-2):

$$x(t + \Delta t) = x(t) + \frac{dx(t)}{dt} \Delta t + \frac{1}{2} \frac{dx^2(t)}{dt^2} \Delta t^2 + \frac{1}{3!} \frac{dx^3(t)}{dt^3} \Delta t^3 + O(\Delta t^4) \quad (1-2)$$

The Taylor series from t to $t-\Delta t$ is described in Equation (1-3):

$$x(t - \Delta t) = x(t) - \frac{dx(t)}{dt} \Delta t + \frac{1}{2} \frac{dx^2(t)}{dt^2} \Delta t^2 - \frac{1}{3!} \frac{dx^3(t)}{dt^3} \Delta t^3 + O(\Delta t^4) \quad (1-3)$$

The addition of these two equations yields Equation (1-4):

$$x(t + \Delta t) = 2x(t) - x(t - \Delta t) + \frac{dx^2(t)}{dt^2} \Delta t^2 + 2O(\Delta t^4) \quad (1-4)$$

The velocity at time $t+\Delta t$ can be evaluated as Equation (1-5):

$$\vec{v}(t + \Delta t) = \frac{x(t + \Delta t) - x(t - \Delta t)}{2\Delta t} \quad (1-5)$$

here the fourth-order term $O(\Delta t^4)$ and the following Taylor expansion terms are neglected in the Verlet's algorithm.

Periodic boundary conditions

The application of periodic boundary conditions is very important in MD simulations. It is quite tricky to remove the effects of the surface interaction in a small

finite simulation cell, thus making the cell behave with an infinite size⁶². The real small system being studied is surrounded by virtually identical cells in two or three dimensions; and the atoms in the real system are able to interact with those in the surrounding cells under periodic boundary conditions (shown in Figure 1-7).

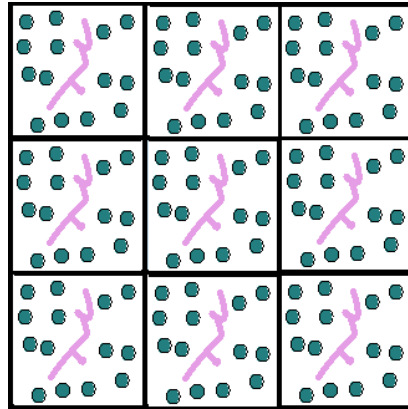


Figure 1-7 Periodic boundary conditions

Particle-mesh Ewald (PME) method

PME method is commonly used to speed up the calculation of long-range electrostatic interactions under periodic boundary conditions in MD simulations. In NAMD, a smooth PME (SPME) is used to compute long-rang electrostatic potential energy⁶³, where a 3-D particle mesh grid represents the configuration of the simulation system. The charge of the system is distributed over the particle mesh with grid size less than 1 \AA ⁶⁴.

Langevin dynamics for temperature control

Langevin dynamics can be used to control the kinetic energy of the simulation system thereby controlling the temperature of the system. The Langevin equation for a single atom is shown as Equation (1-6):

$$m \frac{d^2 x_i(t)}{dt^2} = F_i\{x(t)\} - \gamma_i \frac{dx_i(t)}{dt} m_i + R_i(t) \quad (1-6)$$

here $F_i\{x(t)\}$ is the sum of all forces exerted on the atom i by other atoms present in the system, the second term is a friction damping term applied to the atom i with collision frequency γ_i , and the third term represents the random force acted on the atom i resulting from the solvent interaction. The second and third terms are used to maintain the atom's kinetic energy and thus the temperature of the system.

Pressure control

Constant pressure control is associated with periodic boundary conditions. There are two typical methods applicable to constant pressure control in classical MD simulations, Berendsen pressure bath coupling⁶⁵ and Nose-Hoover Langevin piston pressure control^{66,67}. In current simulations Nose-Hoover Langevin piston pressure control was used, where the Langevin piston method was applied to adjust the size of simulation cell during the simulations. The method is associated with Langevin dynamics for temperature control in order to run simulations under constant temperature and constant pressure. In simulations performed by NAMD, the suggested oscillation time

scale of the Langevin piston method is 200 fs, and the barostat damping time scale is typically smaller than the oscillation time scale, e.g. 100 fs.

Critical parameters: cut-off, switching distance, and pair list distance

Cut-off usually represents the distance beyond which non-bonded interactions, i.e., electrostatic and *van der Waals* interactions are neglected. This definition changes when the Particle Mesh Ewald (PME) summation method is used in NAMD⁶⁰. When PME is used in MD simulations, the cut-off distance specifies the separation point between short and long range non-bonded interactions. Switching distance specifies the distance where switching functions are applied so that electrostatic and *van der Waals* interactions smoothly become zero at the cutoff distance. Pair list distance allows that one atom searches within the distance for other atoms which the atom may interact with by non-bonded interactions. It speeds up the MD simulations because the code does not have to search atoms in the entire simulation cell. On the other hand, the pair list distance must be greater than the cut-off. Figure 1-8 shows the relationship between cut-off, switching distance and pair list distance.

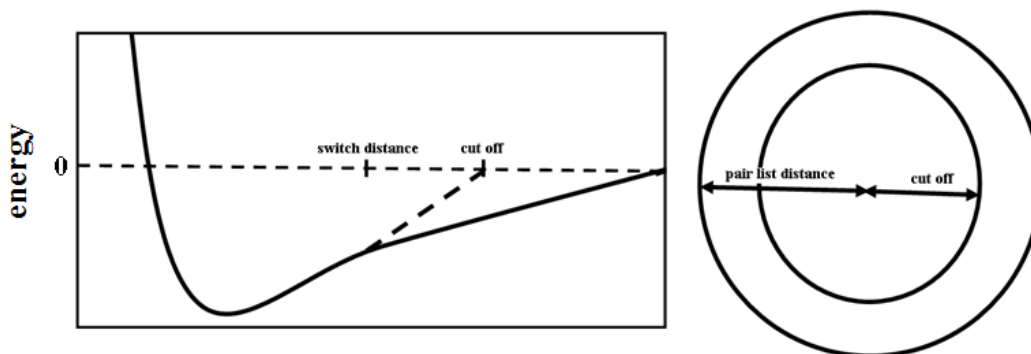


Figure 1-8 Relations of cut-off, switching distance and pair list distance

1.7. THE PROCEDURE TO GENERATE A SIMULATION CELL

1.7.1. Derivation of atomic charges, topology and coordinate files

A saturated structure of the monomer NIPAM capped with H- and CH₃- was generated by VMD. Based on the capped structure, An *ab initio* MD simulation was performed to find the lowest energy structure in gas phase by running CPMD⁶⁸ under constant temperature and constant volume. The structure obtained from CPMD simulation was used to optimize the geometry in gas phase with Gaussian 03⁶⁹. The Gaussian routine line for geometry optimization was:

```
#p B3LYP/6-311+G(d,p) SCF=tight optcyc=200 iop(5/13=1) opt
```

The second step was to calculate an electrostatic potential for the optimized structure by using the following Gaussian routine:

```
#p B3LYP/aug-cc-pvtz SCF=tight Test Pop=MK iop(6/33=2) iop(6/42=6) geom=check  
guess=read
```

The third step was to generate an ac file from the Gaussian output file using antechamber⁷⁰ available in AmberTools 1.2:

```
antechamber -fi gout -fo ac -i gau.out -o saturatednip.ac -c resp
```

The fourth step was to read in *saturatednip.ac* and a backbone definition file to generate prep input file for a monomeric unit NIPAM using prepgen⁷⁰ available in AmberTools 1.2:

```
prepgen -i saturatednip.ac -o nip.prepi -m mainchain.nip -rn NIP -rf nip.res
```

In the backbone definition file, the atom HEAD_NAME is connected the adjacently previous residue and the atom TAIL_NAME is connected to the adjacently post residue; OMIT_NAME atoms are not a part of the residue, but they are necessary to maintain a proper chemical environment. The atoms MAINCHAIN, HEAD_NAME and TAIL_NAME are the backbone atoms. For both terminal residues of PNIPAM, one end doesn't need to specify the atom HEAD_NAME, and the other end doesn't need TAIL_NAME. Here shows the backbone definition file for one middle residue NIPAM in the PNIPAM chain.

```
HEAD_NAME C1
```

```
TAIL_NAME C2
```

```
OMIT_NAME H3
```

```
OMIT_NAME C4
```

```
OMIT_NAME H5
```

```
OMIT_NAME H6
```

```
OMIT_NAME H7
```

```
PRE_HEAD_TYPE c3
```

```
POST_TAIL_TYPE c3
```

```
CHARGE 0.0
```

After the prepi file of NIPAM was generated, the atom types of different atoms needed to be adjusted according to the format of Amber 94 force field because Amber 94 force field was used for PNIPAM in current simulations. With the prepi files for two

terminal residues and middle residues, one 50-unit PNIPAM chain can be generated to obtain the topology and coordinate files for MD simulations in vacuum using Leap (XLeap or TLeap)⁷¹ in AmberTools 1.2. IPA is the residue name of the first residue in the 50-unit PNIPAM chain, NIP is for the middle residues 2-49, and PPA is for the last residue 50. Here the pdb file of the 50-unit PNIPAM chain was saved for easy view in the future, PNIPAM.prmtop is the topology file, and PNIPAM.inpcrd is the coordinate file in Amber format. When the generated PNIPAM chain was viewed here, it was an unphysical linear chain. The following command lines are for the generation process.

```
loadamberprep IPA.prepi
```

```
loadamberprep NIP.prepi
```

```
loadamberprep PPA.prepi
```

```
chain=sequence {IPA NIP NIP ... NIP NIP PPA}
```

```
savepdb chain PNIPAM.pdb
```

```
saveamberparm chain PNIPAM.prmtop PNIPAM.inpcrd
```

The topology files of the residues in PEGMA can be generated similarly following the above procedures. For the generation of the copolymer chain, it needs to be careful to check the bond connections between residues viewed from VMD. If there are unreasonable connections, the wrong connections have to be deleted and new bonds need to be generated using Leap.

1.7.2. MD simulation of PNIPAM in vacuum

The topology and coordinate file can be used for MD simulation in vacuum by directly using Amber force field in NAMD. MD simulation of PNIPAM can be performed in vacuum with/without periodic boundary conditions. After the MD simulation was run at 300 K for a short time, e.g. 100 ps, a reasonable coil-like structure of the PNIPAM could be achieved. Combined with the topology file, a pdb file for the coil-like structure may be obtained from the trajectory file by using VMD. MD simulation of the PNIPAM-co-PEGMA copolymer in vacuum was the same as the MD simulation of PNIPAM in vacuum. The obtained coil-like structure was applied for MD simulations in aqueous solution.

1.7.3. Generation of a PNIPAM-salt-water simulation cell

A pdb file of a salt-water simulation cell with three dimensions of 90 X 90 X 90 Å³ can be generated by a small software package “packmol” available online⁷². A topology file and a coordinate file for the salt-water cell was generated using the pdb file of the salt-water cell and loading Amber 94 force field from the force field library and an ionic parameter file of the version 2008 in AmberTools 1.2. A MD simulation at 300 K was carried out to equilibrate the salt-water simulation cell. The equilibrated cell was obtained at the end of the MD simulation. Referred to Appendix 2 of the PERL program, a single PNIPAM chain can be inserted and centered in the salt-water cell by removing the overlapped water molecules and salt ions and keeping the net charge of 0 for the obtained PNIPAM-salt-water cell. Finally, the PNIPAM-salt-water cell was loaded in Leap to generate the topology and coordinate files in Amber format which were directly used in MD simulations using Amber 94 force field, the prepri files of NIPAM residues

and the ionic parameter file. For the copolymer PNIPAM-co-PEGMA, the prepi files for the residues in the PEGMA side chain were also needed in Leap.

1.8. SUMMARY

PNIPAM is the most popularly studied thermo-responsive polymer, which is commonly used for drug delivery and surface modification of films and membranes. The LCST of PNIPAM is 305 K in water, and is influenced by polymer chain length, concentration, and solution pH only slightly. However, salts have significant impacts on the LCST of PNIPAM and its copolymers. Till now, it is not clear how the salt ions interact with PNIPAM or its copolymers and how they affect the LCST. In order to clarify the mechanisms of LCST reduction of PNIPAM caused by the salt ions, various MD simulations of PNIPAM and the PNIPAM-co-PEGMA copolymer were carried out in different salt solutions.

CHAPTER 2 THE EFFECTS OF SALT ON THE LOWER CRITICAL SOLUTION TEMPERATURE OF POLY (N- ISOPROPYLACRYLAMIDE)

PUBLISHING STATEMENT

This chapter is based on the published paper, “Hongbo Du, Ranil Wickramasinghe and Xianghong Qian, Effects of Salt on the Lower Critical Solution Temperature of Poly (N-Isopropylacrylamide), Journal of Physical Chemistry B, 2010, 114, 16594–16604”. The contents different from the published paper are the addition of hydrogen bonding analyses and more discussions about pair distribution functions between atoms on PNIPAM or salt ions and water.

2.1. INTRODUCTION

PNIPAM has been widely studied as a prototype temperature responsive polymer which exhibits hydrophobic-hydrophilic phase transition at its lower critical solution temperature (LCST)^{10-14,73}. The LCST for PNIPAM in pure water is around 305 K (32 °C). The LCST is slightly affected by polymer molecular weight and concentration, and the observed variation in LCST is less than 2 K^{12,29,30}. Lower molecular weight samples appear to have slightly higher LCSTs. It has also been found that salt ions have a significant impact on the transition temperature. Most salts are found to reduce the

transition temperature^{40,41,74-77}. For example, the transition temperatures for PNIPAM (1.4 wt %) in 1 M NaCl, NaBr, NaI and KCl salt solutions are found to be reduced to 293, 298, 303 and 292 K respectively^{11,32}.

Earlier researchers suggested that anions play a critical role and cations play a minor role in LCST conformational transitions of PNIPAM.^{10,11,42-44} After Cremer et al.^{1,2} investigated the effects of sodium salts on the LCST of PNIPAM at different salt concentrations, they suggested that the anionic effect arises most likely from the direct bonding of the anions to the amide groups of PNIPAM. This is in conflict with the finding by Jungwirth and coworkers⁷⁸, which is the high affinity of cations to the peptide bond of NMA in aqueous salt solutions. However, NMA is only a small organic molecule containing one peptide bond, very different from a polymer or protein. It appears that ion interactions with the proteins in salt solutions^{46,47,50} may be explained via “matching water affinity”^{39,48,49}. However, recent MD simulations of alkali-acetate solutions⁷⁹ show that the ion-pairing effect cannot explain the cation-carboxylate binding affinity.

In order to investigate the interactions between ions and PNIPAM and discover a possible mechanism of the effects of salt ions on the LCST of PNIPAM and on protein stability, MD simulations of PNIPAM with degree of polymerization (DP) of 50 and a corresponding molecular weight (MW) of 5660 in pure water, 1 M NaCl, NaBr, NaI and KCl solutions were carried out above and below their respective LCSTs. PNIPAM conformation, the number of water molecules associated with the first hydration shell of the polymer, the pair correlation functions $g(r)$ between the ions and amide O, N as well as C from carbonyl, backbone and isopropyl groups in the polymer were determined. As far as we are aware, it is the first molecular dynamics study of the effects of salts in

solution on the LCST of PNIPAM. Earlier MD simulations focused on the LCST behavior of polymers in water only^{15,54,55,80}. The simulation results clearly indicate that it is the cation that interacts strongly with PNIPAM, and more importantly, this interaction is modulated by the cation-anion pair interaction of the salt in solution.

2.2. COMPUTATIONAL METHODOLOGY AND SIMULATION DETAILS

MD simulations were performed using NAMD⁶⁰, a highly parallelized code for large scale simulations. The non-polarized Amber 94 force field⁵³ was used for the polymer together with the TIP3P water model. Recent MD simulation results⁷⁸ show polarized and non-polarized force fields yield virtually the same interaction strength between the salt ions (both alkali cations and halide anions) and the peptide bond. However, the polarized force field does show an enhanced interaction between the anions and the alkyl groups in NMA, though the interaction appears to be rather weak using both force fields. The non-polarized force field used here will not affect the results on salt ion interactions with the peptide bond in PNIPAM. In addition, Amber 94 force field has been used successfully to investigate PNIPAM conformations and the LCST phase transition in pure water. For the salt ions in water, the improved parameters developed for the TIP3P water model were used⁸¹. The partial atomic charges of PNIPAM were calculated at B3LYP/aug-cc-pvtz//B3LYP/6-311+G(d,p) level with Gaussian 03⁶⁹. The structures of the monomer NIPAM capped with H- and CH₃- were constructed and the low energy conformations were determined using *ab initio* molecular dynamics simulations with CPMD⁶⁸. Gaussian 03 calculations were carried out for the partial charges of the lowest energy structure based on the RESP protocol⁸². The structure of the

PNIPAM monomer unit is shown in Figure 2-1, and the calculated partial atomic charges, atomic types of atoms and residue positions are listed in Table 2-1.

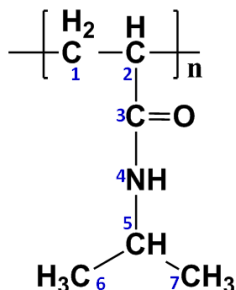


Figure 2-1 The structure of PNIPAM monomer unit. The atoms are numbered for easy discussion in the text.

PNIPAM with DP 50 (MW= 5660) was simulated both in the pure water at 310 and 295 K and salt solutions containing 1 M NaCl at 300 and 288 K, 1 M NaBr at 318 and 278 K, 1M NaI at 328 and 288 K, and 1 M KCl at 307 and 277 K respectively. A total of 22875 water molecules were used to solvate a single 50 DP PNIPAM chain in pure water. For PNIPAM in the salt solutions, a total of 22075 water molecules and 400 ion pairs were included in the simulation cell with a corresponding PNIPAM concentration of 1.4 wt %. Periodic boundary conditions were applied and the dimensions of the simulation unit cell at the start of the simulation were 90 X 90 X 90 Å³. The simulations were conducted under NPT ensemble with the target pressure of P=1 atm using the Langevin-Hoover scheme⁶⁰. A 12Å cut off was used for the short range electrostatic interactions and *van der Waals* interactions. The long range electrostatic interactions were calculated by particle mesh Ewald (PME) method. For PNIPAM in water, a total of 46 nanosecond (ns) simulations were conducted. For all other systems, a total of 48-85 ns simulations were conducted. The pair correlation functions (g(r)) were

Atom name	Atomic type	Residue 1 (atomic charge units:e)	Residues 2-59 (atomic charge units:e)	Residue 50 (atomic charge units:e)
C1	CT	-0.349419	-0.343472	-0.339928
H11	HC	0.092390	0.094000	0.094959
H12	HC	0.092390	0.094000	0.094959
H13	HC	0.092390		
C2	CT	0.110593	0.112520	0.113669
H21	HC	0.008535	0.008684	0.008773
C3	C	0.706540	0.718855	0.726193
O	O	-0.594108	-0.583996	-0.577971
C8	CT			-0.339928
H81	HC			0.094959
H82	HC			0.094959
H83	HC			0.094959
N4	N	-0.806922	-0.793188	-0.785004
H41	H	0.316265	0.321777	0.325062

C5	CT	0.658250	0.669725	0.676562
H51	H1	-0.017558	-0.017259	-0.017081
C6	CT	-0.480233	-0.472056	-0.467185
H61	HC	0.108520	0.110411	0.111538
H62	HC	0.108520	0.110411	0.111538
H63	HC	0.108520	0.110411	0.111538
C7	CT	-0.480233	-0.472056	-0.467185
H71	HC	0.108520	0.110411	0.111538
H72	HC	0.108520	0.110411	0.111538
H73	HC	0.108520	0.110411	0.111538

Table 2-1 Calculated partial atomic charges on PNIPAM monomer units, where the H atom H_{xy} represents the H atom bonding to the C atom C_x, C₈ is the C atom located at the end residue 50 of PNIPAM, and y is the order number of the H atom.

obtained averaging the last 20-30 ns of the simulations after the polymer at higher temperatures went through the LCST transition in solutions. For comparison, simulations were also carried out for aqueous solutions containing only 1M NaCl, NaBr, NaI and KCl without PNIPAM at the same corresponding temperatures with PNIPAM. Moreover, simulations were also carried out for the 1 M corresponding salt solutions at the same

temperature of 300 K. A total of 1897 water molecules and 34 ion pairs were included in each simulation system with box dimensions of 40 X 40 X 40 Å³. The other simulation parameters were kept the same as those with PNIPAM. A total of 40 ns simulations were carried out for the salt solutions without PNIPAM. PNIPAM's radius of gyration (R_g), end-to-end distance, and the number of water molecules in the first hydration shell were calculated during the MD simulations. Both R_g and the end-to-end distance describe polymer dimension and its variation as a function of time during the MD simulations. The number of water molecules closely associated with the polymer (the first hydration shell) is another measure of the size and state of the polymer. The cut-off distance for the first hydration shell is chosen to be 3.5 Å from the surface of the polymer which is conventionally defined⁸³. The cut-off distance is somewhat arbitrary. However, the trend associated with the number of water molecules in the first hydration shell will remain more or less the same for the two temperatures above and below the LCST using different cut-off distances. Three types of hydrogen bonding were analyzed to evaluate the hydrophilic-hydrophobic transition of the polymer at the lower and higher temperatures. The three types of hydrogen bonding are intra-chain hydrogen bonding, hydrogen bonding between O or N on NIPAM units and water molecules. In addition, pair correlation functions between the ions and the O, N, C atoms of the amide group, the C atoms on the backbone and isopropyl groups were determined. Pair correlation functions between the cations and anions in solution were also calculated for both the systems with and without PNIPAM. Pair correlation functions between the salt ions and O atoms of the H₂O molecules were also evaluated.

2.3. RESULTS AND DISCUSSION

MD simulations of PNIPAM in water were conducted at 310 and 295 K above and below its LCST of 305 K. Figure 2-2 tracks the radii of gyration of PNIPAM in water during the 46 ns MD simulations. The radius of gyration for PNIPAM at 310 K starts to decrease at about 3 ns of simulation time and keeps decreasing till about 11 Å is reached. On the other hand, the radius of gyration at 295 K increases slightly during the simulation and reaches around 25 Å at the end of simulation. Figure 2-3 shows the numbers of water molecules in the first hydration of PNIPAM at 310 and 295 K. The number of water molecules for PNIPAM at 310 K starts to decrease at around 6 ns of simulation time and keeps decreasing till it reaches 470, whereas the water number at 295 K remains more or less the same at 530-550. Figure 2-4 shows two final PNIPAM conformations at the ends of simulations, and a folded structure (Figure 2-4b) was observed at 310 K and an extended structure was observed at 295 K (Figure 2-4a).

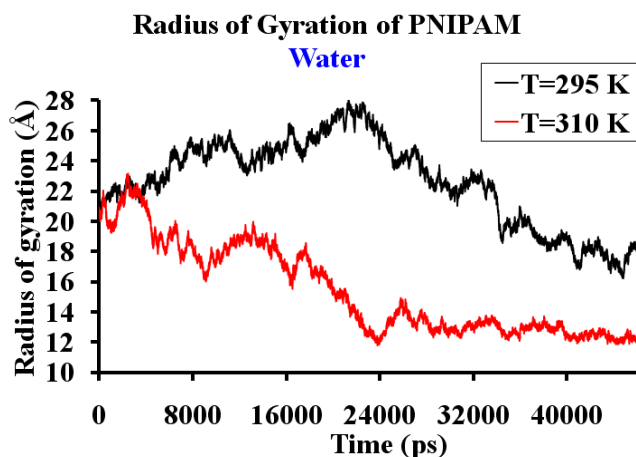


Figure 2-2 Radii of gyration of PNIPAM in water at 310 K (red line) and 295 K (black line) respectively during the 46 ns MD simulation.

The driving force for the PNIPAM's LCST transition is still not fully understood. It was generally thought that the conformational transition from the extended to the folded states is entropy-driven. The mechanism for the LCST transition is not the subject of this discussion. Instead, the spotlight here focuses on how the presence of salt ions in solution affects the transition temperature. From the PNIPAM simulations in water, it was demonstrated that the LCST transition of PNIPAM could be simulated in water in a temperature window of only 15 K.

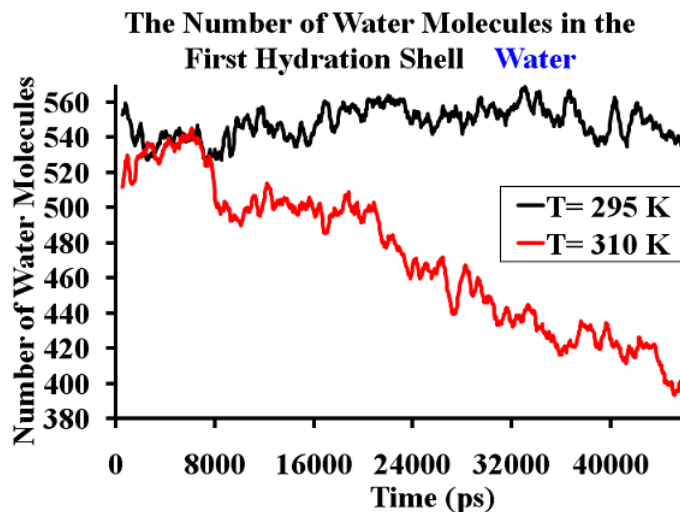


Figure 2-3 The numbers of water molecules within the PNIPAM's first hydration shell in pure water at 310 K (red line) and 295 K (black line) respectively during the 46 ns MD simulations.

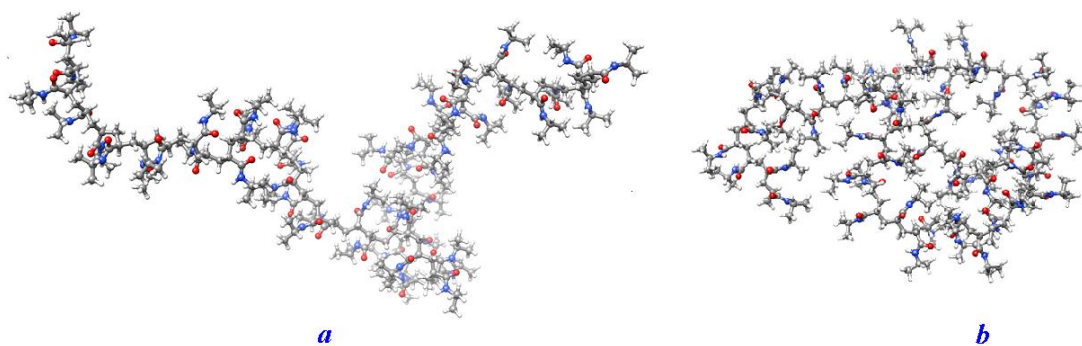


Figure 2-4 PNIPAM conformations after 46 ns MD simulations in water at 295 K (the extended structure shown in 2-4a) and at 310 K (the folded structure shown in 2-4b). Molecular graphics images of PNIPAM and PNIPAM-co-PEGMA in the text were produced using the UCSF Chimera package from the Computer Graphics Laboratory, University of California, San Francisco (supported by NIH P41 RR-01081)⁸⁴.

The numbers of hydrogen bonds (H-bonds)⁸⁵ during the simulations of PNIPAM in water were determined including the intra-chain H-bonds within PNIPAM, intermolecular H-bonds between the O, N atoms on PNIPAM and the water molecules. The time evolution of the numbers of H-bonds along the simulations at 295 and 310 K is shown in Figure 2-5. The criterion used to determine the presence of a hydrogen bond is that the hydrogen bond length between the two heavy atoms ($A \cdots H-B$) is greater or equal to 3.5 Å, and that the cut-off for the hydrogen bond angle ($\angle A \cdots H-B$) is 130° , where A and B are heavy atoms (O or N) in PNIPAM and water molecules. For the simulation of the polymer at 295 K in water, the number of the intra-chain H-bonds fluctuates around the average number of 4 during the simulation. However, the number of intra-chain H-

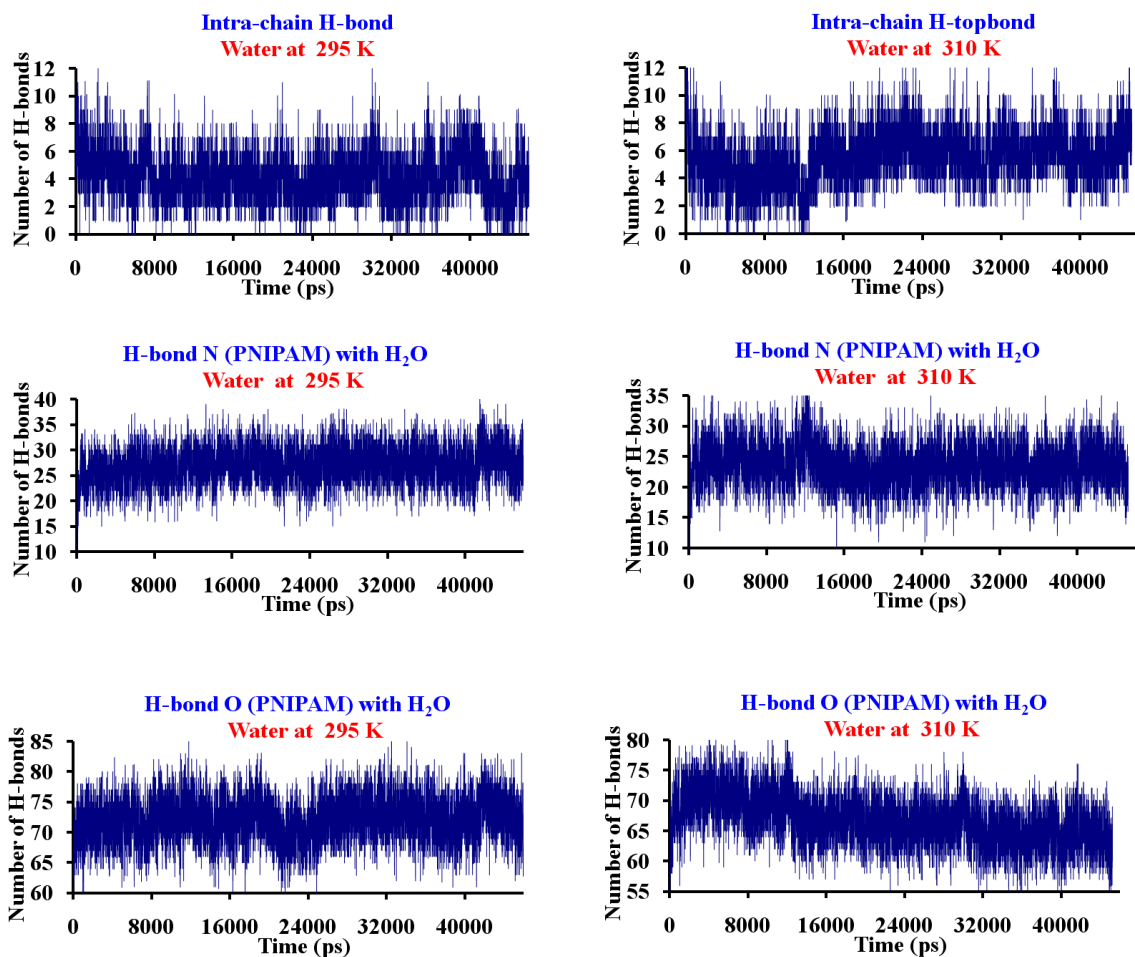


Figure 2-5 The numbers of H-bonds during the course of MD simulations for PNIPAM in water at 295 K (left) and 310 K (right)

bonds obviously increases from the average number of 3 to the average number of 6 along the simulation at 310 K. In the 295 K simulation the number of the H-bonds between the amide N on PNIPAM and water molecules increases a little from the beginning and keeps fluctuating in the range of 20-30 till the end of the simulation. In the 310 K simulation, the number of H-bonds between the amide N on PNIPAM and water molecules fluctuates and decreases slightly along the simulation. In the 295 K simulation,

the number of H-bonds between the amide O on PNIPAM and water molecules fluctuates and is kept in the range of 65-77. In the 310 K simulation, the number of the H-bonds between the O on PNIPAM and water molecules decreases by 8-10 to reach a stable status. We can see that the numbers of intra-chain H-bonds, H-bonds between the amide N or O on PNIPAM and water molecules keep more or less the same along the simulation of PNIPAM at 295 K in water, however, the number of intra-chain H-bonds increases and the number of H-bonds between the amide O or N and water molecules decreases at 310 K due to the hydrophilic-hydrophobic phase transition of PNIPAM at a temperature above its LCST. On the other hand, it can be deduced that the conformation of PNIPAM is more compact at the end of the 310 K simulation than that at the end of the 295 K simulation base on the number variations of three types of H-bonds at both temperatures.

MD simulations of PNIPAM in 1 M NaCl, NaBr, NaI and KCl solutions were carried out subsequently at temperatures above and below their respective LCST values. The experimental LCST values for 1.4 wt % PNIPAM are estimated to be at around 293 K, 298 K, 303 K and 292 K in 1 M NaCl, NaBr, NaI and KCl solutions respectively³³. The transition temperature varies slightly depending on the experimental conditions (polymer concentration and molecular weight) as discussed earlier. Except for NaCl with a temperature difference of 12 K, it was found that the temperature window between the higher and lower temperatures had to be increased to around 30 K for KCl and around 40 K for both NaBr and NaI in order to successfully simulate the LCST transition from the hydrophilic state to the hydrophobic phase. Here we focus on evaluating the properties of this thermo-sensitive polymer and investigating how salt ions interact with this polymer above and below its transition temperature.

Figure 2-6 shows the radii of gyration and the numbers of water molecules in the first hydration shell of PNIPAM in 1 M NaCl, NaBr and NaI salt solutions having the same cation Na^+ above and below their respective LCSTs. A clear reduction in radii of gyration for the higher temperatures are observed after about 8 ns simulation in NaCl solution, after about 20 ns simulation in NaBr solution and after about 40 ns simulation in NaI. The radii of gyration at lower temperatures are seen to fluctuate around 16-20 Å and remain consistently larger than the corresponding higher temperature values of about 10 Å. Additional 30-50 ns of simulations were carried out to ensure that the results are consistent and to obtain the various pair correlation functions sampled from the thermodynamic quasi-equilibrium states. In the higher temperature simulations, the numbers of water molecules in the first hydration shell are significantly reduced compared to the lower temperatures. The numbers of water molecules in the first hydration shell of PNIPAM are reduced to approximately 360 at higher temperatures compared to close to 520 at lower temperatures for all three pairs of systems. Figure 2-7 shows the corresponding results for PNIPAM in 1 M KCl solution. The results in KCl solution resemble those of PNIPAM in the Na^+ salt solutions. The end-to-end distances of the polymer for all the systems shown in Figure 2-8 demonstrate very similar behaviors to that of the radii of gyration.

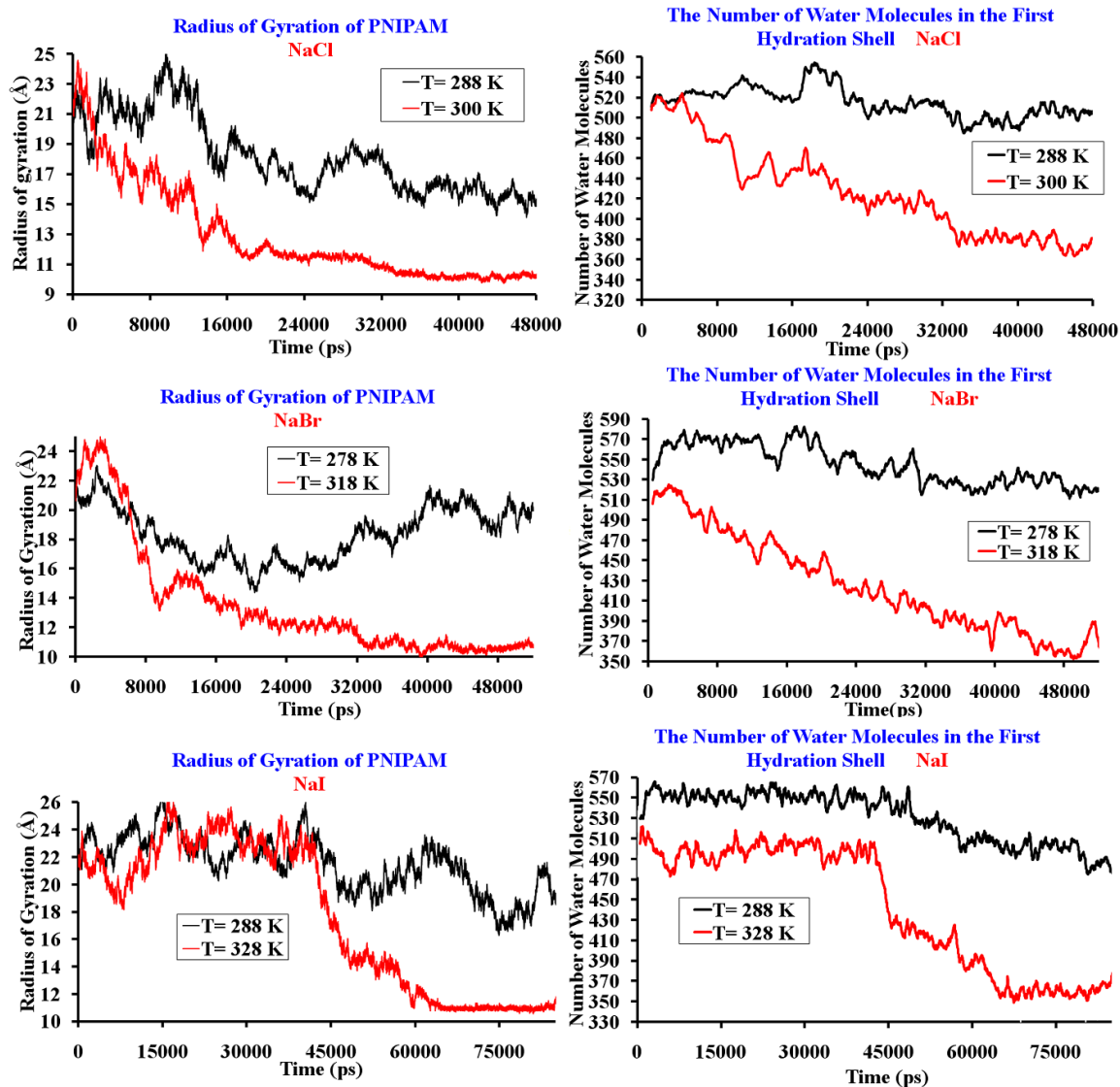


Figure 2-6 Radii of gyration (left) and the numbers of water molecules in the first hydration shell of PNIPAM (right) in 1 M NaCl, NaBr and NaI solutions above and below their respective LCSTs.

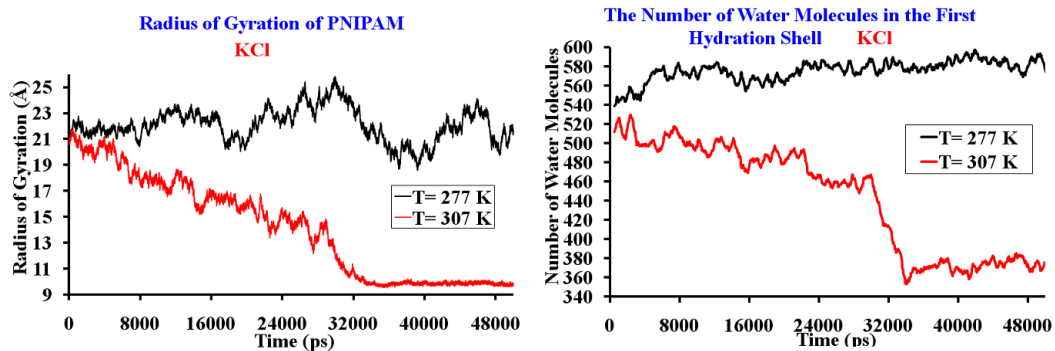


Figure 2-7 Radii of gyration (left) and the numbers of water molecules in the first hydration shell of PNIPAM (right) in 1 M KCl solution above and below its LCST.

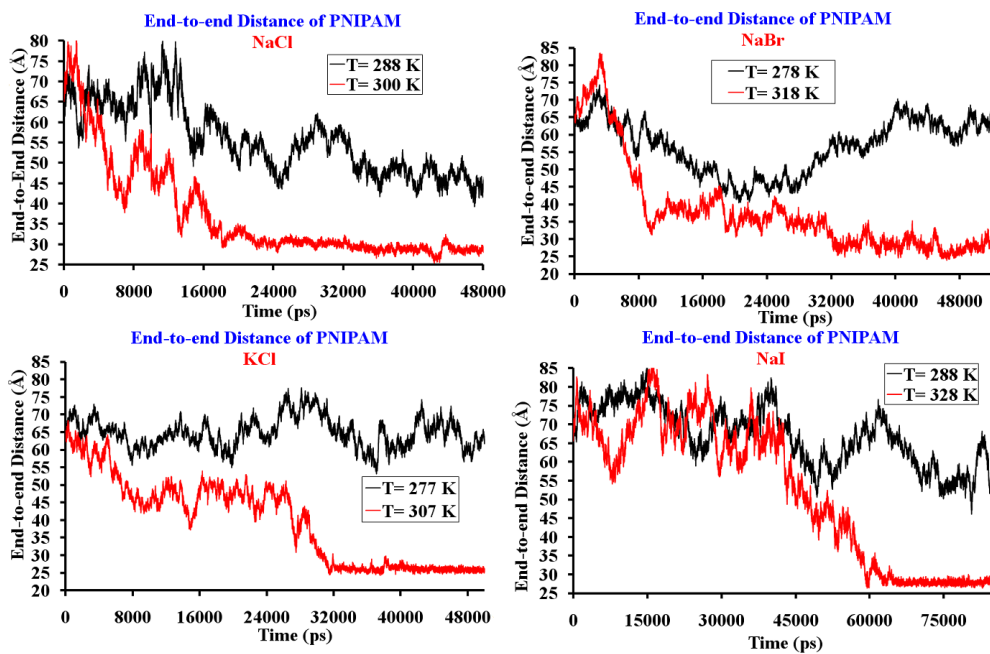


Figure 2-8 End-to-end distances of PNIPAM in 1 M NaCl, KCl, NaBr and NaI solutions above and below their respective LCST during MD simulations.

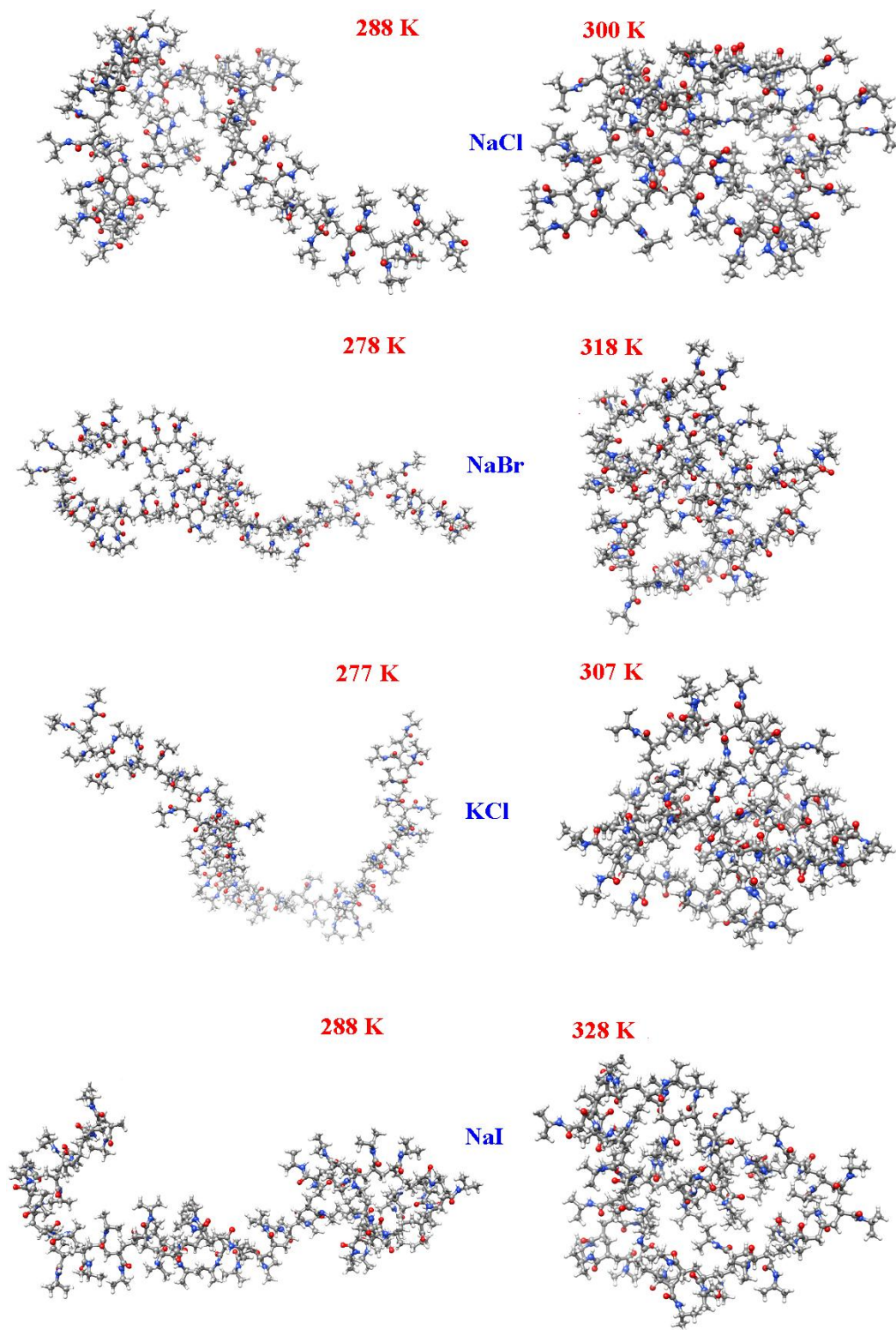


Figure 2-9 Conformations of PNIPAM at the ends of simulations in different salt solutions

Figure 2-9 shows the conformations of PNIPAM at the ends of the simulations of PNIPAM in different salt solutions. After the PNIPAM conformations at the ends of simulations in different salt solutions were checked, it could be found that the conformations at higher temperatures appear to be folded whereas the conformations at lower temperatures show extended structures, similarly to the pure water case.

Figure 2-10 shows the numbers for the same three types of H-bonds during the simulations of PNIPAM at 288 and 300 K in NaCl solution. The criterion used to determine whether a hydrogen bond exists or not is the same as that used for PNIPAM in water. For the simulation of the polymer at 288 K, the number of the intra-chain H-bonds fluctuates around 2-7 along the simulation. In the 300 K simulation, the number of the intra-chain H-bonds increases from the average number of 4 to about 7 during the simulation time of 14-40 ns, and then keeps stable to the end of the simulation. For the number of H-bonds between N in PNIPAM and water molecules, the number increases marginally from about 28 to 30 during the simulation time of 0-30 ns, and then keeps more or less the same around 30 till the end of simulation at 288 K. However, the number decreases by about 5 from the beginning of the simulation to 24 ns and then fluctuates around the average number of 20 till the end along the 300 K simulation. The increasing number of the intra-chain H-bonds and the decrease of the H-bond number between the amide N or O on PNIPAM and water at 300 K show that there are more intra-chain interactions for PNIPAM, and that the final PNIPAM conformation is more compact at 300 K than that at 288 K.

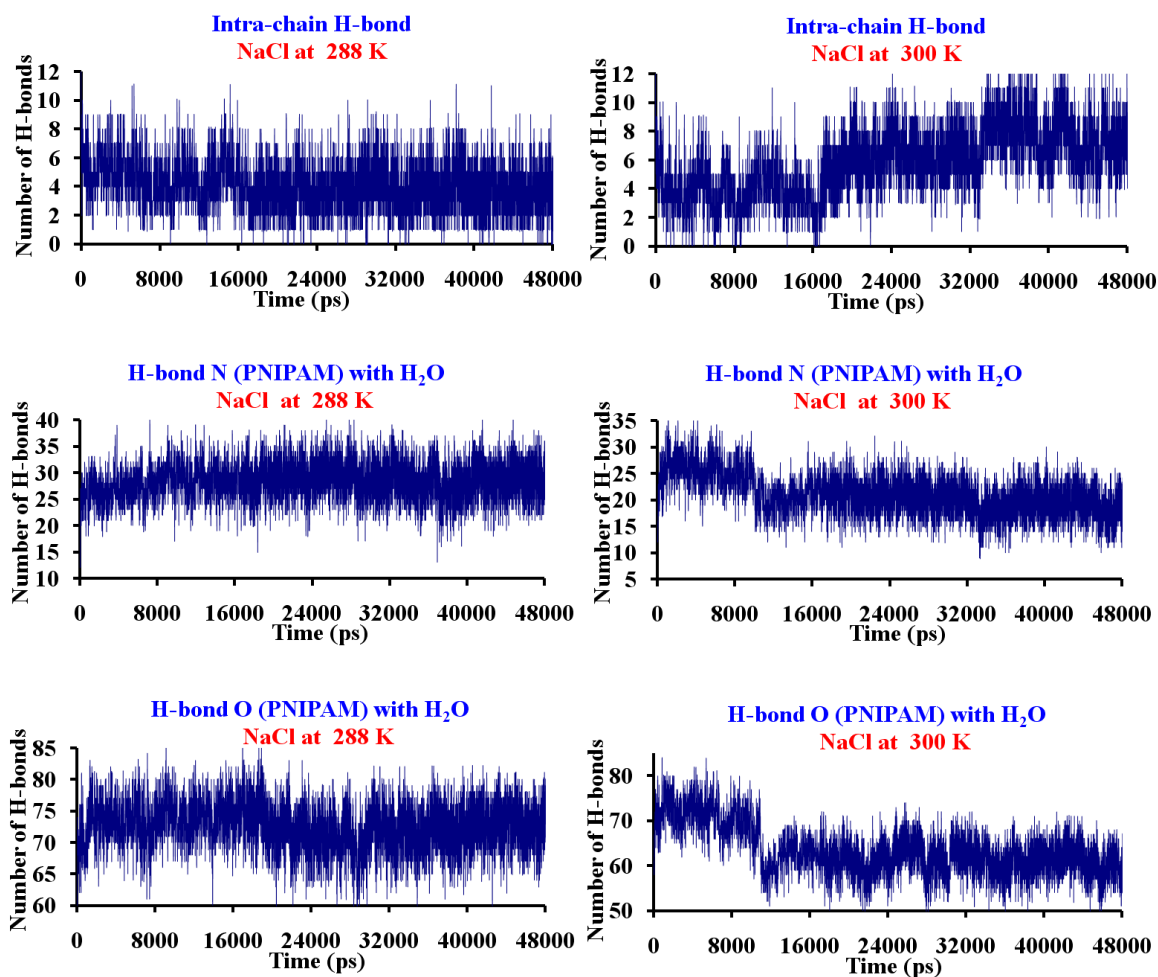


Figure 2-10 The number of H-bonds during the course of MD simulations for PNIPAM in 1 M NaCl solution at 288 K (left) and 300 K (right)

Figures 2-10, 11 and 12 show the results of the hydrogen bonding analyses for the simulations of PNIPAM in NaBr, NaI and KCl solutions below and above the respective LCSTs using the same criterion. We can see that the number of intra-chain H-bonds keeps more or less the same along each simulation at lower temperatures. However, it increases by 4-5 for the simulations along the higher temperature simulations. For the

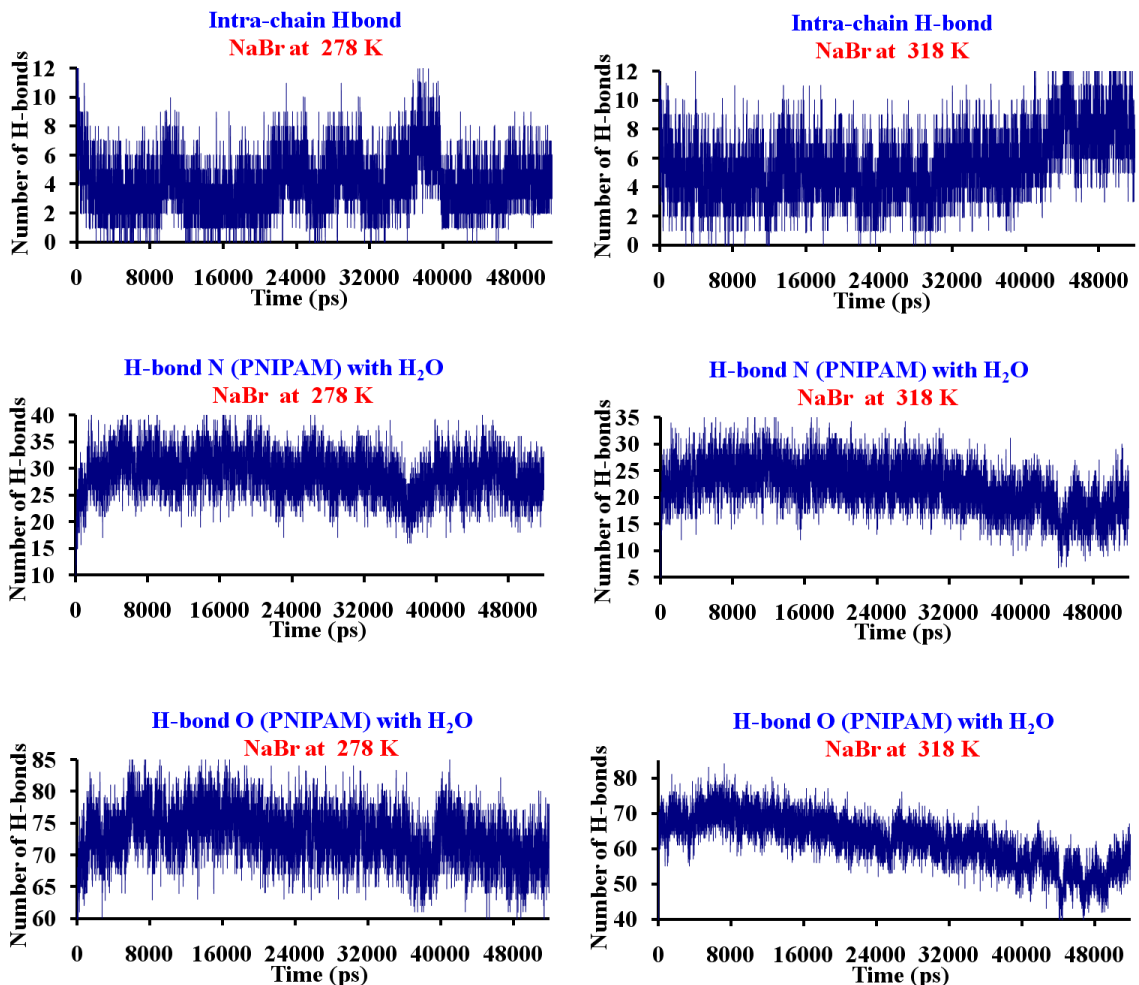


Figure 2-11 The number of H-bonds during the course of MD simulations for PNIPAM in 1 M NaBr solution at 278 K (left) and 318 K (right)

number of H-bonds between the N atoms in PNIPAM and water molecules, the number also keeps more or less the same along the NaBr and KCl simulations at lower temperatures, and there is a slight decrease for the NaI simulation at 288 K. However, the number decreases by 8-10 for the simulations along the higher temperature simulations. For the number of H-bonds between the amide O in PNIPAM and water molecules, the calculated results show the similar trends compared to H-bonds between the amide N in

PNIPAM and water molecules for lower and higher temperatures, but the number decreases more significantly compared to the decrease of the number of H-bonds between the amide N in PNIPAM and water molecules at higher temperatures. Compared to the simulations of PNIPAM in water, the increase degree of the number of intra-chain H-bonds and the decrease degree of the H-bond number between the amide O or N and water molecules is greater due to the presence of salt ions.

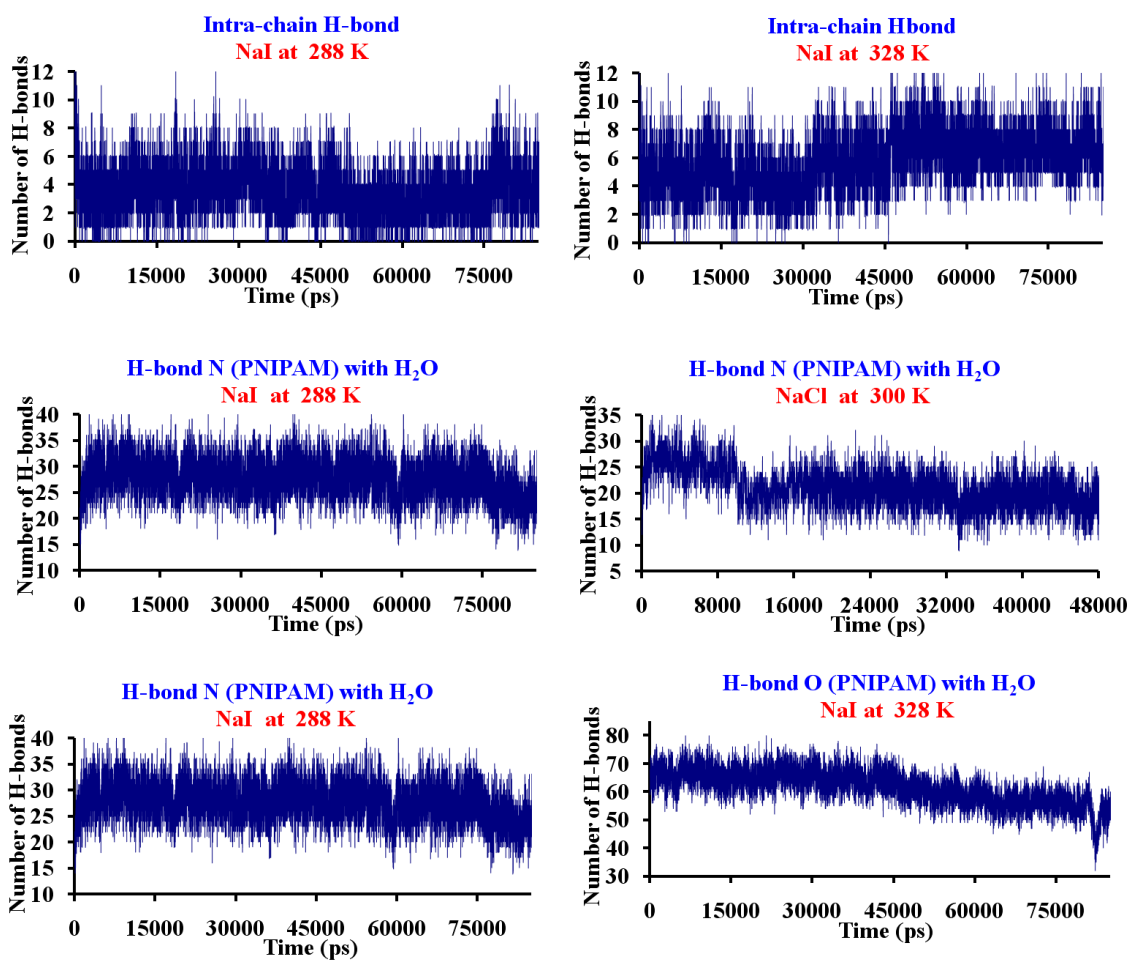


Figure 2-12 The number of H-bonds during the course of MD simulations for PNIPAM in 1 M NaI solution at 288 K (left) and 328 K (right)

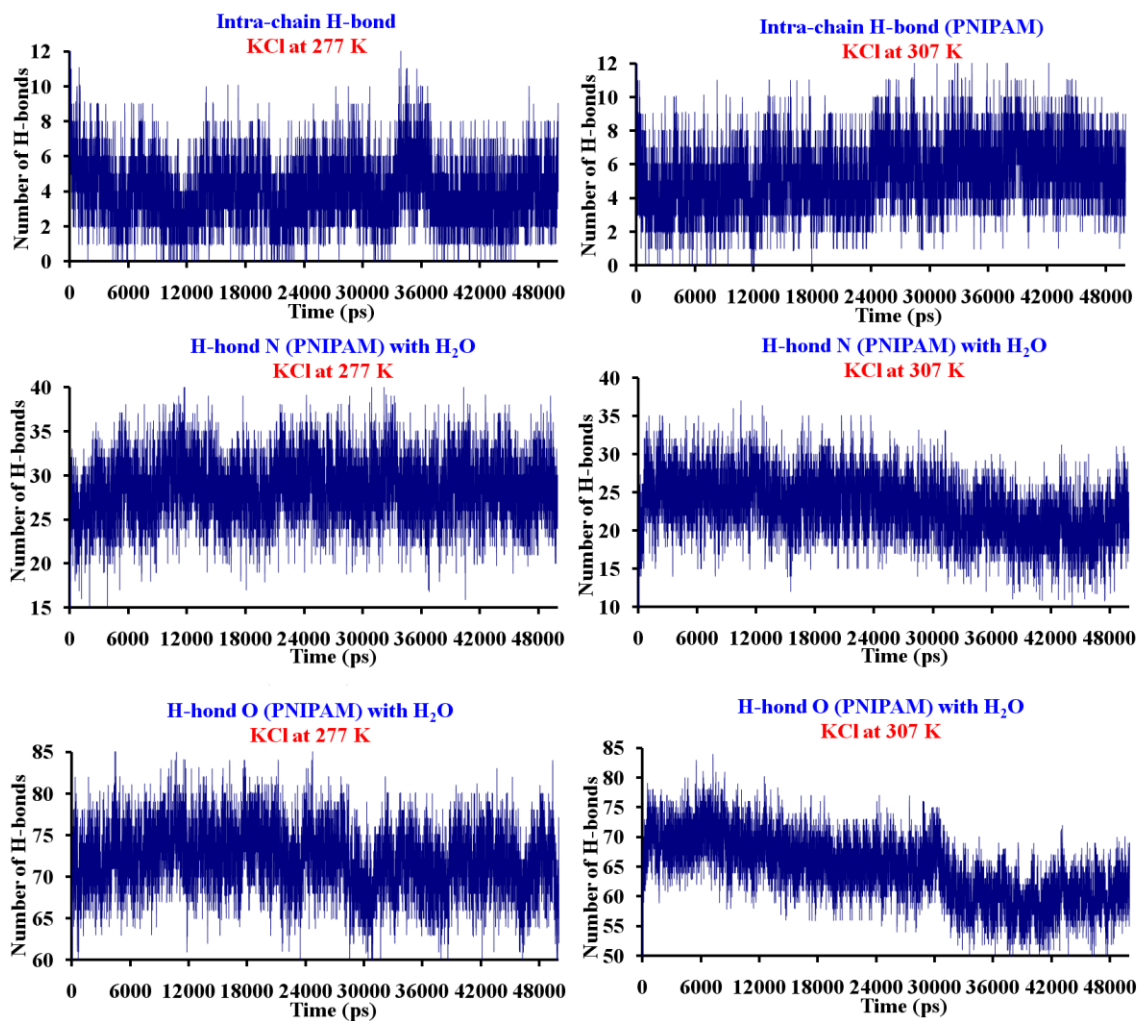


Figure 2-13 The number of H-bonds during the course of MD simulations for PNIPAM in 1 M KCl solution at 277 K (left) and 307 K (right)

The internal energies of the polymer-polymer and polymer-water interactions for PNIPAM in 1 M NaBr solution are shown in Figure 2-14. The results show that both energies remain more or less the same as a function of time for the PNIPAM simulated below its LCST. However, the polymer-polymer interaction energy decreases whereas polymer-water interaction energy increases for PNIPAM simulated above its LCST indicating the phase transition from an extended structure to a folded structure.

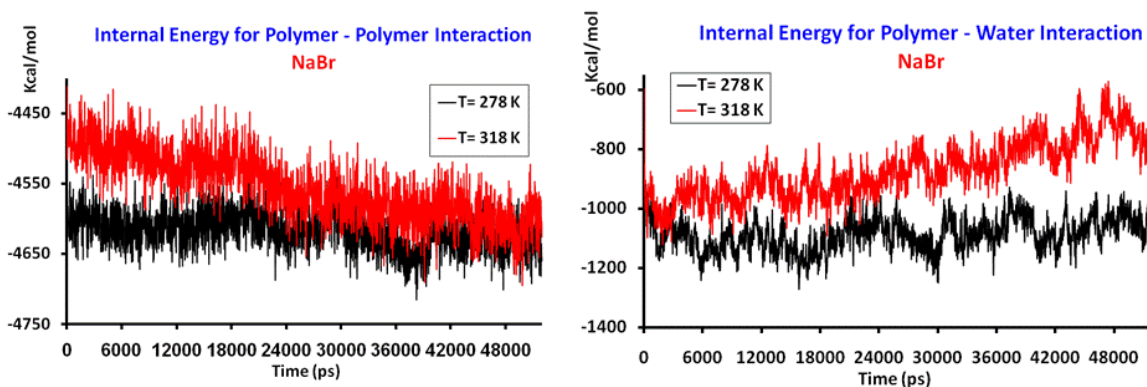


Figure 2-14 The internal energies for polymer-polymer (left) and polymer-water interactions (right)

The pair correlation functions $g(r)$ between the polymer and salt ions were calculated after the phase transition was observed and the systems reached quasi-equilibrium. The pair correlation functions were averaged for the last 20-30 ns of simulation time in each case. Figure 2-15 shows the pair correlation functions between the ions in salt solutions and the O, C atoms on the C=O of the peptide bond at temperatures above and below their respective LCSTs. For the pair correlation functions between the amide O and the cations (Na^+ and K^+), peaks at 2.3 Å and 2.8 Å were observed for Na^+ and K^+ respectively indicating direct contact between the O atoms and the cations. Further, it can be seen that Na^+ in NaI has the strongest interaction with the amide O at temperatures both above and below its LCST whereas K^+ in KCl has the weakest interaction with the amide O. Moreover, the cation-O interaction is slightly favored at lower temperature than at higher temperature for all the cases except for NaCl. The effects of temperature on the strength of the pair interaction will be discussed later in more detail. The interaction strength between the Na^+ and amide O follows the order NaI > NaBr > NaCl. The K^+ in KCl appears to have even weaker affinity with the amide O than the corresponding Na^+ in NaCl. The stronger binding interaction between the Na^+ in

NaI and the amide O than the corresponding interaction in NaCl clearly indicates that anion also plays an important role in the cation interaction with the polymer. However, for the $g(r)$ factors between the salt anions and amide O shown in Figure 2-15, only small and broad peaks at around 4.5 Å, 4.8 Å and 5.0 Å were observed for Cl^- , Br^- and I^- respectively. This indicates that the interactions of the salt anions with the amide O are significantly weaker compared to those of the cation...amide O interactions. Since both amide O and the anions are negatively charged, their interaction must be mediated via the positively charged Na^+ ions. Indeed, considering the $\text{Na}^+\cdots\text{O}$ interacting distance of 2.3 Å and the direct ion pair interacting distances of 2.6 Å, 2.8 Å and 3.1 Å for $\text{Na}\cdots\text{Cl}$, $\text{Na}\cdots\text{Br}$ and $\text{Na}\cdots\text{I}$ respectively, the maximum distances between the amide O and the anions would be around 4.9 Å, 5.1 Å and 5.4 Å when all the atoms involved align linearly close to the peaks observed here. Even though much weaker, the interactions between the anions and amide O follow the trend $\text{I}^- > \text{Br}^- > \text{Cl}^-$. This trend is observed repeatedly for the interactions between the halide anions and the polymer. It is probably due to the fact that I^- ion is the least hydrated ion among I^- , Br^- and Cl^- ions thus having the highest affinity for PNIPAM. The results indicate that anions have very weak affinity and do not bind directly with the amide O. Previously observed anion effect on the interaction between salt cation and amide O is probably due to the fact that halide anions mediate the interactions between the cations and amide O thus affecting the corresponding $g(r)$ factor indirectly. Examining the interactions between the salt ions and amide C, a similar trend was again observed. The Na^+ ion in NaI solution demonstrates the highest affinity for the amide C whereas the lowest affinity was observed for the amide C and K^+ interaction. However, the peak position for the $\text{C}\cdots\text{Na}^+$ correlation is located at around 3.4 Å

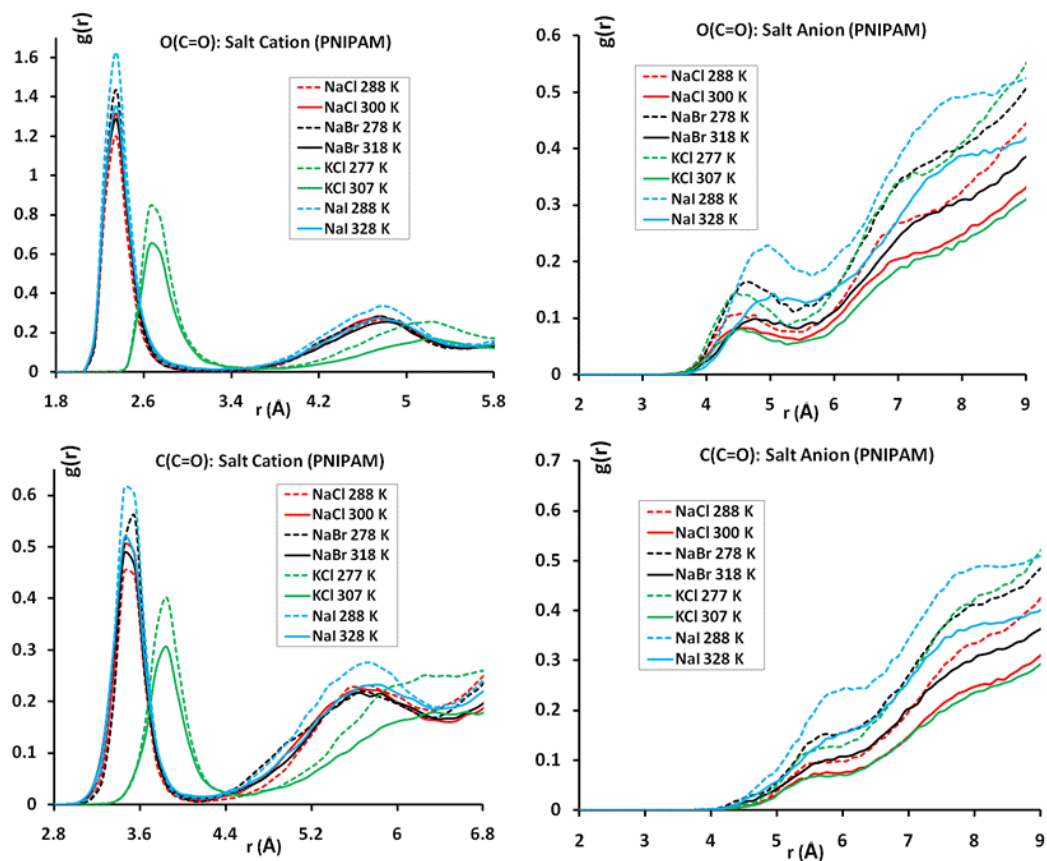


Figure 2-15 Pair correlation functions between the O, C atoms on the amide groups and the cations, anions of the salt solutions containing PNIPAM

compared to 2.3 Å for the $O\cdots Na^+$ interaction. Since both amide C and Na^+ are positively charged, a direct binding between them is unlikely. Moreover, the strength of the interaction between the amide C and cation is much weaker than that of the amide $O\cdots$ cation interaction. The peak height is reduced by about half. The $C\cdots Na^+$ distance is about the distance of $O\cdots Na^+$ plus the $C=O$ bond length of about 1.2 Å. All this indicates that the first peak in $Na^+\cdots C(C=O)$ correlation function arises from the binding between Na^+ and amide O. Moreover, based on the $g(r)$ factor (shown in Figure 2-16) between amide C and O (H_2O) which exhibits a first peak at around 3.7 Å, the first peak in $g(r)$ of

the C and Na^+ correlation cannot come from their indirect binding with a water molecule mediating their interaction. The anions do not appear to bind at all with the amide C atoms, even though the amide C has large positive charge and anions are negatively charged. It appears that the amide C and halide interaction is even weaker than the corresponding amide O and halide interaction. Here the results are in conflict with the suggestion made by Cremer and coworkers^{10,11} earlier that the anions bind directly with amide C, and that is one of the main reasons for the observed salt effects on the LCST of PNIPAM in different sodium salt solutions.

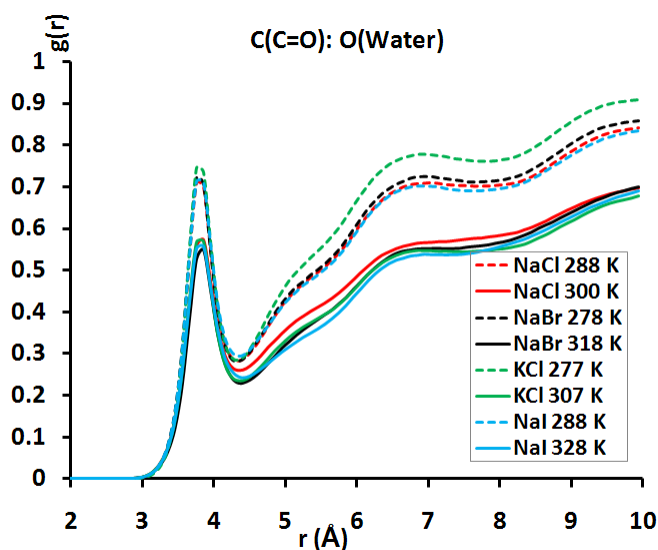


Figure 2-16 Pair correlation functions between the amide N and O (H_2O)

The interaction between cation and amide N follows the same trend as that between cation and amide O, albeit with much weaker strength as shown in Figure 2-17. The Na^+ in NaI has the strongest binding with the amide N, followed by Na^+ in NaBr and Na^+ in NaCl with K^+ in KCl having the lowest correlation. However, the overall

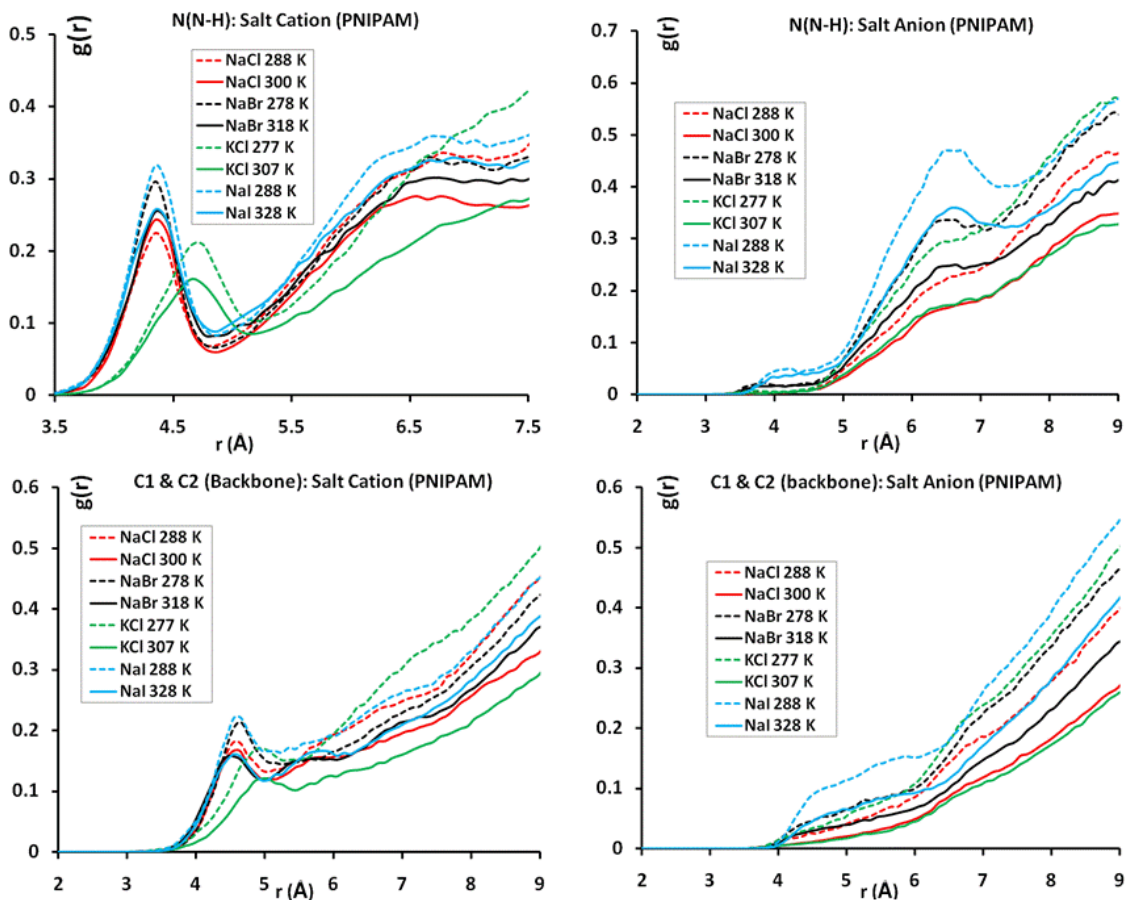


Figure 2-17 Pair correlation functions between the amide N, backbone C and the cations, anions of the salt solutions containing PNIPAM.

cation...N interaction is significantly weaker than the cation...O interaction as seen from the peak heights of the $g(r)$ factors. Further, it appears that cations do not bind directly with the N atoms in PNIPAM since the first peak on N...Na⁺ $g(r)$ function is located at around 4.4 Å. Examining the structure of PNIPAM and its surroundings, this correlation appears to arise indirectly from the interaction between amide O and Na⁺, similar to the observed correlation between amide C and Na⁺. Since the distance between O and N in an amide bond is observed to be approximately 2.3 Å and the O...Na⁺ binding distance is

about 2.3 Å, the interaction distance at around 4.0-4.6 Å for the amide N and Na⁺ interaction is expected. Moreover, the first peak of g(r) (shown in Figure 2-18) between the oppositely charged amide N and H (H₂O) appears at around 3 Å. This indicates that amide N and water do not form strong hydrogen bond and that the first peak in the amide N and Na⁺ correlation must come from the Na⁺ binding to amide O. The anions do not appear to interact directly with the amide N similar to the interaction with amide C. The simulation results agree with earlier theoretical^{46,47,50,78} and experimental⁸⁶ studies suggesting that cation-protein interaction has a significant impact on protein stability.

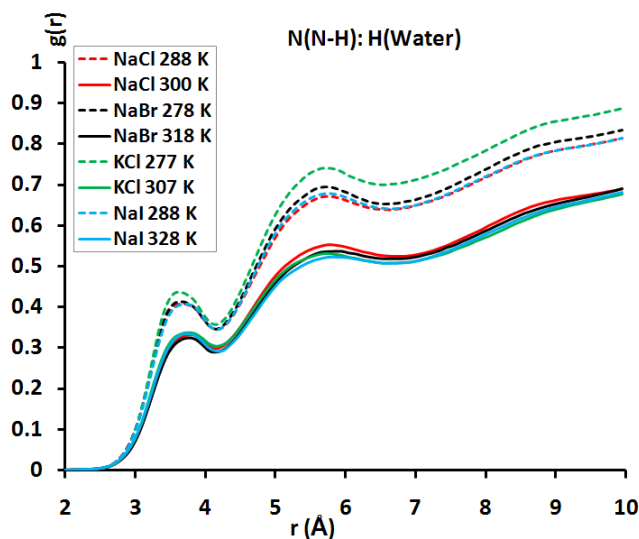


Figure 2-18 Pair correlation functions between amide N and H(water)

Earlier studies⁷⁸ suggested that protein denaturation by the Hofmeister anions arise possibly from the direct interaction of the anions with the C atoms on peptide side chains (corresponding to the C atoms on the backbone or isopropyl groups of the PNIPAM, where the amide groups are in the side chains). The pair correlation functions between the salt cation, anion and the C atoms on the backbone and isopropyl groups in

PNIPAM were calculated. Figure 2-17 (lower panel) shows the $g(r)$ factors between the backbone C (C1 and C2) and cations (left), anions (right) respectively in four different salt solutions. Broad peaks located at around 4.4-5.0 Å were observed for the $\text{Na}^+\cdots\text{C}$ interactions in NaI, NaBr and NaCl solutions. From the calculated pair correlation functions between C1, C2 and O (H_2O) (shown in Figure 2-19), it appears that the peaks observed here can again be attributed to the binding between the Na^+ and amide O. No peaks were observed between the anions and the backbone C except for I^- at lower temperature, where a slightly enhanced $g(r)$ correlation was seen. This is again probably due to the more hydrophobic nature of I^- . Since the first peak in the C1, C2 and Na^+ correlation comes from the amide O and Na^+ interaction, it is not unexpected that Na^+ in NaI again exhibits the strongest association with the backbone C, followed by NaBr and NaCl, whereas K^+ in KCl shows the lowest affinity, even though the association is overall much weaker than the interactions with the amide groups. Moreover, the cations, in particular Na^+ , have relatively stronger correlation with the backbone C, whereas anions virtually have no affinity with these C atoms.

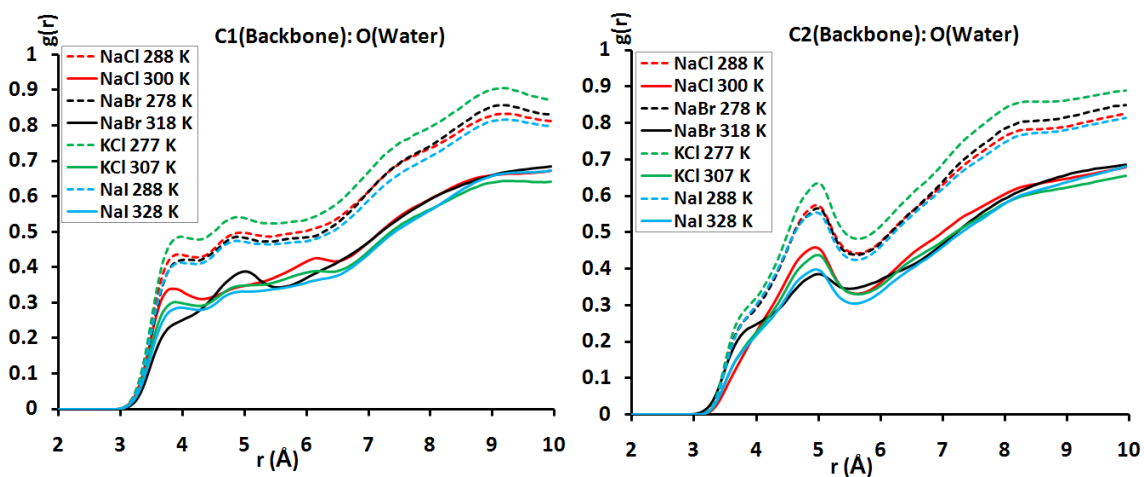


Figure 2-19 Pair correlation functions between C1, C2 and O(water)

Figure 2-20 shows pair correlation functions between the C atoms on the isopropyl groups of PNIPAM and the cations (left), anions (right) of the salt solutions. The interactions between the isopropyl C5, C6, C7 and the cations appear to be rather weak. Though visible, the peaks are very broad and the $g(r)$ factors continue to increase with the increase of the cation...C distance. This indicates that there is no specific interaction mechanism existing between the cations and the isopropyl C atoms. However, the interaction between anion and isopropyl C shows interesting trends. Both isopropyl C5 and C6, C7 atoms appear to interact relative strongly with the anions, particularly with I⁻ compared to the interaction with the cations. Interestingly, the peak positions are located differently at around 5.5 Å and 4.5 Å respectively for anion interacting with the C5 and C6, C7. The interaction between isopropyl C and anion doesn't appear electrostatic in nature. The charges on the two types of the C atoms show opposite signs with a positive charge of $\sim +0.67 e$ for C5 and a negative charge of $\sim -0.47 e$ for C6 and C7 as shown in Table 2-1. If the interaction originates from electrostatic force, the interaction between C6, C7 and anion should be mediated by the positively charged cation since both C6, C7 and anion are negatively charged. However, the interactions between C6, C7 and cation are non-specific and very weak with a binding distance close to 4 to 5 Å, cation does not appear to mediate the interaction between anion and C6, C7 with a binding distance of 4.5 Å only. Moreover, the oppositely charged C5 and C6, C7 exhibiting similar interaction strength with anion means that charge plays a minor role here. The interaction between anion and isopropyl is most likely hydrophobic in nature. Among the three kinds of halide ions, the interaction strength with isopropyl follows the order $I^- > Br^- > Cl^-$ in accordance with the hydration free energies of the anions. The

highly hydrated Cl^- has the weakest binding with the hydrophobic isopropyl groups whereas the least hydrated I^- has the strongest binding. The slightly larger binding distance observed between C5 and anion is probably due to the location of the C5, which it is not easily accessible.

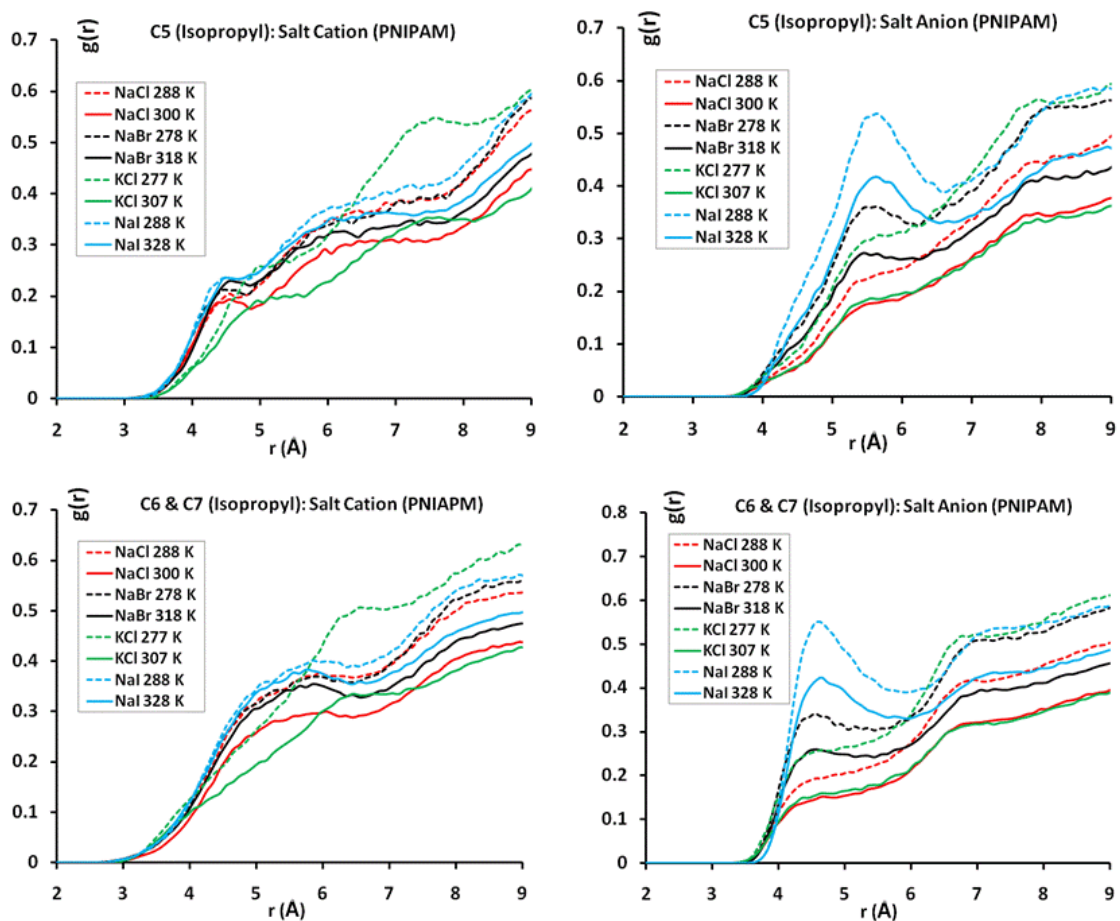


Figure 2-20 Pair correlation functions between the C atoms on the isopropyl groups of PNIPAM and the cations (left), anions (right) of the salt solutions

From the pair correlation functions between the cations, anions and amide groups in PNIPAM, it can be seen repeatedly that the cation interaction with the amide groups is affected by the types of the anions present. Na^+ in NaI has the strongest interaction

whereas Na^+ in NaCl has the weakest. *This begs the question, why does the same Na^+ interact differently with the polymer when paired with different anions?*

Earlier experimental results show that bulk water structure is not affected by the presence of different salts in solution^{36,37}. In order to elucidate the nature of the effects of salt on the LCST of PNIPAM, and similarly on protein stability, the pair correlation functions between the water $\text{O}\cdots\text{O}$ were determined in different salt solutions with and without the presence of PNIPAM. It was found that bulk water structure is indeed not altered by the different salts present in solution. In addition, the salt cation-anion pair correlation functions were also calculated both with and without PNIPAM. Figure 2-21 shows the cation \cdots anion $g(r)$ functions for PNIPAM in 1 M NaCl, NaBr, NaI and KCl simulated above and below their respective LCSTs with (upper) and without (lower) PNIPAM. The first peak on the $g(r)$ function is the contact ion pair peak which could be observed at 2.7, 2.8, 3.0 and 3.1 Å for the ion pairs NaCl, NaBr, NaI and KCl respectively. As with other pair correlation functions, the peak position indicates the contact ion-pair distance, whereas the peak height indicates the binding strength. The results show that K^+ and Cl^- contact ion pair has the strongest association constant, whereas Na^+ and I^- ion pair has the weakest association constant for both higher and lower temperatures investigated. The interaction strength follows the order $\text{KCl} > \text{NaCl} > \text{NaBr} > \text{NaI}$. The current results agree very well with the ion-pair association constants of 0.28, 0.12, 0.090 and 0.048 m^{-1} for KCl, NaCl, NaBr and NaI respectively calculated in aqueous solution using TIP3P water model⁸⁷. The ion pair correlation functions remain more or less the same with and without PNIPAM. Further, cation-anion pair interaction is

stronger at higher temperature than at lower temperature in agreement with earlier results⁸⁸.

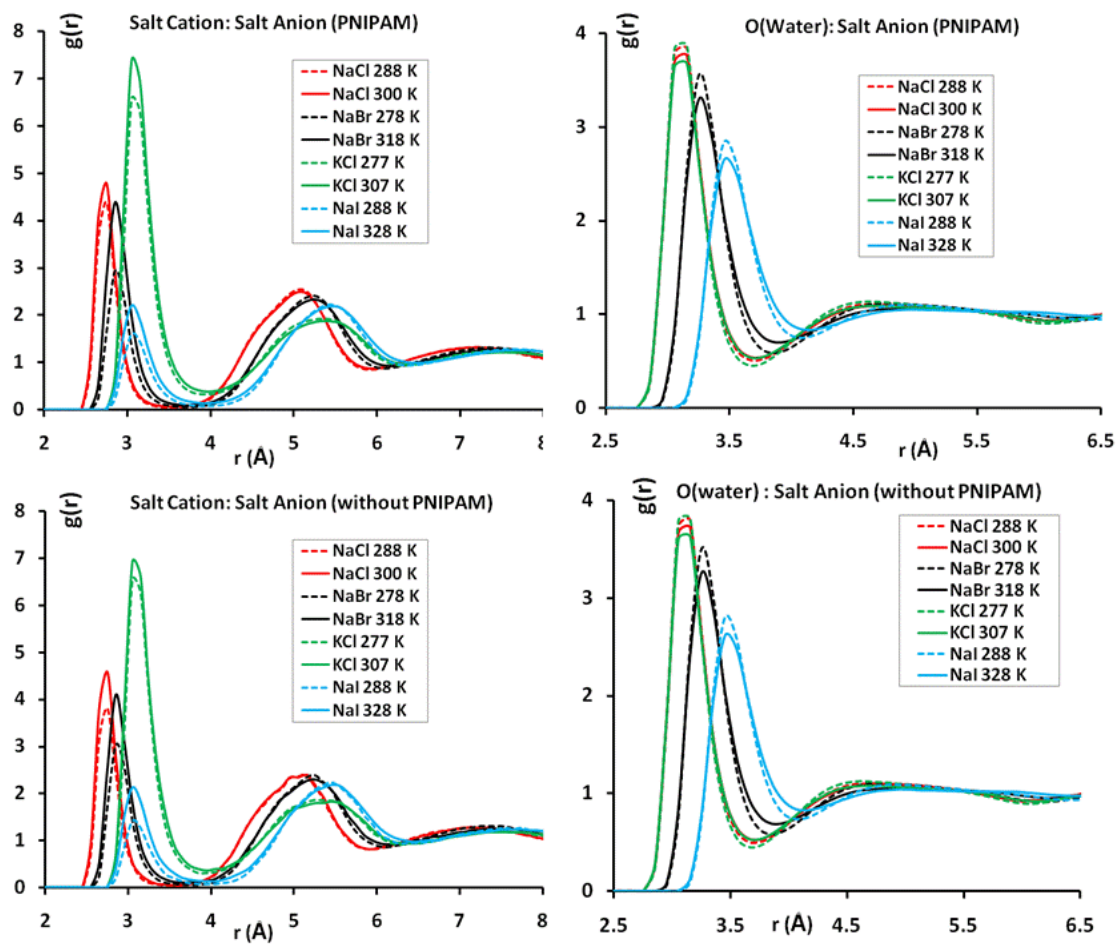


Figure 2-21 Cation-anion pair correlation functions for 1 M NaCl, NaBr, NaI and KCl solution with (upper left) and without (lower left) PNIPAM. The pair correlation functions between the O of water and salt cation (upper right), anion (lower right).

The effects of temperature on the contact ion pair correlation function of NaCl has been studied before^{89,90}. The increase of the Na^+ and Cl^- contact pair association constant

with temperature is thought due to the reduction of the dielectric constant of water at higher temperature thus promoting stronger interaction. In order to test this hypothesis, the pair correlation functions between the cation and O (H₂O) were determined for the four salt solutions as shown in Figure 2-22. It can be seen that the cation...O interaction is stronger at lower temperature than at higher temperature. Since the cation and O (H₂O) are oppositely charged, the observed increase in interaction strength at lower temperature does not come from the dielectric constant increase. The interaction strength between anion and O in H₂O also increases as temperature decreases as shown in Figure 2-21 (right panel). It is known that higher temperature tends to weaken binding interaction including hydrogen bonding interaction resulting in a weaker correlation. In return, the weaker ion-water interaction at higher temperature promotes stronger ion-ion interaction for each salt pair in aqueous solution. That is to say, ion-water interaction is inversely correlated with the cation-anion contact pair interaction for the same salt ion pair at different temperatures. This is not surprising since water and cation (anion) are competing for binding with the anion (cation).

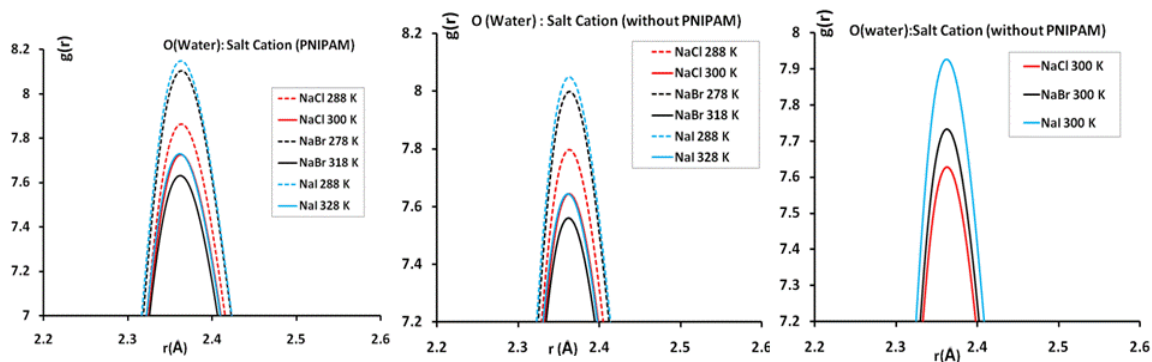


Figure 2-22 The pair correlation functions between cation and O (H₂O) in 1 M NaCl, NaBr and NaI solutions with (left panel) and without (middle panel) PNIPAM determined above and below their respective LCSTs. The pair correlation functions were also determined for the three systems at constant temperature of 300 K (right panel). Only the first peaks are shown in order to show the temperature and ionic effects more clearly.

In order to separate the temperature effects from ionic effects, MD simulations were carried out for 1 M NaCl, NaBr, NaI and KCl at the same temperature of 300 K. Figure 2-23 shows the pair correlation functions for the contact ion pairs (left) as well as between salt anion and O in H₂O (right). It can be seen that at the same temperature, the contact ion pair interaction follows the same observed order with KCl > NaCl > NaBr > NaI. The interaction strength between anion and O (H₂O) follows Cl⁻ > Br⁻ > I⁻. This is not unexpected since Cl⁻ is the most hydrated whereas I⁻ is the least hydrated. The ability for the anions to form hydrogen bonds with water also follows the same order. The $g(r)$ between salt cation and O (H₂O) is shown in Figure 2-22 (right). Interestingly, the interaction between cation (Na⁺) and O (H₂O) in 1 M NaCl, NaBr and NaI shows that Na⁺ has the strongest interaction with O (H₂O) in NaI solution whereas it has the weakest

interaction in NaCl solution. The pair correlation function between K^+ and O (H_2O) is significantly weaker (not shown). *The same question arises, why the same cation (Na^+) has different interaction strength with water when paired with different anions?*

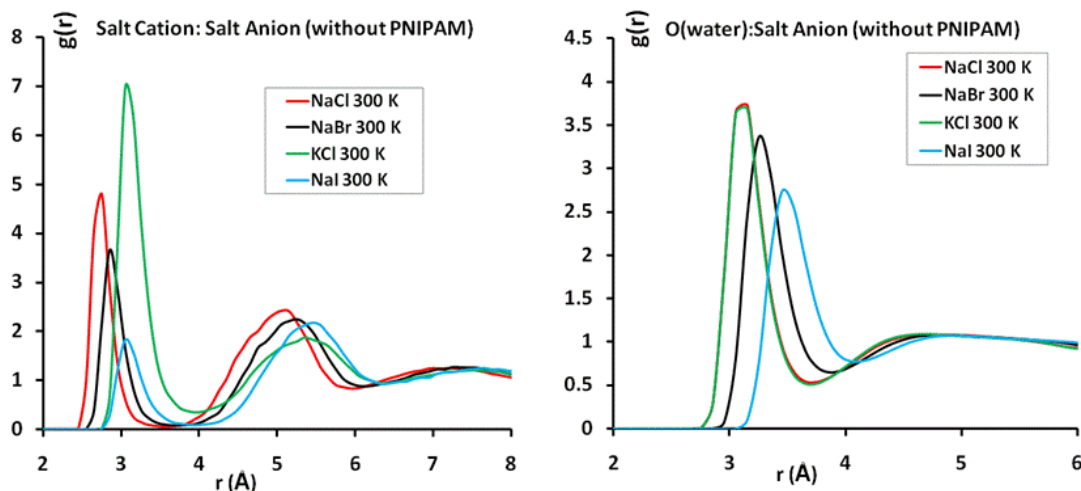


Figure 2-23 Contact ion pair correlation functions in 1 M KCl, NaCl, NaBr and NaI solutions at 300 K (left). The pair correlation functions between anion and O (H_2O) are also shown (right).

The simulation results demonstrate that the binding affinity between the Na^+ and amide group (specifically the amide O) in PNIPAM is affected by the anions. Similar to the interaction between cation and O (H_2O), the binding affinity between Na^+ and amide O in PNIPAM is inversely correlated with the contact pair interaction strength between Na^+ and various anions. The stronger the cation-anion interaction is, the weaker the cation-polymer interaction becomes. This could explain why Na^+ ion in NaI has a stronger association with the amide O in PNIPAM than those of the Na^+ ion in NaCl and NaBr solutions. Moreover, Na^+ at lower temperature tends to bind more strongly with the amide group than at higher temperature as shown in Figures 2-15 and 2-17. This is

partially due to the weaker contact ion pair interaction at lower temperature thus promoting stronger binding of the cation with the polymer. In addition, the polymer adopts a folded structure at higher structure with less exposed surface area. This will decrease the overall binding affinity between cations and the polymer. However, in the case of PNIPAM in 1 M NaCl, it appears that the binding affinity between the Na⁺ and amide O is slightly larger at higher temperature, in contrast to the results observed in the other solutions. This is maybe due to several reasons. For the folded PNIPAM, sites on the surface could exist with several amide O atoms in close proximity. In this case, the binding affinity with the cation will be enhanced for the folded structure. In addition, the higher and lower simulation temperature difference in NaCl is only 12 K, much smaller than other systems (with 40 K in NaBr and NaI, and 30 K in KCl). As a result, the differences in radii of gyration and end-to-end distances are also smaller in NaCl. These additional factors could probably reverse the temperature effect on the binding affinity.

The observation can be used to partially interpret the effects of anion on the LCST of PNIPAM for the series of sodium salts with ΔT shift of LCST from pure water following the Hofmeister series as Na₂CO₃ > Na₂SO₄ > Na₂S₂O₃ > NaH₂PO₄ > NaF > NaCl > NaClO₄ > NaBr > NaNO₃ > NaI > NaSCN. The current simulation results indicate that the stronger the contact pair Na⁺-anion interaction, the weaker the Na⁺ ion's ability to bind with the amide O in PNIPAM. Assuming the presence of the salts (irrespective of the salt type) will decrease the LCST of the polymer to a common temperature due to potentially excluded volume effect³⁷ or the increase of the surface tension due to the presence of salts¹⁰ as suggested by earlier researchers, the interaction of the cations with PNIPAM will increase the PNIPAM's LCST depending on the specific ionic species

present. The stronger the binding between the cation and PNIPAM is, the larger the increase in LCST. The strength of cation-polymer interaction is modulated via the cation-anion interaction in the polymer solution.

2.4. CONCLUSION

The LCST phase transition of PNIPAM in pure water and 1 M NaCl, NaBr, NaI and KCl salt solutions was investigated. It was found that cations have higher affinity with the amide O in the polymer, whereas anions virtually have no association with the polymer. Further, the cation's interaction strength with the polymer is inversely correlated with the cation-anion contact pair association constant. The stronger the cation-anion interaction is, the weaker the cation binds to the polymer. The results can further be used to interpret the shift of LCST for PNIPAM in various sodium salt solutions. Moreover, cations appear to interact directly with protein thus affecting its stability, anions appear to affect protein stability via the cation-anion interaction.

CHAPTER 3 MOLECULAR DYNAMICS SIMULATIONS OF PNIPAM IN MIXED SALT SOLUTION

3.1. INTRODUCTION

After completing the MD simulations of PNIPAM in 1 M NaCl, NaBr, NaI and KCl solutions, the mechanisms for the interactions between the salt ions and PNIPAM were elucidated. The previous results show that cations bind strongly to the amide O on the peptide bond in PNIPAM whereas anions exhibit very weak affinity for the peptide bond as well as on the hydrophobic residues in PNIPAM. In addition, the results show that the association strength between cation and amide O is inversely correlated with the cation–anion interaction strength for the same cation (e.g. Na⁺). Finally it was shown that the Hofmeister order of the salt ions affecting the LCST of PNIPAM could be explained via the direct cation interaction with PNIPAM. The effects of anion on the LCST are modulated via the cation–anion interaction. In order to further investigate the effects of different salts on the LCST of PNIPAM in the same solution, MD simulations of PNIPAM in a mixed salt solution were carried out above and below its estimated LCST. The mixed salt solution is composed of 0.5 M Na⁺, K⁺ and 0.5 M Cl⁻ and Br⁻ with a total salt concentration equivalent to 1 M monovalent salt solutions studied earlier.

3.2. COMPUTATIONAL METHODOLOGY AND SIMULATION DETAILS

MD simulations were also performed using NAMD⁶⁰. The force field parameters of PNIPAM were the same as those for the MD simulations of PNIPAM in different salt solutions. The ionic parameters for each kind of salt ion were also the same as those described in Chapter 2. The MD simulations performed in the mixed salt solution used the same starting structure for simulations of PNIPAM in different salt solutions. The experimental LCSTs of PNIPAM in 1 M NaBr, KBr, NaCl and KCl solution are ~298, 297, 293 and 292 K respectively when the polymer concentration of PNIPAM is 1.4 wt %. The LCST of PNIPAM in a mixed salt solution is estimated to be in the range of 292 K to 298 K with salt ionic concentrations of 0.5 M Na⁺, K⁺, Cl⁻ and Br⁻ each.

The MD simulations of PNIPAM in the mixed salt solution were performed at 278 K below its LCST and 318 K above its LCST for a total of 75 ns each. A total of 22075 water molecules, 200 Na⁺ ions, 200 Cl⁻ ions, 200 K⁺ ions and 200 Br⁻ ions was included in the simulation unit cell. The unit cell contains one PNIPAM chain consisting of 50 NIPAM units with a corresponding PNIPAM concentration of 1.4 wt %. The initial dimension of the unit cell is 90 x 90 x 90 Å³. The simulations were conducted under NPT ensemble with a target pressure of P=1 atm using the Langevin-Hoover scheme⁶⁰. A 12Å sphere cut-off and a 15Å pair list distance were applied to the *van der Waals* and short range electrostatic interactions respectively⁹¹⁻⁹⁸. Long range electrostatic interactions were treated by particle mesh Ewald (PME) method⁶³. The TIP3P water model⁹⁹ was applied to water molecules. The simulations with 1fs time step were performed under periodic boundary conditions.

The radius of gyration of the polymer backbone⁵⁴, the number of water molecules in the first hydration shell of the polymer and the end-to-end distance of the polymer were analyzed by Ptraj¹⁰⁰ in AmberTools 1.2 according to the same protocols for the simulations of PNIPAM in the different salt solutions in Chapter 2.

The pair correlation functions ($g(r)$) between the ions and specific atoms on PNIPAM were evaluated based on the 30 ns simulation period after PNIPAM went through the LCST transition in the mixed salt solution at the higher temperature of 318 K. For the purpose of comparison, MD simulations were also carried out for the mixed salt solution containing only 0.5 M Na⁺, K⁺, Cl⁻ and Br⁻ ions without PNIPAM at the same corresponding temperatures. A total of 1897 water molecules and 17 ions each for Na⁺, K⁺, Cl⁻ and Br⁻ ions were included in the simulation unit cell with the initial cell dimensions of 40 X 40 X 40 Å³. The rest of the simulation parameters were kept the same as those of the mixed salt solution in the presence of PNIPAM. A total of 40 ns simulations were carried out for the mixed salt solution without PNIPAM. Pair correlation functions between the cations and anions in solution were calculated for both systems with and without PNIPAM. Pair correlation functions between the salt ions and the O atom of the H₂O molecules were also evaluated.

3.3. RESULTS AND DISCUSSION

MD simulations of PNIPAM in the 0.5 M Na⁺, K⁺, Cl⁻ and Br⁻ mixed salt solution were carried out at temperatures 318 K above its estimated LCST value and 278 K below the LCST. Figure 3-1 shows the radius of gyration (a) and the number of water molecules

(b) in the first hydration shell of PNIPAM along simulation time in the mixed salt solution at 278 and 318 K respectively.

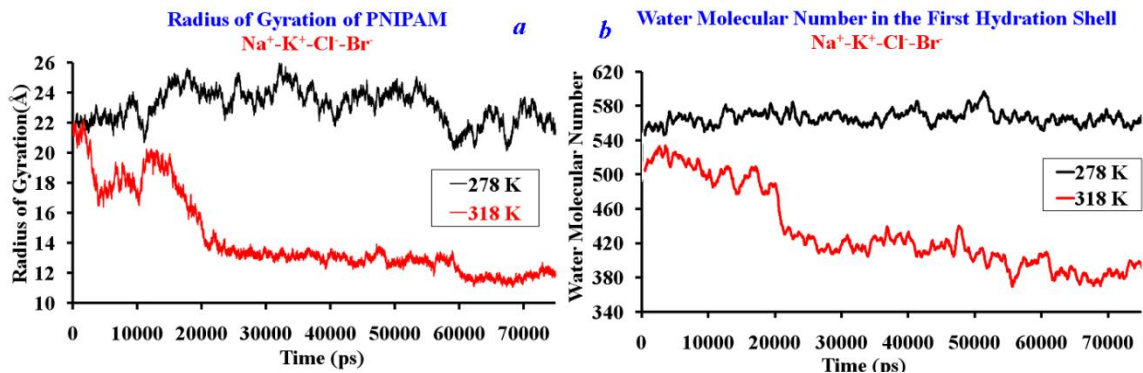


Figure 3-1 Radii of gyration (a) and the number of water molecules in the first hydration shell of PNIPAM (b) in the mixed salt solution above and below its estimated LCST value.

There is a significant decrease of the radius of gyration of PNIPAM along the higher temperature simulation, but not at the lower temperature. A reduction in the radius of gyration of PNIPAM from about 22 Å at the beginning to about 14 Å along the 318 K simulation is observed during the first 20 ns of simulation in the mixed salt solution. After that, the radius of gyration decreases slowly during the last 55 ns of the simulation and reaches the value of about 12 Å at the end. The radius of gyration along 278 K simulation was found to fluctuate at around 22-24 Å remains consistently larger than the corresponding higher temperature value at about 12 Å. There is a significant reduction of the number of water molecules in the first hydration shell of PNIPAM along the higher temperature simulation, in contrast to the observation at lower temperature. The number of water molecules in the first hydration shell of PNIPAM along the higher temperature simulation decreases from about 560 at the beginning of the simulation to about 380 after

60 ns of simulation. After that, the water molecule number fluctuates in the range of 380-400 till the end of the simulation. However, the number of water molecules in the first hydration shell of PNIPAM is observed to fluctuate in the range of 550-570 throughout the entire simulation period at the lower temperature. Figure 3-2 shows the end-to-end distances of the polymer along both temperature simulations. Along the higher temperature simulation, the end-to-end distance decreases dramatically from the beginning at around 70 Å to about 40 Å after about 20 ns of simulations. It then fluctuates at around 40 Å for the remaining 55 ns of the simulation. At the lower temperature, the end-to-end distance fluctuates between 70-80 Å from the first 55 ns of simulation time. Then it decreases to about 60 Å and then fluctuates in the range of 60-70 Å till the end of the simulation.

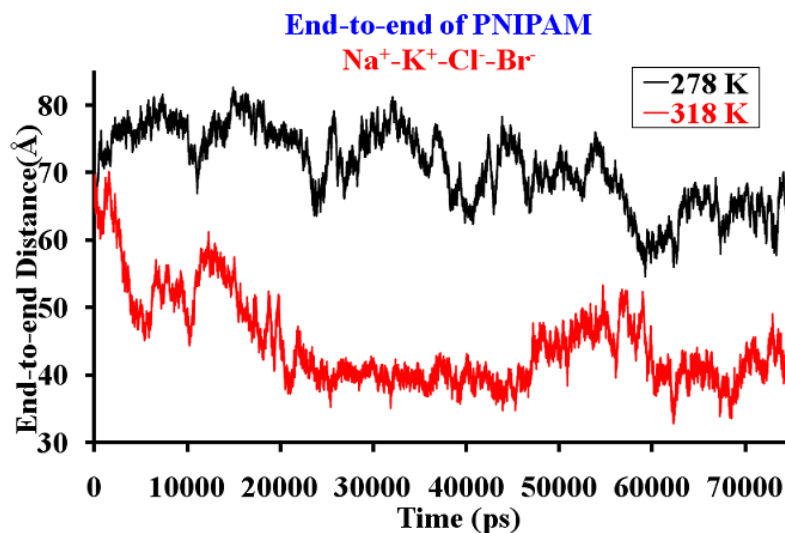


Figure 3-2 The end-to-end distances of PNIPAM along MD simulations in 1 M mixed salt solution at 278 K and 318 K respectively.

Figure 3-3 shows the conformations of the polymer after 75 ns of simulations at 278 K (a) and 318 K (b) respectively. It can be seen that the final conformation of PNIPAM (Figure 3-3a) remains extended at 278 K whereas the conformation of PNIPAM (Figure 3-3b) becomes folded at 318 K after the LCST phase transition.

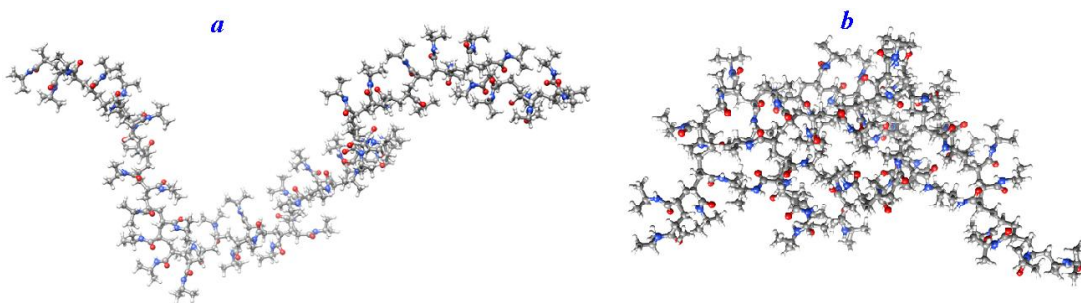


Figure 3-3 The conformations of PNIPAM after the 75 ns simulations in 1 M mixed salt solution at 278 K (a) and 318 K (b) respectively

The numbers of H-bonds⁸⁵ were also determined including the intra-chain H-bonds within PNIPAM and inter-molecular H-bonds between the O, N atoms in PNIPAM and the water molecules. The variations of the number of H-bonds along the simulations at both temperatures are shown in Figure 3-4. The criterion used to determine whether a hydrogen bond exists or not is the same as that used in the earlier studies. The hydrogen bond length cut-off between the two heavy atoms ($A \cdots H-B$) is 3.5 Å, and the cut-off for the hydrogen bond angle ($\angle A \cdots H-B$) is 130°, where A and B are heavy atoms (O or N). As shown in Figure 3-4, the number of intra-chain H-bonds remains more or less the same for the PNIPAM simulation carried out at 278 K in the mixed salt solution. The number of H-bonds fluctuates at around 4 throughout the 75 ns simulation time. This is easy to understand since the conformation of the PNIPAM remains extended during the

course of the simulations. For the PNIPAM simulation carried out at 318K, the number of H-bonds increases from the initial 2-5 to about 6-8 at the end of 75 ns simulations. The enhanced intra-chain hydrogen bonding interaction is caused by the folding of the PNIPAM chain after it goes through the hydrophilic to hydrophobic LCST phase transition.

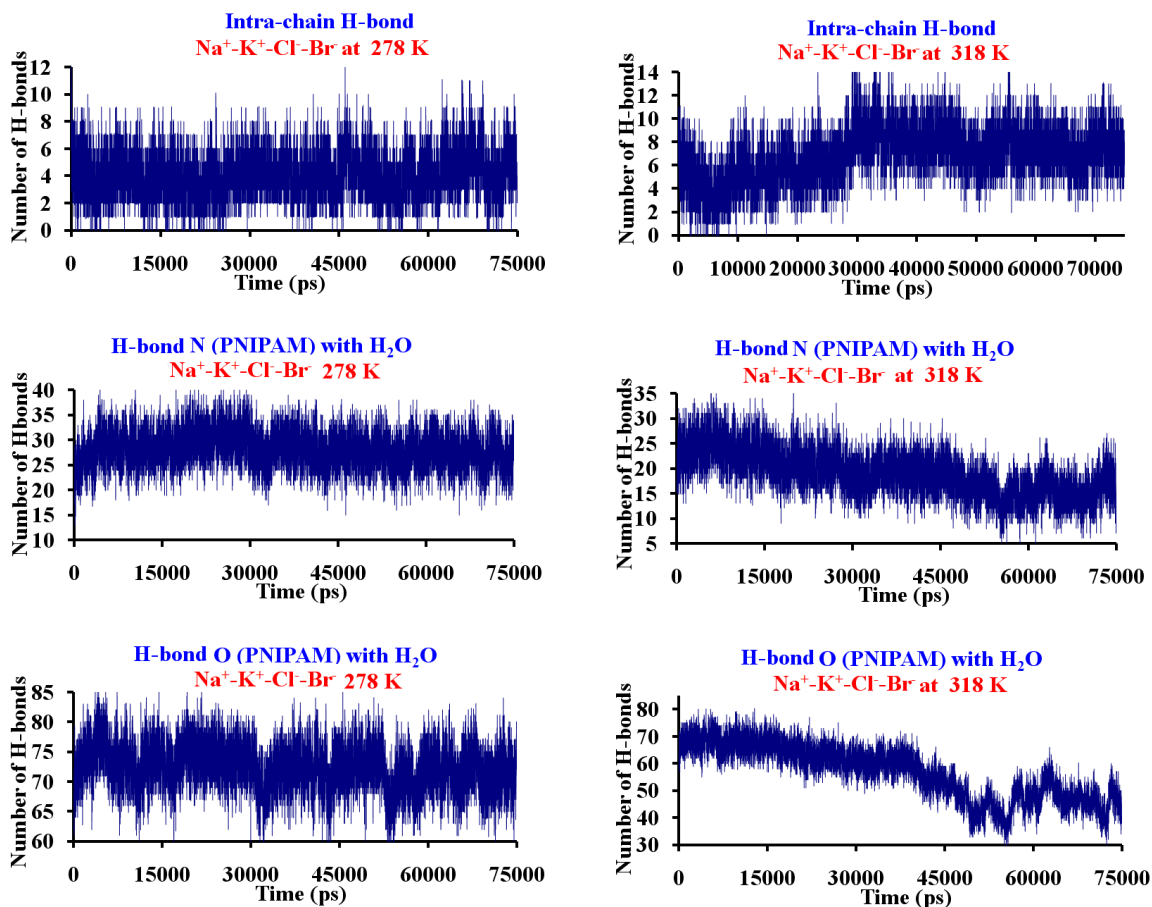


Figure 3-4 The number of H-bonds during the course of MD simulations for PNIPAM in 1 M mixed salt solution at 278 K (left) and 318 K (right)

The intermolecular hydrogen bonding interaction exhibits a similar trend to the ones for PNIPAM in 1 M various salt solutions. The number of H-bonds between the

amide N and the water molecules fluctuates around 25-30 for the entire simulation period at lower temperature where the conformation of the polymer remains in an extended hydrated state. However, the number of H-bonds formed between the amide N and water decreases sharply from about 25 at the beginning to about 10-15 after 75 ns of simulation at higher temperature. This is undoubtedly due to the conformation change of PNIPAM after the LCST phase transition. The increased intra-chain hydrogen bonding interaction is accompanied by the reduced intermolecular hydrogen bonding interaction. The number of H-bonds between the amide O and water demonstrates very similar behavior as shown in Figure 3-4. However, it is worthwhile to point out that the number of hydrogen bonds formed between the amide O and water is significantly higher than that between amide N and water. As a result, the reduction in the H-bonds at higher temperature is much larger from 70 at the beginning of the simulation to about 40 at the end of the 75 ns simulation.

The pair correlation functions $g(r)$ between the polymer and salt ions were calculated after the LCST phase transition at higher temperature was observed and the systems reached quasi-equilibrium state. The pair correlation functions were averaged for the simulation period between 24 to 54 ns. Figure 3-5 shows the pair correlation functions between the amide O and salt ions, between the amide N and salt ions, and between the amide C and salt ions at temperatures above and below its estimated LCST. For the pair correlation functions between the amide O atoms and the cations (Na^+ and K^+), two peaks at 2.3 Å and 2.8 Å were observed for Na^+ and K^+ respectively indicating direct contact binding between the O atoms and the cations (shown in Figure 3-5a). Both kinds of cations show a relative high affinity with the amide O. The magnitudes of the first peaks on $g(r)$ are larger at higher temperature than at lower temperature indicating

stronger binding at 318 K. This is in contrast to the trend observed for PNIPAM in 1 M NaBr, NaI and KCl salt solutions. However, the phenomenon of higher binding affinity at higher temperature agrees with the previous results for PNIPAM in 1 M NaCl solution. The effects of temperature on $g(r)$ will be discussed in more detail later in the chapter. Further from Figure 3-5, it appears that Na^+ has a stronger interaction with the amide O than the K^+ ion in agreement with the previous observations. The previous results show that the cation interaction with the amide group on PNIPAM is modulated by the cation–anion interaction. For the $g(r)$ factors between the salt anions and amide O shown in Figure 3-5b, only small and broad peaks at around 4.5 Å and 4.8 Å were observed for amide O $\cdots\text{Cl}^-$ and amide O $\cdots\text{Br}^-$ interactions respectively. This indicates that the interactions of the salt anions with the amide O are significantly weaker compared to those of the amide O \cdots cation interactions. The interaction between amide O and Br^- is slightly stronger than that between amide O and Cl^- . This again agrees with the earlier observation that the more polarizable the anion is, the stronger the interaction will be. Interestingly, the effects of temperature on interactions between the amide O and anions appear to be quite different from those between the amide O and cations. Here a slightly enhanced binding is observed at the lower temperature compared to binding at higher temperature. The results presented here agree well with the ones from PNIPAM in 1 M various salt solutions. The cations bind strongly to the amide O, whereas anions only exhibit very weak hydrophobic interactions with the amide O.

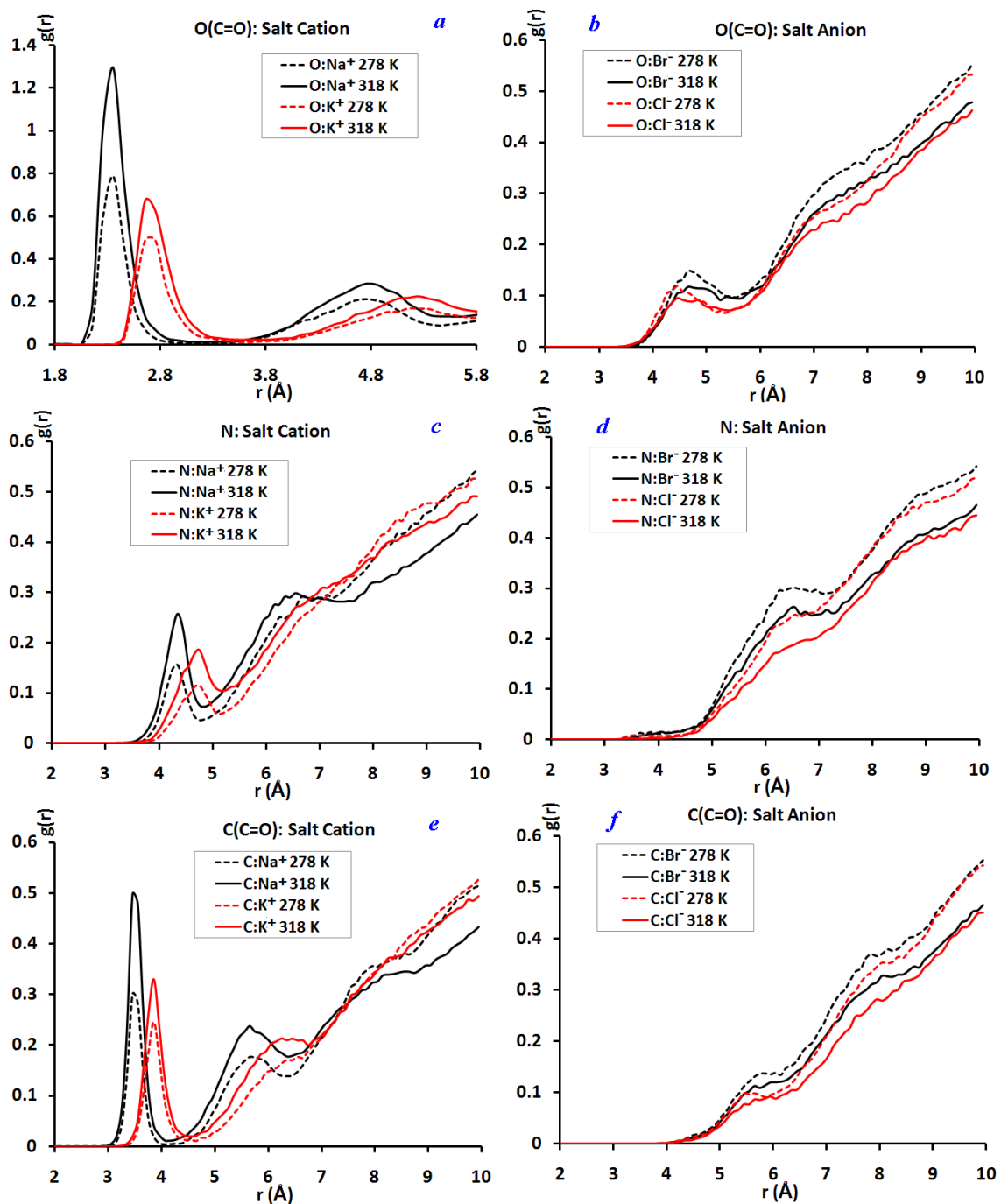


Figure 3-5 Pair correlation functions between the O, N, C atoms on the amide group and the cations, anions of the salt solutions with PNIPAM.

The pair correlation functions between the salt ions and amide N, C show very similar trend as was observed in the previous results in different salt solutions. For the

pair correlation functions between the amide N atoms and the cations, peaks at 4.2 Å and 4.8 Å were observed for amide N ··Na⁺ and amide N ··K⁺ interactions respectively (shown in Figure 3-5c). Both kinds of cations exhibit much weaker correlation with amide N at both temperatures compared to the amide O ··cation interaction. As was discussed in Chapter 2, the amide N ··cation correlation arises from the direct binding of the cations with the amide O. It appears that cations do not bind directly with the N atoms in PNIPAM because the first peaks on the amide N··Na⁺ or amide N ··K⁺ g(r) functions are located at around 4.2 Å or 4.8 Å respectively. The observed amide N ··cation correlation comes from the proximity of the N atom to the amide O as was discussed in detail in Chapter 2. Neither do the anions appear to interact directly with the amide N as shown in Figure 3-5d. The correlation appears to be stronger at higher temperature than at lower temperature in agreement with the amide O ··cation interaction. The interactions between the amide N and anions are even weaker than the interactions between the amide O and anions again in agreement with previous results. It is distinctive that lower temperature exhibits a slight enhanced correlation for the amide ··anions interaction compared to the higher temperature one. For the pair correlation functions between the amide C and cations, peaks at 3.4 Å and 3.8 Å were observed for amide C ··Na⁺ and amide C ··K⁺ interactions respectively as shown in Figure 3-5e. Both kinds of cations show stronger correlation with the amide C than that between the amide N and cations, but significantly lower than that between amide O and cations at both higher and lower temperatures. Further, it appears that cations do not bind directly with the C atoms on PNIPAM either because the first peaks on amide C··Na⁺ or amide ··K⁺ g(r) functions are located at around 3.4 Å or 3.8 Å respectively. The Na⁺ ion demonstrates higher

correlation with the amide C than that between amide C and K^+ . The amide $C\cdots Na^+$ distance is about the distance of amide $O\cdots Na^+$ plus the $C=O$ bond length of about 1.2 Å. All this again indicates that the first peak in the $Na^+\cdots C(C=O)$ correlation function arises from the binding between Na^+ and amide O as was discussed in more detail earlier. The anions do not appear to bind at all to the amide C atoms, even though the amide C has large positive charge and anions are negatively charged. The interactions between the amide C and anions are similar to those between the amide N and anions. It also appears that the amide C and salt anion interaction is weaker than the corresponding amide O and anion interaction. Moreover, based on the $g(r)$ factors between the amide C or N and O (H_2O) which exhibit a first peak at around 3.7 or 3.1 Å respectively as shown in Figure 3-6, the first peaks in $g(r)$ factors between the C or N and Na^+ or K^+ correlations cannot come from their indirect binding with a water molecule mediating their interactions. After the structure of PNIPAM and its surroundings was examined, it was found that the correlations between the amide C or N and cations appear to arise indirectly from the interaction between amide O and Na^+ . Since the distance between O and N in an amide bond is observed to be approximately 2.3 Å and the $O\cdots Na^+$ binding distance is about 2.3 Å, the interaction distance at around 4.0-4.6 Å for the amide N and Na^+ interaction is expected. Similarly, the interaction distance between the amide N and K^+ interaction is expected at around 4.5-5.1 Å; the interaction distance between the amide C and Na^+ interaction is expected to be around 3.3-3.5 Å; and the interaction distance between the amide C and K^+ interaction is expected to be around 3.7-3.9 Å. Moreover, the first peak of $g(r)$ as shown in Figure 3-7 between the oppositely charged amide N and H (H_2O) appears at around 3.7 Å. This indicates that amide N-H only acts as a proton donor for

the N··O (H₂O) hydrogen bonds formed. For the pair correlation functions shown in Figures 3-6 and 3-7, it appears that lower temperature has a stronger correlation in agreement with the interactions between the anions and the amide group. All in all, the results agree with earlier theoretical^{46,47,50,78} and experimental⁸⁶ studies suggesting that cation-protein interaction has a significant impact on protein stability.

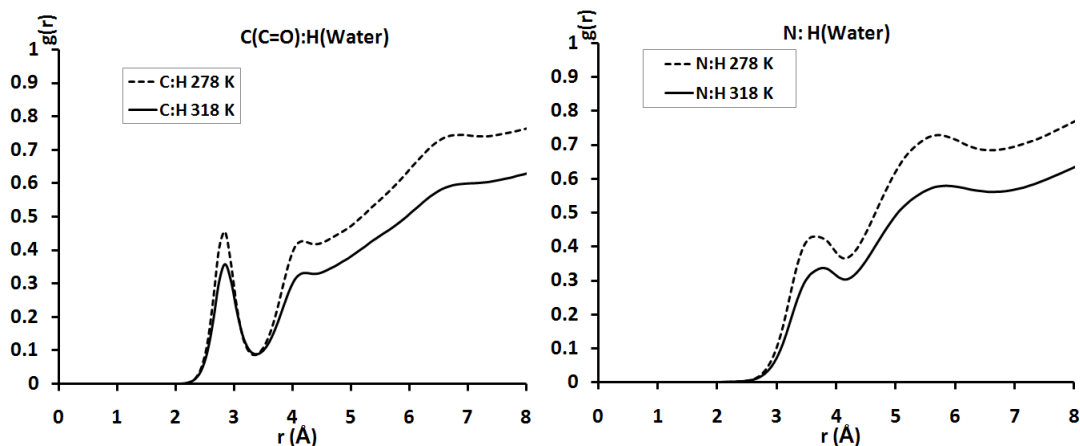


Figure 3-6 Pair correlation functions between the C, N atoms on the amide groups and O atoms on water molecules.

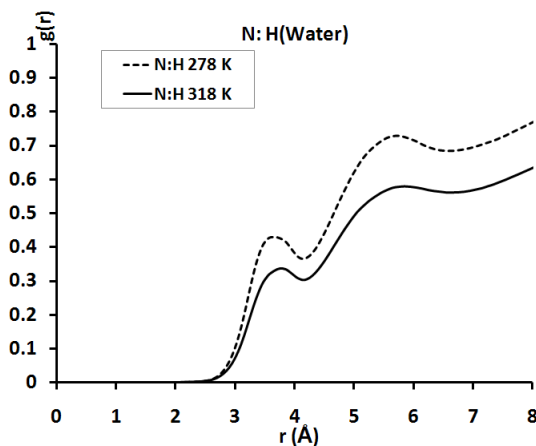


Figure 3-7 Pair correlation functions between the N atoms on the amide groups and H atoms on water molecules.

Figure 3-8 shows the pair correlation functions between the isopropyl C (C5, C6, C7) and cations, anions respectively at 278 and 318 K in the mixed salt solution. The interactions between the isopropyl C5, C6, C7 and cations appear to be rather weak. Though visible, the peaks are very broad and the $g(r)$ factors continue to increase with the increase of the cation...C distance. This indicates that there is no specific interaction mechanism existing between the cations and the isopropyl C atoms. However, the interaction between anion and isopropyl C also shows interesting trends similar to the trends discussed in Chapter 2. Both isopropyl C5 and C6, C7 atoms appear to interact relative strongly with the anions, particularly with Br^- compared to the interaction with the cations. Moreover, the oppositely charged C5 and C6, C7 exhibiting similar interaction strengths with the anions mean that charge plays a minor role here. The interaction between Br^- and isopropyl group is slightly stronger than that between Cl^- and isopropyl group in accordance with the hydration free energies of the anions. The more hydrated Cl^- has a weaker binding with the hydrophobic isopropyl groups whereas the less hydrated Br^- has a stronger binding. The slight larger binding distance observed between C5 and anion is probably due to the location of the C5, which it is not easily accessible. These results agree well with the results shown in Chapter 2. The only difference is that temperature effects on the pair correlation functions between the cations and isopropyl C atoms in the mixed salt solution appear to be opposite to the earlier results in various individual salt solutions. This will be discussed further in more detail later.

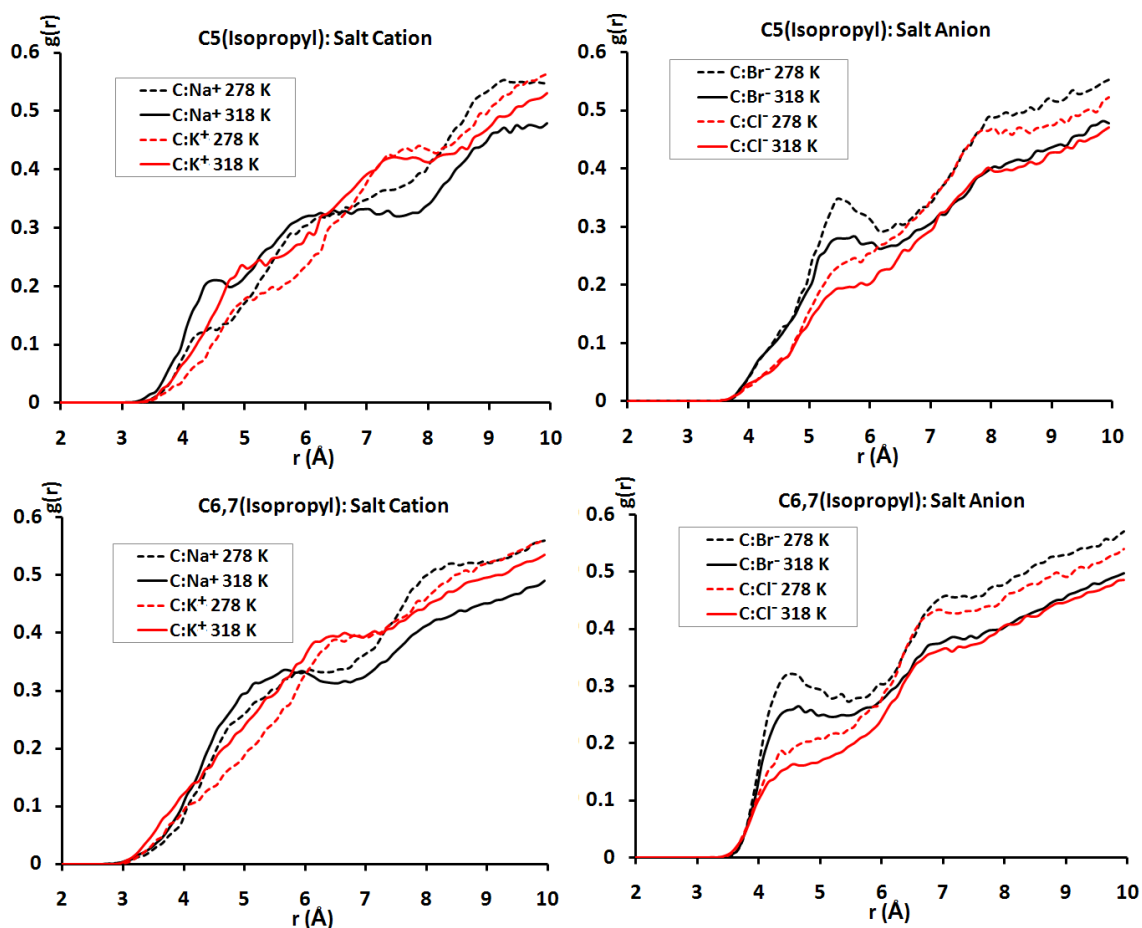


Figure 3-8 Pair correlation functions between the C atoms on the isopropyl group of PNIPAM and the salt ions (cations on left panel and anions on right panel) in the 1 M mixed salt solution.

Figure 3-9 shows the $g(r)$ factors between the C atoms (C1 and C2) on the backbone of PNIPAM and salt ions (cations and anions) at 278 and 318 K in the mixed salt solution. A broad peak located at around 4.7 Å was observed for the backbone C \cdots Na⁺ interactions, and a broad peak located at around 5.0 Å was observed for the backbone C \cdots K⁺ interactions in the mixed salt solution. It is consistent with the fact that K⁺ has a larger radius than the Na⁺. In addition, Na⁺ exhibits the stronger correlation with the backbone C than the K⁺ at both higher and lower simulation temperatures. Moreover,

the magnitude of the peak at higher temperature appears to be larger than the corresponding lower temperature one in agreement with the pair correlation functions between the cations and amide group observed. The anions appear to have very weak affinity with the backbone C atoms for both Br⁻ and Cl⁻ ions. The lower panel of Figure 3-10 shows the calculated pair correlation functions between the backbone C1, C2 and O (H₂O). Since the closest interaction distance between the backbone C and water is located at around 3 Å and above, the correlation distance observed at around 4.5-5 Å between the cations (Na⁺ and K⁺) must come from the correlation between the cations and amide O since the cation ··O direct interaction distance is close to 2.3 Å for Na⁺ ion and 2.8 Å for the K⁺ ion. The weak correlation observed between the cation and backbone C is due to the proximity of the backbone C2 atom to the amide O. The temperature effects on the pair correlation functions are also consistent with the phenomenon observed between the amide O and cation interactions. The temperature effects on the pair correlation functions between the backbone C and water show the opposite trend. That is an additional confirmation that the correlation between the backbone C and cation is not mediated by the water molecules.

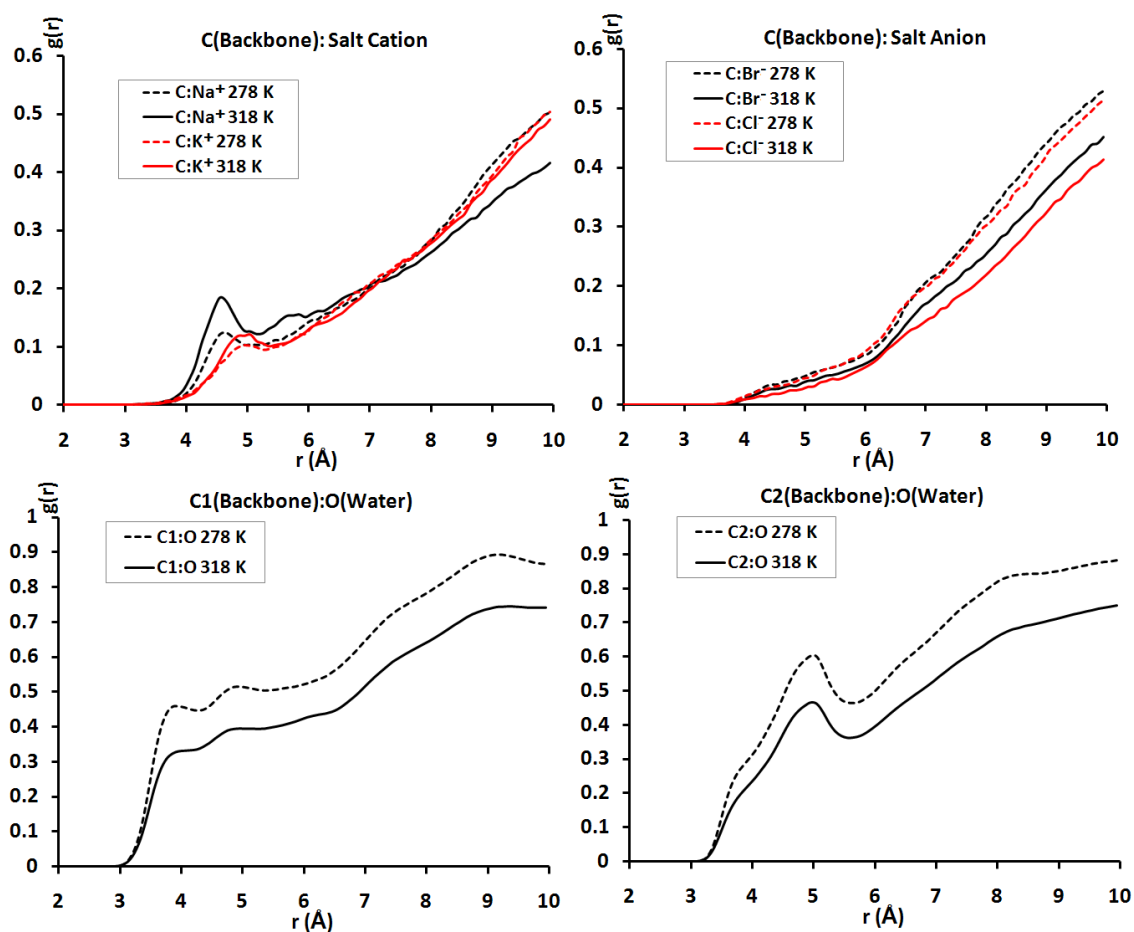


Figure 3-9 Pair correlation functions between the backbone C atoms (C1 and C2) in PNIPAM and the salt ions in the mixed salt solution (upper panel); the pair correlation functions between the backbone C1, C2 and the O atom in H₂O (lower panel).

The effects of temperature on the pair correlation functions are rather perplexing. On the one hand, the $g(r)$ s between cation and amide O show that higher temperature tends to increase the cationic affinity to amide group than the corresponding lower temperature one in the mixed salt solution investigated here. On the other hand, the affinity between the anions and the amide group is generally very weak. Nevertheless, it appears that lower temperature tends to have a higher affinity. The pair correlation

functions between the C atoms on the backbone as well as the isopropyl group and the salt ions exhibit the same behavior with opposite temperature effects. In addition, other pair correlation functions between the atoms on the amide group and water show that lower temperature generally improves the binding affinity. This is understandable since higher temperature tends to weaken chemical, physical and hydrogen bonding interactions between the atoms. The fact that cationic affinity with the amide group for PNIPAM in mixed salt solution increases when temperature increases is puzzling, particularly the earlier simulations in 1 M NaBr, NaI and KCl show the opposite trend. However, the earlier results for the affinity between Na^+ and amide O also show that higher temperature appears to increase the cationic binding.

In order to elucidate the true nature of the effects of temperature on cationic and anionic binding affinities, the structures of the PNIPAM were examined at both higher and lower temperatures, and before and after the LCST transition at higher temperature. The distances between the salt cations close to the PNIPAM chain and the neighboring amide O were calculated. It was found that one cation simultaneously binds two neighboring amide O atoms at higher temperature after the LCST phase transition when the PNIPAM chain is in a folded dehydrated state as shown in Figure 3-10. At lower temperature when the PNIPAM chain is in an extended hydrated state, simultaneous binding of two amide O atoms by the cation was not observed. As shown in Figure 3-10, one Na^+ ion binds to two amide O atoms, where the distance (a) between Na^+ and one amide O is 2.34 Å and the distance (b) with another amide O is 2.37 Å. It is reasonable to expect that the collapsed PNIPAM structure after LCST phase transition during higher temperature simulation will have neighboring NIPAM units close to each other thus

promoting binding of the one cation to multiple amide O atoms. Due to this enhanced interaction at higher temperature caused by multiple binding, the pair correlation functions at higher temperature will exhibit higher affinity. Since anions do not bind directly to the PNIPAM chain at either temperature, their interaction is guided by the more normal temperature effects where lower temperature improves the interaction strength. In addition, lower temperature will have less disorder in the system therefore more pronounced correlation is expected.

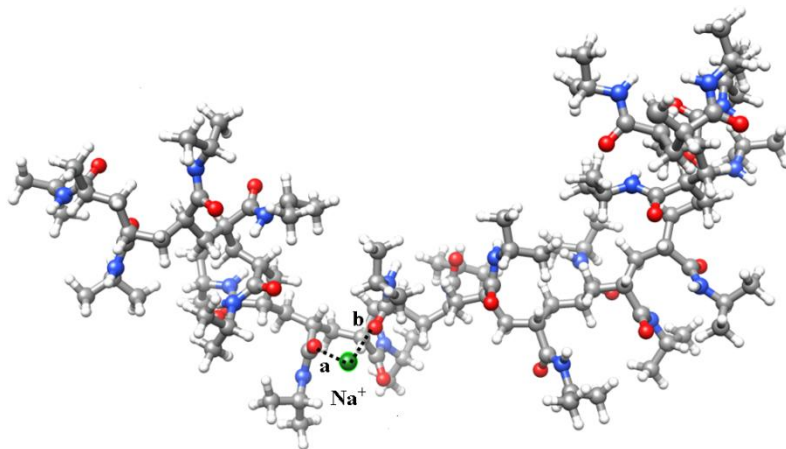


Figure 3-10 The Na^+ binds simultaneously to two amide O atoms on PNIPAM after it goes through LCST phase transition at the higher temperature of 318 K. Only part of the PNIPAM chain is shown. The Na^+ ion is shown in green, O atoms in red, N atoms in blue, C atoms in gray and H atoms in light white.

Earlier experimental results show that bulk water structure is not influenced by salt ion in solution^{36,37}. In order to further understand how salt affects the LCST of PNIPAM in the mixed salt solution, salt cation–anion pair correlation functions were calculated both with and without the presence of PNIPAM. In addition, the pair correlation functions between the O atoms in H_2O and salt ions were determined in mixed

salt solutions with and without the presence of PNIPAM. Figure 3-11 shows the cation-anion $g(r)$ functions in the mixed salt solutions simulated above and below the LCST with (left panel) and without (right panel) PNIPAM. The first peaks on the pair correlation functions are contact ion pair peaks which could be observed at 2.7, 2.8, 3.0 and 3.2 Å for the ion pair NaCl, NaBr, KCl and KBr respectively. As with other pair correlation functions, the peak position also indicates the contact ion-pair distance, and the peak height indicates the strength of ion association between cation and anion. The pair correlation functions for the mixed salt solution were evaluated based on the simulation time of 20-40 ns. The results in the mixed solution without PNIPAM show that K^+ and Br^- contact ion pair has the strongest ion association, whereas Na^+ and Br^- ion pair has the weakest ion association for both higher and lower temperatures. The interaction strength follows the order $KBr > KCl > NaCl > NaBr$. The results agree very well with the ion-pair association constants of 0.30, 0.28, 0.12, 0.090 m^{-1} for KBr, KCl, NaCl, and NaBr respectively calculated in aqueous solution using the TIP3P water model⁸⁷. In the simulations of PNIPAM in the mixed salt solutions, there are some changes on the strength of ion association affinity due to the presence of PNIPAM. For example, the height of the first peak of KCl is slightly higher than that of the first peak of KBr in the 318 K simulation with PNIPAM, but the latter is slightly higher in the 318 K simulation of the mixed salt solution without PNIPAM. This is probably affected by the stronger Br^- binding to the PNIPAM than that of Cl^- in the mixed salt solution with PNIPAM. Further, the cation-anion pair interaction is stronger at higher temperature than at lower temperature in agreement with the earlier simulation results in different salt solutions. The pair correlation functions between the salt ions and O atoms on water

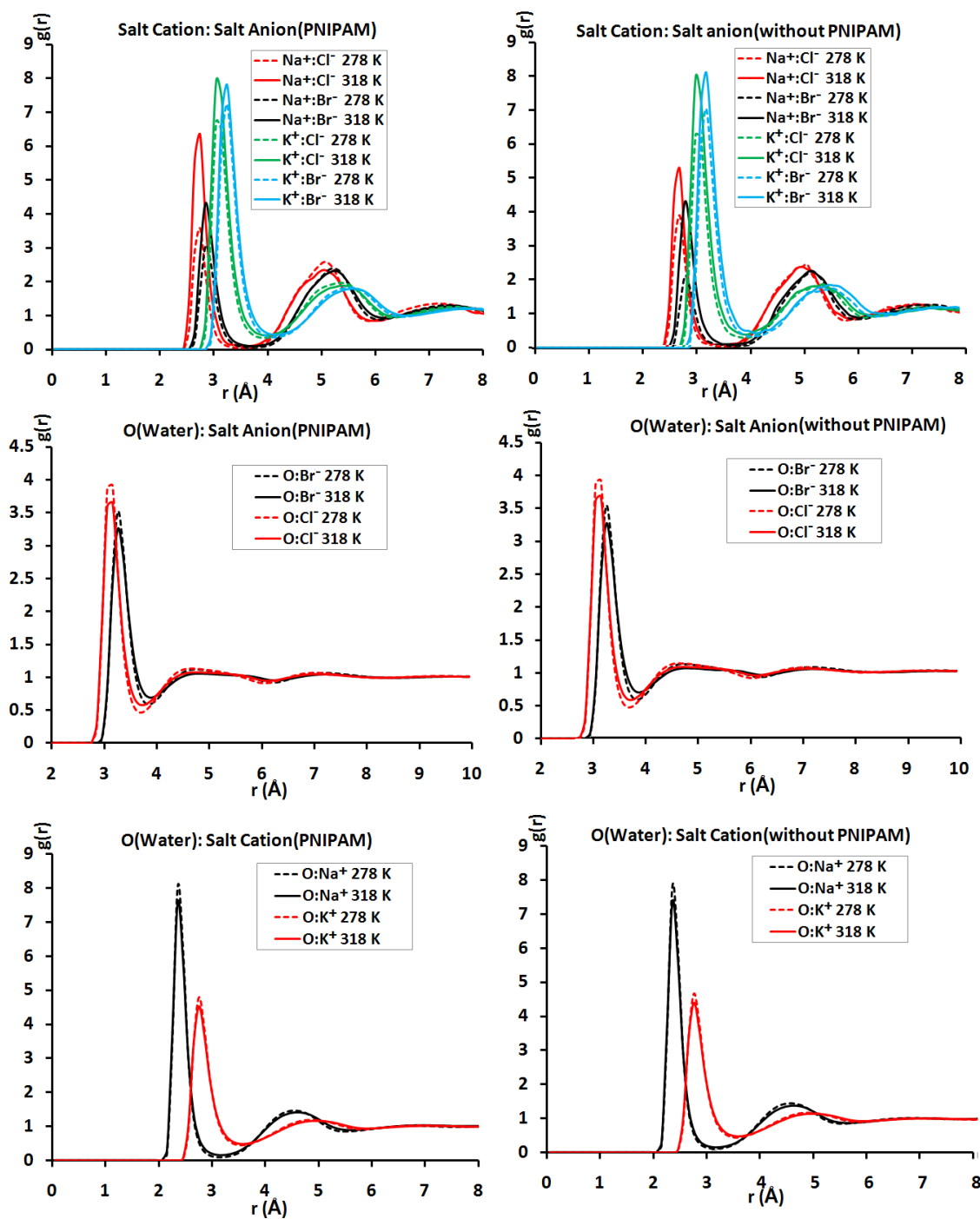


Figure 3-11 Pair correlation functions between cation and anion, between anion and O(water) and between cation and O(water) with and without PNIPAM at both temperatures in the mixed salt solution.

molecules with PNIPAM are very similar to the corresponding ones without PNIPAM for both temperatures. The PNIPAM chain doesn't appear to influence the pair correlation functions between salt ions and water. In addition, pair correlation functions between salt ions and water are stronger at lower temperature than at higher temperature in agreement with earlier results⁸⁸. The effects of temperature on the contact ion pair correlation function were discussed in Chapter 2 and earlier in this chapter. The ion-water interaction is inversely correlated with the cation-anion contact pair interaction for the same salt ion pair at different temperatures. It is due to the relative weaker binding interaction including hydrogen bonding interaction at higher temperature in aqueous solution. This can also be applied to explain the relative higher affinity of salt anions to PNIPAM at lower temperature than that at higher temperature.

The results of pair correlation functions from PNIPAM simulations in mixed salt solutions demonstrate the high affinity between salt cations and the amide group (specifically the amide O) in PNIPAM, especially the affinity of Na^+ is higher than that of K^+ . The cationic affinity with the amide O appears to be inversely correlated with the cation-anion interaction strength in that Na^+ -anion (Cl^- , Br^-) interaction is weaker than that of K^+ -anion. The strength of cation-polymer interaction is modulated via the cation-anion interaction in the polymer solution. The simulation results of PNIPAM at 278 K and 318 K in the mixed salt solution further validated the mechanisms proposed in Chapter 2.

3.4. CONCLUSION

The LCST phase transition of PNIPAM was investigated in the mixed salt solution using MD simulations. Similar to the simulation results of PNIPAM in different salt solutions, it was found that cations have a high affinity to the amide groups of PNIPAM, whereas anions virtually have no association with the polymer. In particular, the affinity of Na^+ to amide group appears to be higher than that of K^+ . Further, cations exhibit higher affinity to amide group of PNIPAM at higher temperature than that at lower temperature due to the multiple binding of the cation to the amide O in a folded PNIPAM structure. This is different from the corresponding results for the simulations of PNIPAM in different salt solutions except in NaCl solution. Many factors affect the binding affinity including the specific cations present, the cation-anion association constant, temperature and the specific conformations of the PNIPAM. The strength of the cation's interaction with the polymer is inversely correlated with the cation-anion contact pair association constant. The stronger the cation-anion interaction is, the weaker the cation's ability to bind to the polymer.

CHAPTER 4 MOLECULAR DYNAMICS SIMULATIONS OF THE LCST PHASE TRANSITION OF PNIPAM-CO-PEGMA IN NACL SOLUTION

4.1. INTRODUCTION

PNIPAM and poly(ethylene glycol) (PEG) have been widely studied as typical thermo-responsive polymers which exhibit volume phase transitions around their LCSTs^{1,7,9,16,101-103}. The LCST of PNIPAM in water is about 305 K (32 °C)¹⁰⁴, which is lower than the body temperature of mammals. The LCST of PEG may vary from 455 K for short chains to 363 K for long chains¹⁰⁵. The volume phase transition of PNIPAM mainly originates from the solvation balance of a hydrophilic amide group on the side chain and a hydrophobic isopropyl group in each NIPAM unit as well as a hydrophobic carbon backbone. The PEG's LCST is much higher than that of PNIPAM due to its much higher hydrophilicity. In order to overcome the limited temperature range of LCST of PNIPAM in aqueous solutions, the derivatives of PNIPAM, especially PNIPAM copolymers¹⁰⁶⁻¹⁰⁸, are investigated with PEGs¹⁰⁹. Veena Choudhary et al.²² investigated PNIPAM-co-PEGMA, a copolymer of PNIPAM and poly (ethylene glycol) methacrylate (PEGMA) for cell culture applications. They demonstrated that the LCST of the PNIPAM-co-PEGMA copolymer varied from 308 K to 312 K in water when they increased the PEGMA content from 1 to 20 wt %. In addition, experiments demonstrated

that salts have a significant impact on the LCSTs of PNIPAM and PEG^{10,32,110}, more significant for the LCST of PEG^{111,112}. In Chapter 2, the effects of salt ions on the LCST of PNIPAM were investigated. The salt ions, particularly anions, appear to follow the so-called Hofmeister series. The MD simulation results show that this order appears to arise from the relative high affinity between the cations and the amide O in PNIPAM. The influence of the anions on the LCST of PNIPAM is modulated by cation-anion interactions in solution.

In order to further test the hypothesis on the effects of salt on LCST of PNIPAM, MD simulations of PNIPAM-co-PEGMA in 1 M NaCl solution were performed above and below its LCST.

Using Leap in AmberTools 1.2, one single chain of the PEGMA-co-PNIPAM copolymer was artificially synthesized so that it contained 38 NIPAM units and 2 PEGMA units, with each PEGMA chain containing 4 ethylene glycols (PEGs) and one methacrylate unit. One PEGMA side chain was located at residue 15 on the carbon backbone of the copolymer, and the other was at residue 30. The force field parameters of NIPAM units in the copolymers were the same as those used for MD simulations of PNIPAM in salt solutions. The atomic charges of PEGMA were also determined using *ab initio* calculations at B3LYP/aug-cc-pvtz//B3LYP/6-311+G(d,p) level with Gaussian 03⁶⁹. Gaussian 03 calculations were carried out to compute the partial atomic charges for the low energy structures⁵². The atom name, atomic types and partial charges of atoms on the PEGMA unit are shown in Table 4-1. The copolymer was pretreated in vacuum to obtain a relaxed low energy structure as the starting structure for MD simulations in 1 M NaCl solution. Figure 4-1 shows the structures of units NIPAM and PEGMA, and the starting

Atom name	Atom type	Partial atomic charge(e)
C11	CT	-0.363904
H111	HC	0.060031
H112	HC	0.060031
H113	HC	0.060031
C12	CT	0.176926
C13	CT	0.079235
H131	HC	-0.036175
H132	HC	-0.036175
C14	C	0.697411
O1	O	-0.429553
O2	OS	-0.267858
C21	CT	0.383474
H211	H1	0.011912
H212	H1	0.011912
C22	CT	0.056419
H221	H1	0.042545
H222	H1	0.042545

O3	OS	-0.541927
C31	CT	0.458147
H311	H1	-0.018780
H312	H1	-0.018780
C32	CT	0.126509
H321	H1	0.021706
H322	H1	0.021706
O4	OS	-0.597388
C41	CT	0.036070
H411	H1	0.049746
H412	H1	0.049746
C42	CT	0.019678
H421	H1	0.049677
H422	H1	0.049677
O5	OS	-0.254594
C51	CT	0.269962
H511	H1	-0.005665
H512	H1	-0.005665

C52	CT	0.217080
H521	H1	-0.011007
H522	H1	-0.011007
O6	OH	-0.793609
H61	HO	0.339911

Table 4-1 Partial charges of atoms in PEGMA calculated with Gaussian 03, here O_x atoms are the O atoms of PEGMA numbered in the following Figure 4-1, C_{xy} atoms are the C atoms associated with O_x, H_{xyz} are the hydrogen atoms bonding to C_{xy}, the order of C_{1y} is from the top to the C atom bonding to O₁, and H₆₁ is the H atom bonding to O₆.

structure of the copolymer for the simulations in which two PEGMA units are shown in green. Force field parameters of PEGMA were taken from Amber 99 force field because they are not available in Amber 94 force field⁵². Based on the LCST of PNIPAM in 1 M NaCl solution and the LCST variation of the PNIPAM-co-PEGMA copolymer with PEGMA content, the estimated LCST of the copolymer should be in the range of 296-300 K in 1 M NaCl solution.

Although *van der Waals* parameters of Na⁺ and Cl⁻ ions are available in the Amber 94 or 99 force fields, recent simulations in high-concentration salt solutions¹¹³ showed that those parameters failed because the ions developed into clusters in the

solutions during the simulations. Improved ionic parameters of Na^+ and Cl^- ions corresponding to the TIP3P water model¹¹⁴ have been adopted in the current work.

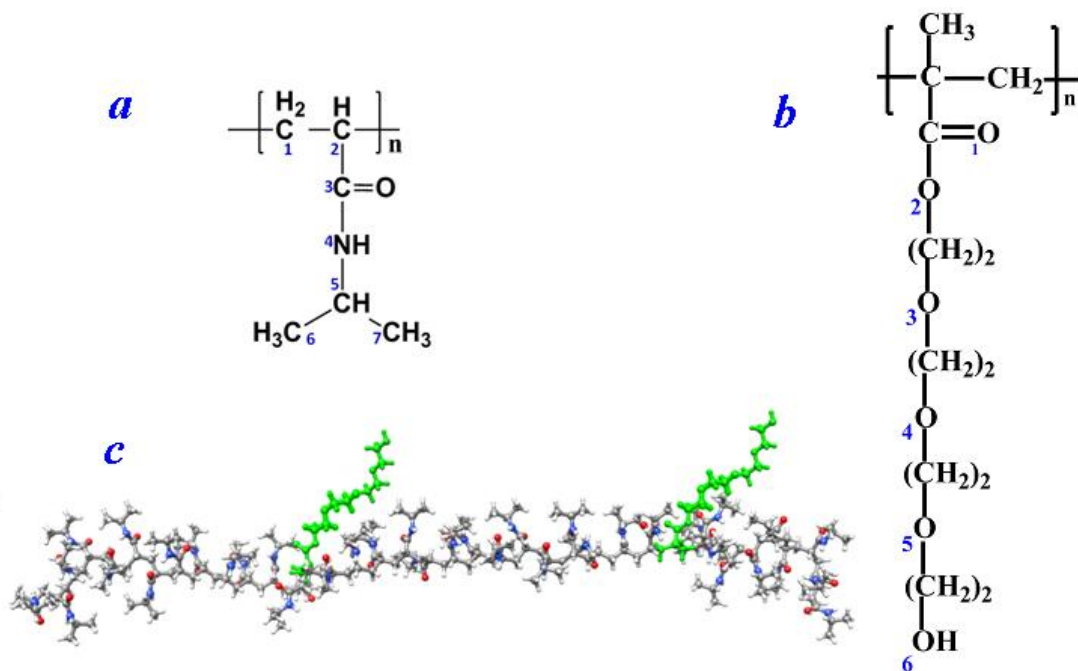


Figure 4-1 The structures of monomer unit NIPAM (a) and PEGMA side chain (b), and the starting structure (c) of the copolymer for the simulations. The atoms are numbered for easy discussion in the text.

Radius of gyration (R_g) of the copolymer's backbone⁵⁴ was analyzed by Ptraj¹⁰⁰ in AmberTools 1.2 according to the following protocol for the simulations. The radius of gyration of the copolymer which shows the time evolution of the conformation change along a simulation, is defined in Equation (4-1) :

$$R_g = \sqrt{\frac{\sum_{i=1}^N m_i (r_i - R)^2}{\sum_{i=1}^N m_i}} \quad (4-1)$$

here r_i and m_i are the position vector and the mass of atom i respectively, and R is the position vector of the centroid of the chosen atoms, identified by the C1 and C2 atoms of NIPAM units in the backbone. The end-to-end distance of the copolymer was also evaluated based on the C1 and C2 atoms on the carbon backbone. The number of water molecules in the first hydration shell was calculated within a distance of 3.5 Å from the surface of the copolymer chain, which represented the first hydration shell of the copolymer.

Four types of hydrogen bonding were analyzed to evaluate the hydrophilic-hydrophobic transition of the copolymer at the lower and higher temperatures. These include intra-chain hydrogen bonding, hydrogen bonding between O or N on NIPAM units and water molecules and hydrogen bonding between the two PEGMA units and water. Pair correlation functions ($g(r)$) between the salt ions and atoms on PNIPAM and PEGMA were evaluated based on a simulation time period from 35 to 55 ns. These atoms on PNIPAM include the amide O, C, N and C5, C6, C7 atoms on the isopropyl group of each NIPAM unit as well as C1 and C2 on the backbone.

4.2. SIMULATION DETAILS

MD simulations were also performed using NAMD⁶⁰. Two simulations of the PNIPAM-co-PEGMA copolymer in 1 M NaCl solution were conducted for 65 ns under NPT ensembles at 278 and 318 K above and below its estimated LCST respectively using the Langevin-Hoover scheme^{66,67}. The pressure is kept at 1 atm. In order to avoid the influences of different dimensions of the simulation box on the polymer chain during MD simulations in 1 M NaCl solution, a cubic water box with a size of 90 X 90 X 90Å³ was generated by VMD⁶¹. A total of 22875 water molecules were used to solvate the copolymer to reach the targeted experimental polymer concentration of 1.4 wt %³². A total of 400 pairs of Na⁺ and Cl⁻ ions were distributed randomly in the water box to achieve the salt concentration of about 0.96 M during MD simulations under 1 atm. The MD simulation of NaCl solution was performed for several ns to equilibrate the system at 300 K. A single PNIPAM-co-PEGMA chain was immersed in the equilibrated salt box by removing the water molecules and salt ions overlapped with the copolymer chain. The obtained NaCl salt solution with the copolymer chain included 22165 water molecules and 400 Na⁺ and Cl⁻ pairs. A 12Å cut-off and a 15Å pair list distance were applied to the short-range *van der Waals* and electrostatic interactions respectively⁹¹⁻⁹⁸. Long range electrostatic interactions were treated using Particle Mesh Ewald (PME) method⁶³. The TIP3P water model⁹⁹ was used for water molecules and the simulations with 1fs time step were constrained under periodic boundary conditions.

4.3. RESULTS AND DISCUSSION

Figure 4-2 shows the conformations of the copolymer at the end of the simulation at 278 and 318 K respectively. The two PEGMA units are again shown in green. It is obvious that the final structure of the copolymer is globular at 318 K after the LCST phase transition, which is much more compact than the corresponding U-shaped conformation at 278 K. Figure 4-3a shows the time evolution of radii of gyration of the copolymer during simulations in NaCl solution at the two temperatures. At higher temperature, the copolymer experiences the LCST phase transition between 8 and 28 ns with R_g decreasing dramatically from about 25 Å from the starting structure to about 10 Å for the final structure. In contrast, at lower temperature the copolymer changes its conformation moderately with R_g decreasing from about 25 Å to 17 Å and a final U-shaped conformation. Figure 3-4b shows the time evolution of the numbers of water molecules in the first hydration shell of the copolymer along the simulations. At 318 K, the number of water molecules in the first hydration shell continues to decrease from 460 at the beginning and reaches about 310 after the LCST phase transition of the copolymer. However, the number of the water molecules remains more or less the same at around 500 at 278 K during the course of simulations.

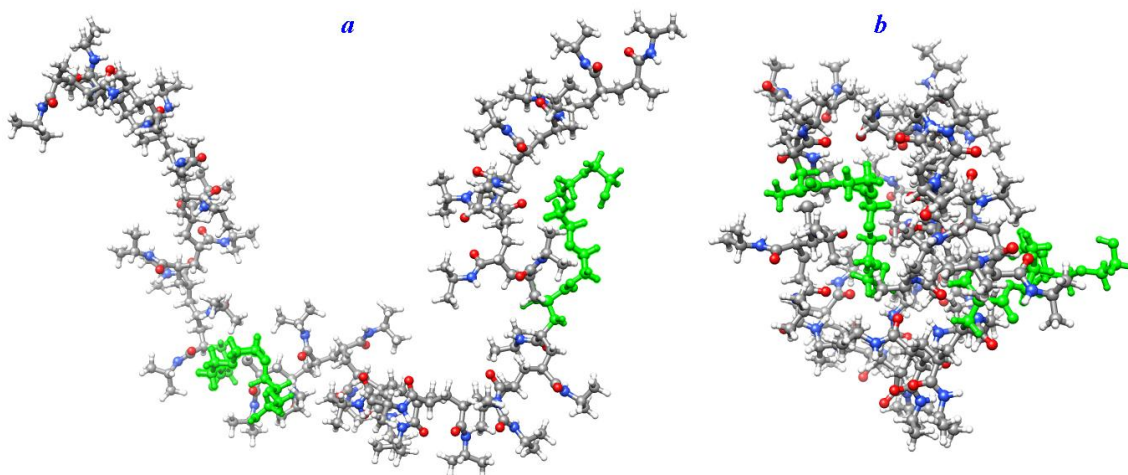


Figure 4-2 The conformations of the PNIPAM -co-PEGMA copolymer after 65 ns of simulations at 278 K (a) and 318 K (b)

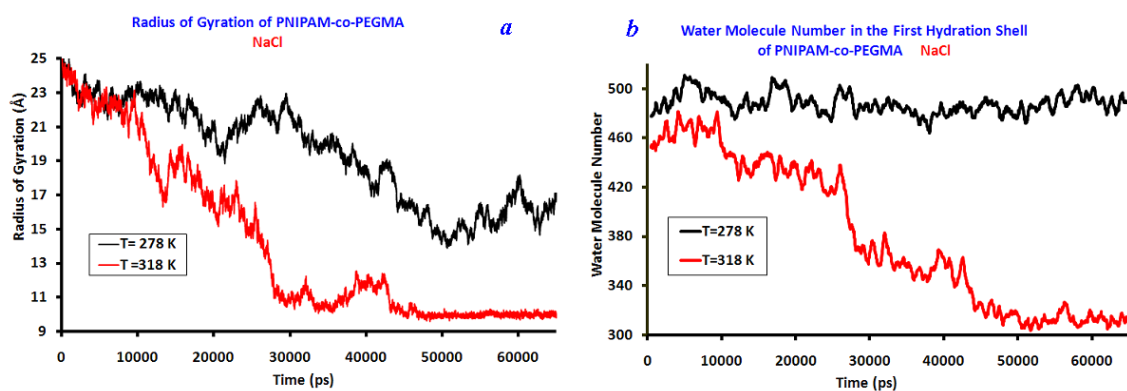


Figure 4-3 Radii of gyration of the PNIPAM -co-PEGMA copolymer (a) and the number of water molecules (b) associated with the first hydration shell of the copolymer in 1 M NaCl solution at 318 K (red line) and 278 K (black line) respectively during the 65 ns MD simulations.

Figure 4-4 shows the time evolution of the end-to-end distances of the PNIPAM-co-PEGMA copolymer at 278 and 318 K along the 65 ns MD simulations. The results show the similar trend to the radii of gyration of the copolymer along the simulations.

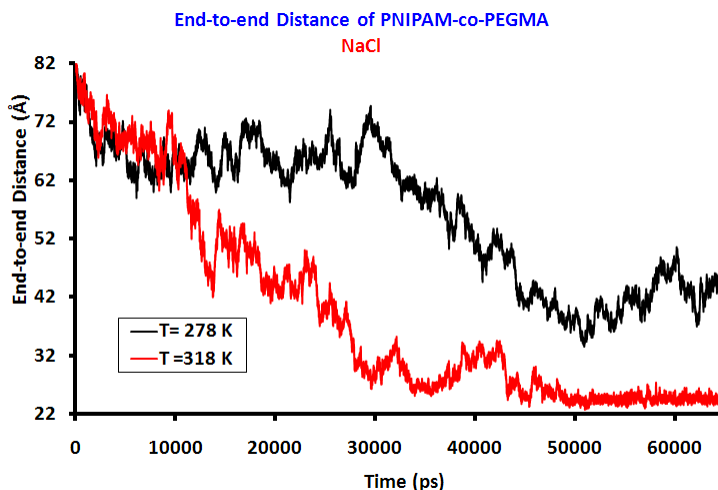


Figure 4-4 End-to-end distances of the PNIPAM-co-PEGMA copolymer at 318 K (red line) and 278 K (black line) during the 65 ns MD simulations.

The number of H-bonds¹¹⁵ were evaluated for the intra copolymer chain, between the N atoms on the NIPAM units and water molecules, between the O atoms on the NIPAM units and water molecules, and between the O atoms on the PEGMA and water molecules (Figure 4-5). The criterion for a hydrogen bond is the same as before with the H-bond length less than 3.5 Å between the two heavy atoms, and the angle is larger than or equal to 130°, where the heavy atoms are O and N on the copolymer and O on water molecules. For the 278 K simulation of the copolymer in NaCl solution, the number of the intra-chain H-bonds fluctuates around 4 during the entire simulation period. However, the number of intra-chain H-bonds increases from about 2-4 to about 6-8 for the simulation conducted at higher temperature of 318 K. This is obviously due to the enhanced intra-molecular interactions in the folded structure. At 278 K, the number of the H-bonds between the N atom in PNIPAM and water molecules fluctuates around 20-25.

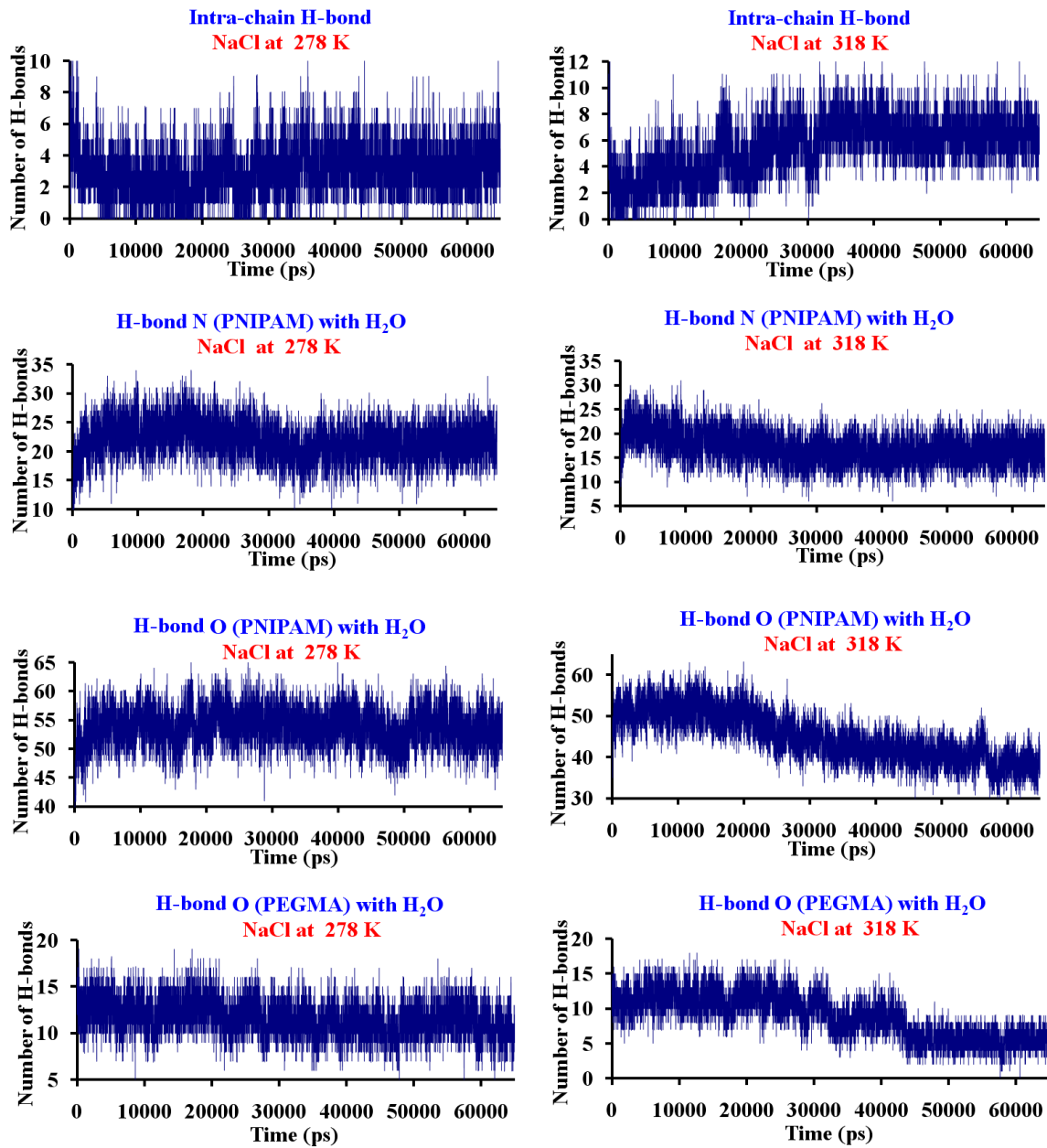


Figure 4-5 Intra-chain hydrogen bonds and intermolecular hydrogen bonds between the copolymer and water during the course of simulations.

At 318 K, the number of H-bonds between the N atoms in PNIPAM and water molecules decreases from 20-25 to around 15-20 during the course of simulations. At 278 K, the number of H-bonds between the O atoms on PNIPAM and water molecules fluctuates at

around 50-55 whereas the number of the H-bonds decreases from 50-55 to about 40-45 at 318 during the course of the simulation period. At 278 K the number of H-bonds between the O on PEGMA and water molecules fluctuates at around 13 whereas this number decreases from about 10-14 to about 4 at the end of the simulation at 318 K. The results for the hydrogen bonding interactions agree with the conformation changes during the course of the simulations at higher and lower temperatures. With a compact folded final structure at higher temperature, an enhanced intra-chain H-bond interaction and a weakened polymer-water H-bonding interaction are expected. When the polymer conformation remains extended at lower temperature, both intra-chain and intermolecular H-bond interactions remain more or less the same.

Pair correlation functions $g(r)$ were evaluated based on the simulation time of 20 ns after the LCST phase transition at 318 K. Figure 4-6 shows the pair correlation functions $g(r)$ between the salt cations, anions and the amide O, N and C on PNIPAM at temperatures above and below the copolymer's LCST. Figure 4-6 top left panel shows the pair correlation functions between amide O and Na^+ . The first peak appearing at about 2.3 Å for both temperatures arises from the direct contact between the amide O on PNIPAM and the Na^+ ion. At the higher temperature, there is a position shift of the first peak to the right and broadening compared to that at the lower temperature. The shift and broadening are significant and it will be discussed later in the chapter. Moreover, it can be seen from the magnitudes of the peaks that Na^+ ion interacts strongly with the amide O on PNIPAM. Higher temperature tends to favor stronger $\text{Na}^+ \cdots \text{O}$ binding. The $g(r)$ factors for the anion $\text{Cl}^- \cdots$ amide O interaction were shown in Figure 4-6 top right panel.

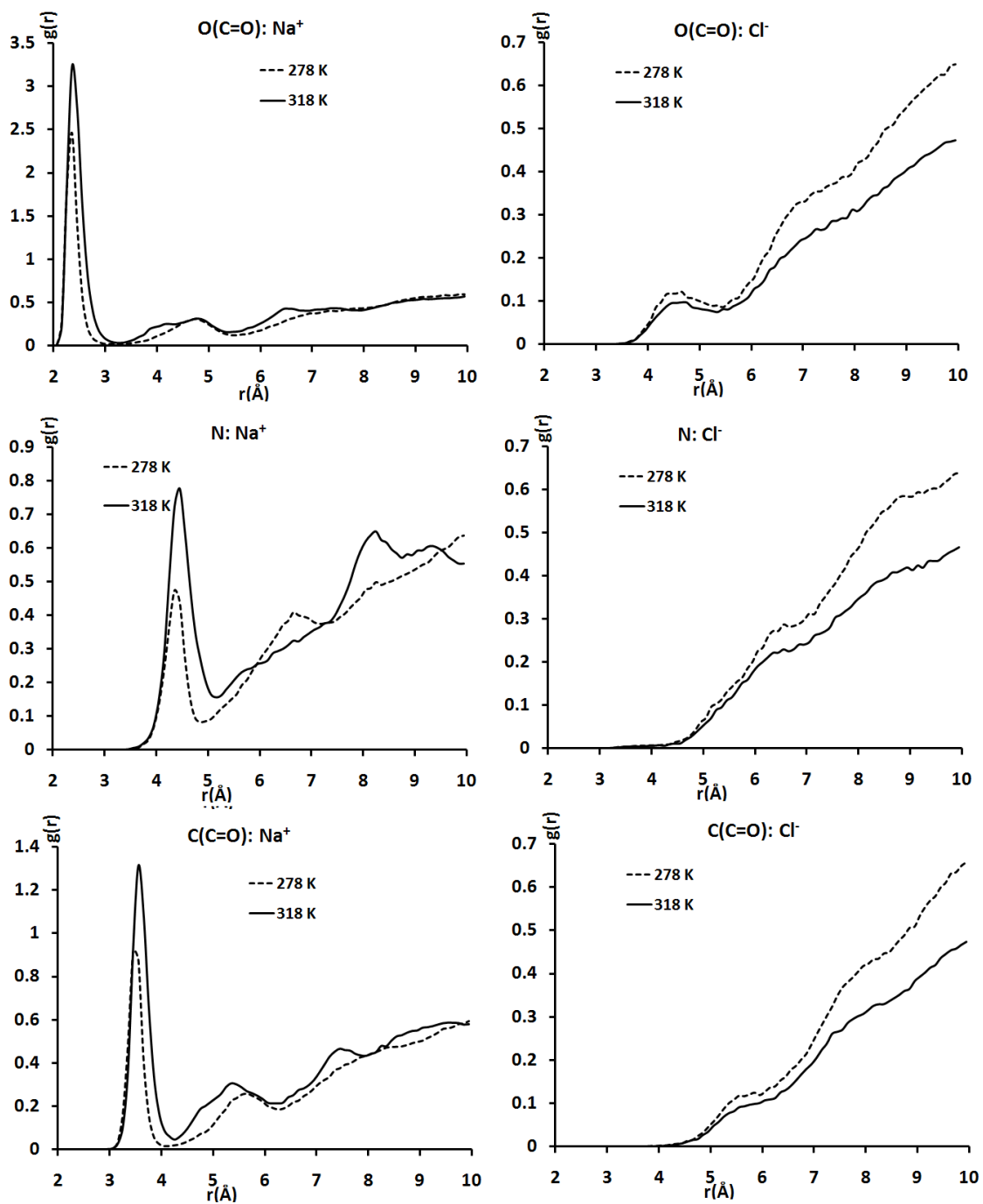


Figure 4-6 Pair correlation functions between amide O, N, C on NIPAM and salt cation (left panel), anion (right panel)

It can be seen that the affinity of Cl^- to the amide O on NIPAM is much weaker compared to that of Na^+ with the first peak appearing at around 4.5\AA . This implies that anions do not bind directly with the amide O on PNIPAM and the interaction between them is significantly weaker than that between Na^+ and amide O. Further, lower temperature tends to favor stronger anion binding in contrast to the cation binding. The pair correlation functions between the amide N, C and salt ions were also determined as shown in the middle and bottom panels in Figure 4-6. The $g(r)$ s appear to be similar to those between the amide O and salt ions. However, the interactions between amide N, C and Na^+ are much weaker than those between amide O and Na^+ . The first peak positions for amide N, C and cation interactions are located at 4.3 and 3.5\AA respectively. It appears that there is no direct binding of Na^+ to the amide N or C atoms. From the conformational structures, it was found that the correlations between the amide N or C and Na^+ come from the direct binding of amide O and Na^+ due to the proximity of the amide N, C and O. The slight peak shift to the right and broadening are also observed for the amide N, C and Na^+ correlations. The interactions between the amide N, C and Cl^- are weak and similar to those between amide O and Cl^- at both temperatures with lower temperature slightly favored.

Compared to the $\text{Na}^+ \cdots$ amide O (N, C) pair correlation functions for PNIPAM in 1 M NaCl salt solutions presented in Chapter 2, the magnitude of the first peak in the copolymer solution at both lower and higher temperatures is much higher than the corresponding peak for PNIPAM in NaCl solutions. This peak broadening and shift at higher temperature will be discussed later in the chapter in more detail.

Figure 4-7 shows the pair correlation functions between the salt ions and the isopropyl C5, C6, C7 or backbone C on PNIPAM. The C5 $\cdot\cdot\text{Na}^+$ pair correlation functions shown in the top left panel in Figure 4-7 exhibit a relatively pronounced peak at around 4.3 Å, particularly at higher temperature. However, the magnitudes of the peaks are much weaker than the corresponding amide O $\cdot\cdot\text{Na}^+$ peaks as well as the amide C, N $\cdot\cdot\text{Na}^+$ peaks indicating much weaker interaction. Similar to the case of PNIPAM in various salt solutions investigated earlier, the C5 $\cdot\cdot\text{Na}^+$ correlation arises from the direct binding between Na^+ and amide O. Examining the structures of the copolymer conformations at 278 and 318 K during the last 20 ns of simulations, there is no evidence to suggest that there exists any direct contact binding between isopropyl C5 and Na^+ . Further, the large peak positions at 4.3 Å indicate the correlation is probably mediated via other atoms. Similar to the earlier findings, the C5 $\cdot\cdot\text{Na}^+$ correlation is due to the close proximity between the C5 atom and the amide group. However, the temperature effects on the $g(r)$ factors show an opposite trend compared to earlier studies. It was found consistently that the cation $\cdot\cdot$ copolymer interaction appears to be stronger at higher temperature with the stronger correlation. This will be discussed in more detail later in the chapter. The same phenomenon was observed from the pair correlation function between backbone C and Na^+ shown in the middle left panel in Figure 4-7. The relatively sharp first peak arises from the close proximity between the C2 atom and the neighboring amide group. The weak affinity between the cation and the hydrophobic backbone and isopropyl group can be further demonstrated by inspecting the pair correlation functions between the isopropyl C6, C7 and the Na^+ ion shown in the middle panel of Figure 4-7. There are no pronounced peaks on the plotted $g(r)$ functions. Further,

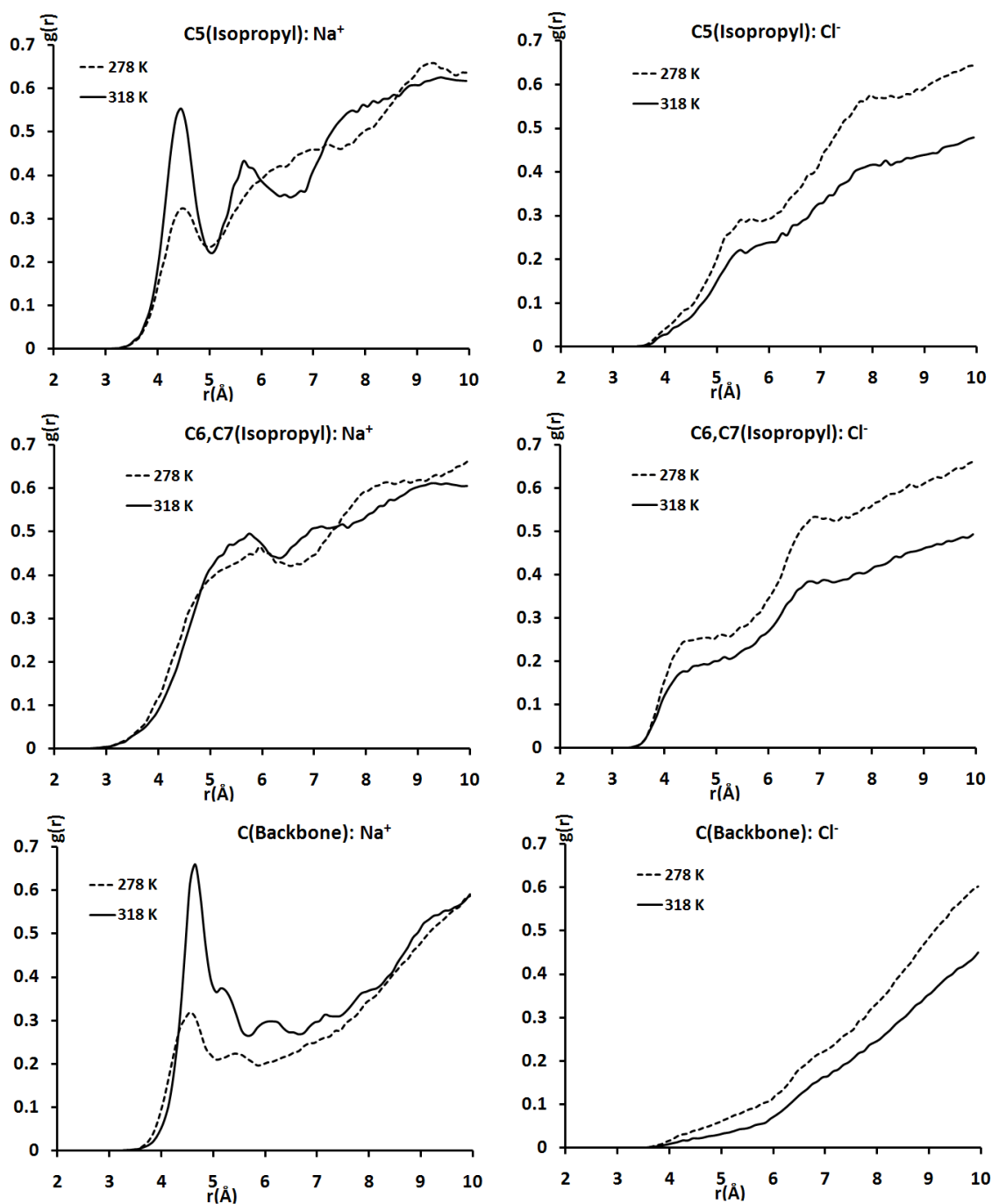


Figure 4-7 Pair correlation functions between isopropyl C5, C6, C7, backbone C on PNIPAM and the salt cation (left panel), salt anion (right panel).

the $g(r)$ function only becomes substantial at a correlation distance of around 4-5 Å. This indicates that the distribution of Na⁺ around the C6, C7 is probably random without much

order, similar to that between the Cl^- and amide O, N or C. In summary, the interactions between the Na^+ and the isopropyl groups or the backbone C are much weaker than those between the Na^+ and the amide group. It appears that the Cl^- anion does not interact strongly with NIPAM unit.

Figure 4-8 shows the pair correlation functions between the various O atoms on one of the PEGMA chains with the salt ions. The pair correlation functions between PEGMA and the salt ions were evaluated for both PEGMA chains separately. For the pair correlation function between the carbonyl O1 on PEGMA chain 1 and Na^+ as shown in Figure 4-8, a strong peak is observed at about 5.8 Å at 318 K. On the other hand, no distinctive peaks were observed for the pair correlation functions between Na^+ and the carbonyl O1 on PEGMA chain 2 at 318 K. The magnitude of the correlation function for the second chain is also significantly lower than that of the O1 $\cdot\cdot\text{Na}^+$ for PEGMA chain 1. The corresponding pair correlation functions at the lower temperature of 278 K for both PEGMA chains are significantly weaker than that between the O1 on PEGMA chain 1 and Na^+ at 318 K indicating much weaker interactions at 278 K. The pair correlation function between the O1 on PEGMA chain 2 and Na^+ at 318 K appears to be even weaker than those at 278 K. For the pair correlation functions between Cl^- and the carbonyl O1 on both PEGMA chains there are no distinctive peaks observed. Further, the $g(r)$ increases as the correlation distance increases indicating random distribution of the Cl^- ions surrounding the PEGMA chains. For the $g(r)$ between the ester O2 on PEGMA and Na^+ , a strong peak at 4.2 Å is observed for PEGMA chain 1 at 318 K, much shorter than the corresponding peak between Na^+ and the carbonyl O1 on PEGMA chain 1 observed at 318 K. Moreover, the peak is also much higher indicating stronger and tighter

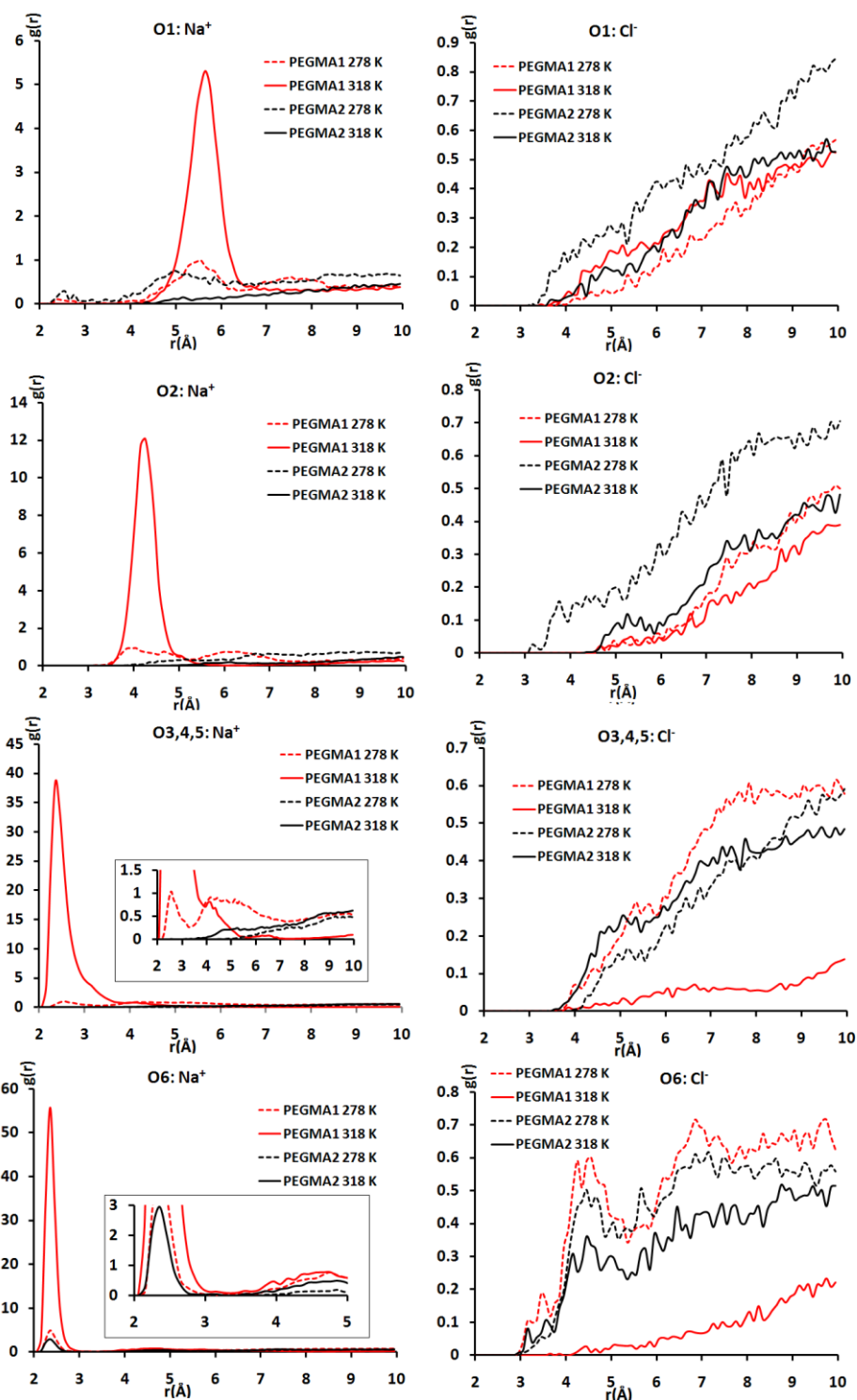


Figure 4-8 The pair correlation functions between salt ions (Na^+ or Cl^-) and various O atoms on PEGMA chain 1 and 2.

association between the ester O2 atom on PEGMA chain 1 and the Na⁺. Similar to the Na⁺ interaction with the carbonyl O1 on PEGMA chain 1 at the lower temperature, the interaction between Na⁺ and the ester O2 on PEGMA chain 1 at 278 K exhibits low magnitude with no distinctive peak indicating very weak affinity. The pair correlation functions between Na⁺ and the O2 on PEGMA chain 2 show very weak interactions at both temperatures similar to the previous case. The interactions between Cl⁻ and the ester O2 on both PEGMA chains also demonstrate similar trend to the Cl⁻ ···O1 correlation with very weak association.

For PEGMA chain 1, the first peaks on the pair correlation functions between ether O atoms (O3, O4 and O5) and Na⁺ are located at about 2.3 Å at 318 K and 2.4 Å at 278 K. The peak height at 318 K is significantly higher than the corresponding peak at 278 K. This indicates a strong association between the ether O atoms on PEGMA chain 1 and Na⁺ at higher temperature whereas only very weak interaction exist between the ether O and Na⁺ at lower temperature. The g(r)s between Na⁺ and ether O (O3, O4 and O5) on PEGMA chain 2 are very weak at both temperatures similar to the previous cases. The g(r) for Cl⁻ ···O (O3, O4 and O5) again demonstrates very weak affinity between the Cl⁻ ion and both of the PEGMA chains at 318 and 278 K.

The pair correlation functions between the O6 of the hydroxyl group on PEGMA chains and the salt ions are shown on the bottom panel of Figure 4-8. The magnitude of the g(r) for the O6 ···Na⁺ on PEGMA chain 1 at higher temperature exhibits the strongest interaction among all the O ···Na⁺ correlations. The magnitude reaches over 55 compared to ~40 for O(3,4,5) ···Na⁺, ~12 for O2 ···Na⁺ and ~ 6 for O1 ···Na⁺ for PEGMA chain 1 at 318K. Not only the peak height increases as the O atom on the PEGMA chain 1 moves

away from the PNIPAM backbone, the peak also becomes narrower as the interaction becomes stronger. This is probably due to lower mobility of the Na^+ when the interaction is stronger. The Na^+ interaction with the O6 atom on PEGMA chain 1 at 278K is again seen to be rather weak with significantly reduced correlations. However, the interaction with the O6 atom is slightly enhanced compared to the other O atoms on PEGMA chain 1 at 278K. This stems from the slightly more negative charge on the O6, thus stronger interaction with the Na^+ . For the second PEGMA chain, the $\text{Na}^+ \cdots \text{O6}$ interaction is again observed to be weak at both temperatures though slightly stronger correlation is observed at higher temperature. The affinity between Cl^- and O6 is again seen to be weak for both PEGMA chains at both temperatures. No specific associations were observed with random distribution of the Cl^- ions surrounding the PEGMA chains.

From Figure 4-8, it can be seen that the interactions between Na^+ and the O atoms on the PEGMA chain 1 at 318 K are much stronger than the corresponding interactions at 278 K as well as than the $\text{Na}^+ \cdots \text{O}$ for the second PEGMA chain at both temperatures. Moreover, compared to the interaction between Na^+ and amide O on NIPAM at both temperatures, the Na^+ interaction with the O atoms on PEGMA chain 1 at higher temperature is also much stronger. Several questions naturally arise. Why is there a significant difference between PEGMA chain 1 and PEGMA chain 2 at higher temperature? Why does Na^+ exhibit much higher affinity with PEGMA chain 1 than for PNIPAM? Why the affinity between Na^+ and PEGMA chain 2 is strongly temperature dependent? Why is there a peak shift as well as a broadening for the first peak for the Na^+ interaction with the amide O on NIPAM at higher temperature compared to the lower temperature one?

Earlier theoretical and experimental work showed that PEG has a very high affinity with alkali ions in the gas phase forming a caged complex with the alkali ions located at the center of the cage¹¹⁶⁻¹¹⁸. The current simulations indicate that there also exist a very high affinity between the Na⁺ ion and one of the PEGMA chains in 1 M NaCl solution at 318 K after the PNIPAM-co-PEGMA copolymer went through a LCST transition exhibiting a hydrophobic folded state as shown in Figure 4-2. Examining the copolymer structure at 318 K as shown in Figure 4-9, a Na⁺ ion was found to complex with multiple O atoms on PEGMA chain 1 as well as the amide O atoms on the PNIPAM units. The structure is similar to the complex observed in the gas phase. From the structures along the simulation trajectory at 318 K, one Na⁺ ion was found to be caged at around 32 ns inside PEGMA chain 1 with the O atoms forming a six coordinated Na⁺ complex. It is similar to the Na⁺ bonding to multiple backbone carbonyls of denatured peptide in an earlier simulation.¹¹⁹ The complex was found to be stable once it is formed. No Na⁺ ion was found to complex with the second PEGMA chain. The O atoms on PEGMA chain 1 forming a complex with Na⁺ include the three ether O (O3, O4, and O5) and the O6 from the end hydroxyl group. The Na⁺ ···O bonds are approximately 2.4 Å and 2.3 Å for the ether O and hydroxyl O6 respectively. The ester O2 is found to be ~4.3 Å away from the Na⁺ ion which indicates no direct bonding between the atoms. The carbonyl O1 on the PEGMA chain was found to be more distant from the Na⁺ ion with a correlation distance of about 5.5 Å. What is more interesting is that the two amide O atoms from the neighboring NIPAM units also form two strong bonds with the caged Na⁺ ion with a distance of ~2.4 Å. In Figure 4-9, the NIPAM units of the copolymer were marked by two ovals. The distances between the amide O on two NIPAM units and the

caged Na^+ are 2.43 and 2.42 Å (shown as *a* and *e* in Figure 4-9). The distances between the O2, O3, O4, O5 and O6 on the PEGMA chain 1 and Na^+ are shown as *b*, *c*, *d*, *f* and *g* in Figure 4-9. The Na^+ is typically six coordinated. Here the two O atoms on the amide groups on the NIPAM units and the four O atoms (O3, O4, O5, O6) on PEGMA chain 1 form a six-coordinated Na^+ complex. The ester O2 appears not involved in the complex probably due to its position. At 278 K below the LCST transition, no Na^+ ion was seen captured by the PEGMA chains during the course of the simulations.

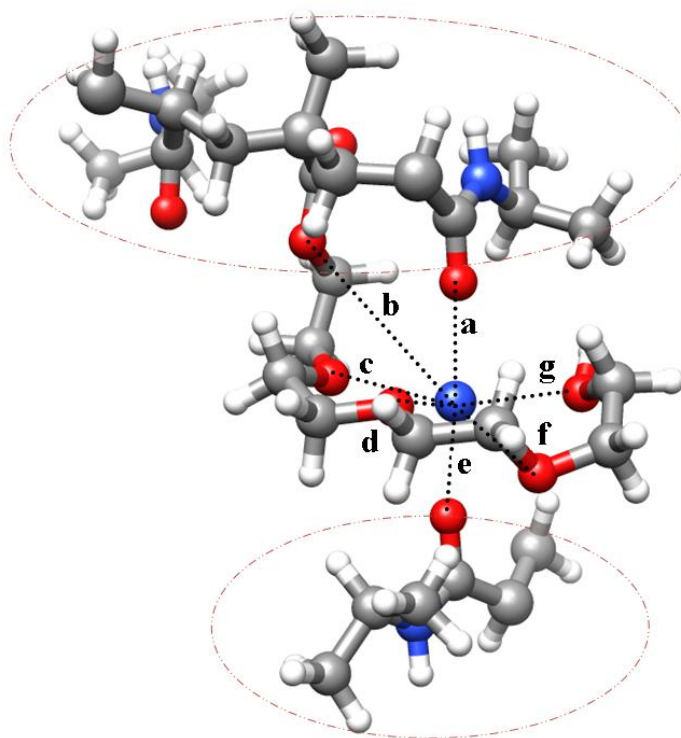


Figure 4-9 The complex formed between the Na^+ ion and the PNIPAM-co-PEGMA copolymer. The center atom in blue is the Na^+ ion. The other blue atoms on the copolymer represent N atoms. The O, C and H atoms are red, gray and white in color respectively. The letters *a*, *c*, *d*, *e*, *f* and *g* indicate the bindings between the various O atoms and the Na^+ .

Earlier experiments reported that the LCSTs of both PEG and PNIPAM are dramatically influenced by the type and concentration of salts present. The LCST of PNIPAM-co-PEGMA in 1 M NaCl solution is estimated to be in the range of 296-300 K between the two simulation temperatures of 278 and 318 K. In the higher temperature simulation, the conformation of the copolymer changes from an extended hydrated state to a folded dehydrated state going through the LCST transition. The dehydration of the copolymer resulted in the O atoms on one of the PEGMA chains to complex with a Na^+ ion forming the observed caged structure shown in Figure 4-9. At 318 K, it appears that only one PEGMA chain is folded to form a complex with the Na^+ ion whereas the other PEGMA chain remains somewhat extended. This is probably due to several factors. One reason is probably due to the positive charge of the copolymer- Na^+ complex to make the second Na^+ complexation energetically unfavorable due to electrostatic repulsion. The second possibility is that the simulations are conducted for 65 ns due to the expensiveness of computation associated with the system. If the simulations were conducted at much longer time scale, the second Na^+ could be captured and complexed with the second PEGMA chain.

The peak shift to the longer correlation distance and broadening of the pair correlation function between Na^+ and the amide O on NIPAM at higher temperature compared to the $g(r)$ at the lower temperature arise from the complexation of the Na^+ with one of the PEGMA chains. Figure 4-10 shows the pair correlation functions between the amide O on PNIPAM and Na^+ with and without caged Na^+ at 318 K. The $g(r)$ between Na^+ and the amide O on PNIPAM at 278K was also shown for comparison. The black dotted line shows the $g(r)$ factor between amide O and Na^+ ions in solution at 278

K. The red solid lines show the $g(r)$ between amide O and all of the Na^+ ions in solution at 318 K. The red dotted lines shows $g(r)$ between amide O and the Na^+ ions without the one Na^+ caged by PEGMA in the 318 K simulation. Compared to the $g(r)$ at 278 K, there is no peak shift observed for the pair correlation function between amide O and Na^+ ions at 318 K when the complexed Na^+ was removed. The shift and broadening of the amide O $\cdot\text{Na}^+$ correlation peak at 318 K come from the coordination of the amide O with the caged Na^+ ion. Due to geometric constraints, the amide O and Na^+ bonding distance is slightly increased from $\sim 2.3\text{\AA}$ for the more mobile Na^+ in solution to $\sim 2.4\text{\AA}$ for the caged Na^+ . This causes the slight shift to a longer distance in the $g(r)$ and the broadening of the peak. Moreover, the magnitude of the peak also increases accordingly due to the stronger association of the amide O with the Na^+ .

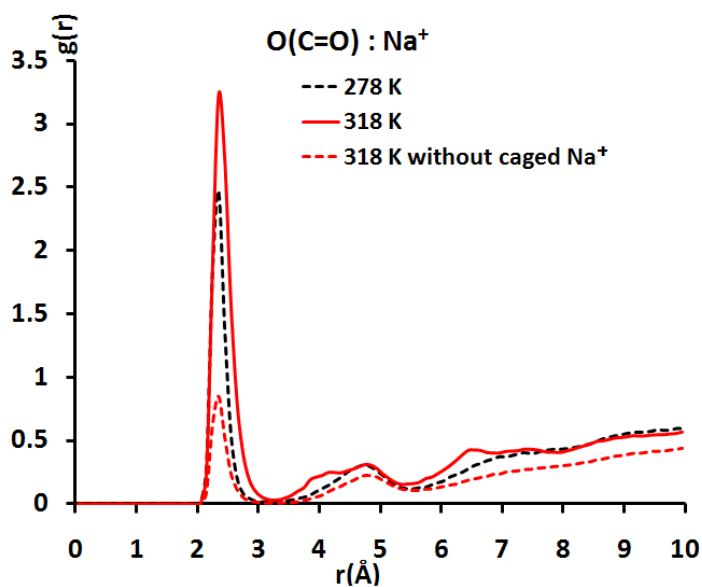


Figure 4-10 The pair correlation functions between the amide O on PNIPAM and Na^+ with and without caged Na^+ at 318K. The corresponding $g(r)$ at 278 K was also shown for comparison.

It is known that PEG has a much higher LCST than PNIPAM due to its more hydrophilic nature. For the PNIPAM-co-PEGMA copolymer, it is expected that its LCST will be higher than that of PNIPAM due to copolymerization with the more hydrophilic PEGMA chains. The effects of salt on the LCST of PEG are more complex due to the strong association of the PEG with the salt cations. It is known that the presence of salt ions will generally decrease the LCST of a polymer such as PNIPAM and PEG. However the strong interaction between the cation and the polymer will cause the LCST to shift to a higher value as was discussed earlier in Chapter 2. This will mitigate the decrease of the LCST depending on the type of the ions present. For the PEG, it is likely that the effects of salt ions will be more complex due to the complexation between the salt cations and the PEG chain as was observed here in the PNIPAM-co-PEGMA copolymer.

4.4. CONCLUSION

The MD simulations of the PNIPAM-co-PEGMA copolymer in 1 M NaCl solution were successfully carried out at 278 and 318 K. The copolymer undergoes LCST phase transition at higher temperature resulting in a folded dehydrated conformation, whereas the conformation of the copolymer at lower temperature remains extended and hydrated. The Na^+ exhibits high affinity for the amide O as well as the O atoms on one of the PEGMA chains at higher temperature. Moreover, one of the Na^+ ions forms a six O-coordinated complex with one of the PEGMA chains on the copolymer. The complex was formed between the Na^+ and two of the amide O atoms on PNIPAM units as well as four of the O atoms (O3, O4, O5 and O6) on PEGMA. The carbonyl O1 and ester O2 on the PEGMA chains do not appear to directly bond with the Na^+ ion, probably due to their geometric restraint. The resulting complexation increases the magnitude of the

correlation peak between Na^+ and the amide O on PNIPAM. In addition, it shifts the peak to a longer correlation distance and as well as broadens the peak. On the other hand, the interaction between Na^+ and the O atoms on the other PEGMA chain at higher temperature is significantly weaker without the complexation. For the extended PNIPAM-co-PEGMA copolymer at lower temperature, the overall interaction between Na^+ and the copolymer is much weaker than at higher temperature. The interactions between Cl^- and the copolymer are weak and non-specific at both temperatures in agreement with the earlier studies of PNIPAM in various salt solutions.

CHAPTER 5 MOLECULAR DYNAMICS STUDY OF THE VOLUME PHASE TRANSITION OF PNIPAM IN HCL SOLUTION

5.1. INTRODUCTION

After the mechanisms for the salt ion and PNIPAM interactions were elucidated and the effects of salt on the LCST of PNIPAM were understood, the effects of pH on the LCST of PNIPAM remain unresolved. The LCST of PNIPAM is about 293 K (20 °C) in 1 M NaCl solution, about 292 K (19 °C) in 1 M KCl solution, however, it is about 302 K (29 °C) in 1 M HCl solution³². The LCST shift of PNIPAM in 1 M HCl solution is only 3 K, which is much smaller than the LCST shift of PNIPAM in 1 M NaCl solution although both solutions have the same ionic strength. Chen et al.³¹ investigated the pH-sensitivity of PNIPAM and change of its LCST due to pH variation in acrylic acid buffer solutions. They reported that the LCST increases from 297.25 K (24.1 °C) to 301.85 K (28.7 °C) when pH decreases from 7 to 1 in acrylic acid buffer solutions. They illustrated pH effects on the hydrogen bonding in the PNIPAM hydrogel network, but they didn't compare and elucidate the differences between pH effects and salt effects on the LCST shift of PNIPAM. In order to uncover the principles of the LCST shift of PNIPAM in acidic solution, MD simulation of PNIPAM was carried out in 1 M HCl solution.

HCl as a strong acid is fully dissociated in water to form hydrated proton and Cl^- in dilute aqueous solution, and the hydrated proton exists in different forms such as hydronium ion (H_3O^+), Eigen (H_9O_4^+) complex, Zundel (H_5O_2^+) ion¹²⁰ or other ($\text{H}_{2n+1}\text{O}_n^+$) complexes mainly depending on the HCl concentration¹²¹⁻¹²⁵. Figure 5-1 shows the structures of Eigen and Zundel models, where O atoms are marked in red and H atoms in gray. Proton transfers between the water molecules could develop or destroy Eigen, Zundel or other complexes with the 1-2 ps proton lifetime at room temperature¹²⁶⁻¹²⁹. Due to the complication of proton transport in aqueous solution, proton transfer is usually ignored in classical MD simulations, which is one of the major limitations of the method. In some packages of classical MD simulation, e.g., Amber and Gromacs,^{130,131} acid solution can be simply treated using constant pH with implicit solvent model. On the other hand, hydronium ion is used to represent proton in solution with explicit solvent model in some classical MD simulations^{121,132-139} although it is not accurate enough that the hydrated proton is treated as a fixed hydronium ion. One typical model of hydronium ion^{137,139} and non-bonded ionic parameters of Cl^- in Amber force field were used in the MD simulations of PNIPAM in 1 M HCl solution here. Compared to the results of the simulations of PNIPAM in different salt solutions, the interaction between hydronium ion and PNIPAM is much weaker than that between salt cation and PNIPAM in salt solutions, and the interaction is modulated by the hydronium- Cl^- interaction in HCl solution.

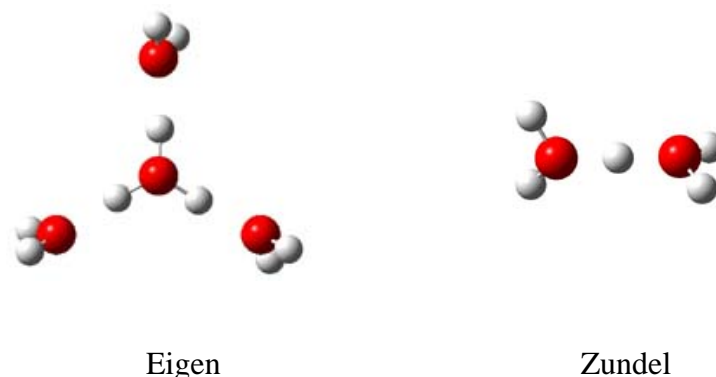


Figure 5-1 The structures of Eigen and Zundel models¹⁴⁰

5.2. COMPUTATIONAL METHODOLOGY AND SIMULATION DETAILS

In the MD simulations of PNIPAM in 1 M HCl solution, the same starting PNIPAM structure as that used in different salt solutions was used. The same parameter set of Amber 94 force field was used for PNIPAM. The estimated LCST of the 50 DP PNIPAM is about 302 K in 1 M HCl solution³². Corresponding to the ionic parameters for salt ions in the simulations of PNIPAM in the different salt solutions, the improved non-bonded parameters of Cl^- were adopted here¹¹⁴. The Urata model of the hydronium ion^{137,139} was applied to the simulations in HCl solution, where the partial atomic charges of hydrogen and oxygen are +0.518 e and -0.554 e respectively. Other force field parameters of hydronium ions were taken from the TIP3P water model.

The radius of gyration of the polymer's backbone⁵⁴ along the simulations was also analyzed by Ptraj¹⁰⁰ in AmberTools 1.2 according to the same protocol for the simulations in different salt solutions. Similarly, the end-to-end distance of the PNIPAM chain was evaluated during the simulations. The number of water molecules in the first

hydration shell was also calculated from ptraj¹⁰⁰ in AmberTools 1.2 using a cut-off distance of 3.5 Å from the surface of the PNIPAM chain.

Pair correlation functions $g(r)$ were calculated between hydronium or chloride ions and some specific atoms on PNIPAM based on the average results of the simulation time of 15-42 ns after the LCST phase transition of PNIPAM at 322 K occurred. The $g(r)$ factors were calculated between H_3O^+ , Cl^- ions in the solution and the amide O, N, C on the peptide bond, the carbon atoms C5, C6 and C7 on the isopropyl group as well as C1 and C2 on the backbone of PNIPAM.

MD simulations were also performed using NAMD⁶⁰. Simulations for PNIPAM in 1 M HCl solution were conducted under NPT ensembles at 282 and 322 K above and below its estimated LCST of 302 K respectively for 42 ns using the Langevin-Hoover scheme^{66,67}. The target pressure is 1 atm. A single PNIPAM chain was immersed in a water box with dimensions of 70 X 80 X 90Å³ generated by VMD⁶¹. A total of 15845 water molecules were used to fully solvate the polymer. A total of 296 pairs of hydronium and chloride ions were randomly distributed in the simulation unit cell to obtain a HCl concentration of about 1 M for MD simulations under 1 atm. A 12Å sphere cut-off and a 15Å pair list distance were used for the short range *van der Waals* and electrostatic interactions⁹¹⁻⁹⁸. PME method was chosen for the long range electrostatic interactions⁶³. A 5 ps⁻¹ collision frequency was used. The TIP3P water model⁹⁹ was used for the water molecules in solution. The simulation time step is chosen to be 1 fs, the same as the ones used in earlier simulations. Periodic boundary conditions were applied to the system.

5.3. RESULTS AND DISCUSSION

Figure 5-2 show the final conformations of the PNIPAM chain at the ends of two simulations after 42 ns simulations at 282 K (Figure 5-2a) and 322 K (Figure 5-2b) respectively. It is obvious that the final conformation of the polymer is a folded structure at 322 K after a LCST phase transition. It is much more compact than the corresponding coil-like structure at 282 K.

Figure 5-3a shows the time evolution of the radii of gyration of the polymer along the simulations at both temperatures in 1 M HCl solution. At higher temperature, the polymer experiences the LCST phase transition from the beginning of simulation to about 12 ns. The radius of gyration reduces from about 21 Å to about 11 Å. It then fluctuates at around 10.5 Å for the rest of the simulation time. At the lower temperature, PNIPAM undergoes a conformation adjustment at the beginning to develop into a dynamically stable coil-like structure for the first 15 ns. The radius of gyration decreases from about 21 Å to about 17 Å. It fluctuates at around 18 Å during the subsequent 27 ns of simulations. Figure 5-3b shows the time evolution of the number of water molecules in the first hydration shell of the polymer along both higher temperature and lower temperature simulations. During the higher temperature simulation at 322 K, the number of water molecules decreases from 500 from the beginning of the simulations to about 360 after the LCST phase transition and continues to decrease slightly during the remaining 25 ns simulation time. However, the number of water molecules in the first hydration shell fluctuates around 510 after the conformation adjustment during the lower temperature simulation at 278 K.

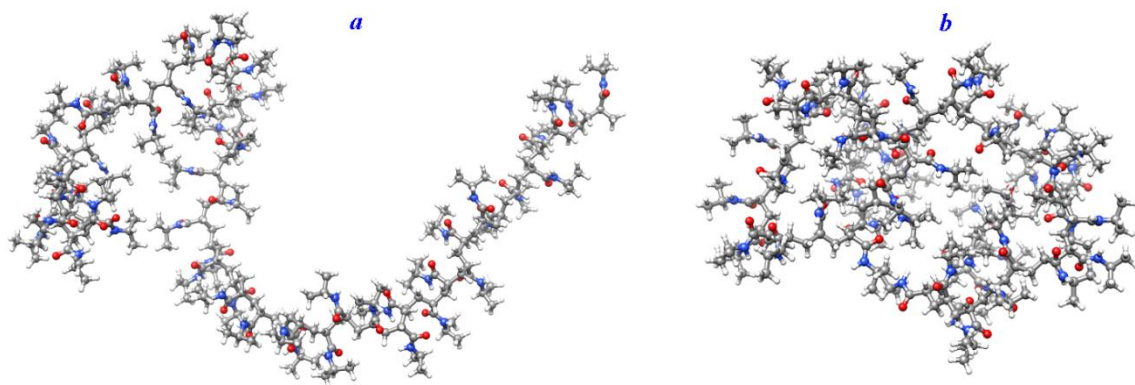


Figure 5-2 The conformations of the PNIPAM chain at the end of 42 ns simulations at 282 K (a) and 322 K (b) respectively.

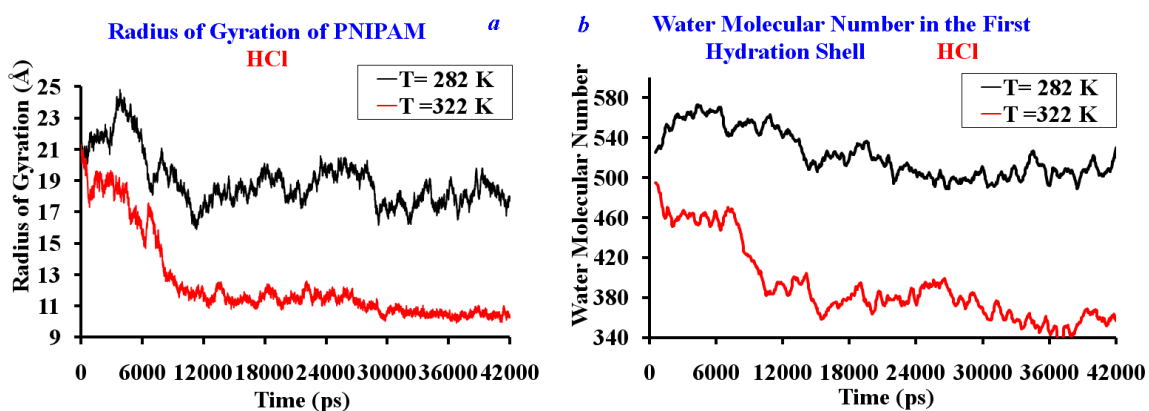


Figure 5-3 Radii of gyration of PNIPAM (a) and the numbers of water molecules (b) associated with the first hydration shell of PNIPAM in 1 M HCl solution at 322 K (red line) and 282 K (black line) respectively during the 42 ns MD simulations.

Figure 5-4 shows the time revolution of the end-to-end distance of PNIPAM at 282 and 322 K along the 42 ns MD simulations. The results show similar trends to the radii of gyration of PNIPAM. The differences between these two properties are a small increase of the end-to-end distance after 24 ns at 278 K and a gradual decrease of the end-to-end distance after 30 ns at 318 K.

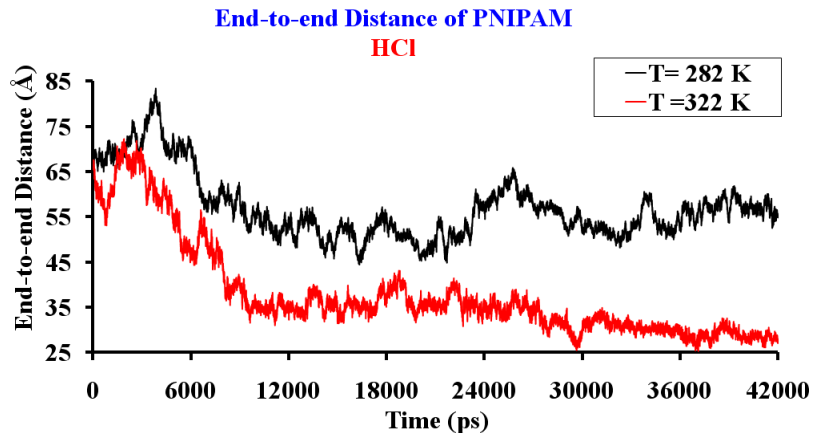


Figure 5-4 End-to-end distances of PNIPAM at 322 K (red line) and 282 K (black line) during the 42 ns MD simulations.

The numbers of H-bonds¹¹⁵ were also evaluated for the PNIPAM intra-chain, between the amide N atoms on the PNIPAM and the water molecules, and between the amide O atoms on the PNIPAM and the water molecules as shown in Figure 5-5. The criterion for the existence of a hydrogen bond is the same as those discussed in the earlier chapters. The hydrogen bond distance cut-off is 3.5 Å between the two related heavy atoms, and the cut-off for hydrogen bond angle is 130°. The heavy atoms are O and N on the polymer and O on the water molecules. For the simulations of the polymer at 282 K in 1 M HCl solution, the number of intra-chain H-bonds first decreases from the starting value of 6 to about 2 during the initial 15 ns of simulation. Then it increases to an average number of about 6 at 21 ns, and keeps more or less the same number during the remaining 20 ns of the simulation. During the higher temperature simulation at 322 K, the number of the intra-chain H-bonds keeps increasing slowly and reaches an average number of about 10 at the end of the 42 ns simulation. For the number of H-bonds between the amide N in PNIPAM and water molecules at 282 K, it increases from the

starting value of 25 to about 35 during the first 4 ns of simulation, then decreases to about 30 and keeps more or less the same value during the rest of simulation period. However, for the simulation at 322 K, the number of the hydrogen bonds between the amide N and water decreases slowly from the initial value of 30 to about 15 during the 42 ns simulation. For the number of H-bonds between the amide O in PNIPAM and the water molecules during lower temperature simulation, it increases from the initial value of 65 to 75 during the first 3 ns simulation time, and then it decreases slightly and fluctuates at around 70 during the remaining 30 ns simulation time. During the higher temperature simulation at 322 K, the number of H-bonds between the amide O and water decreases from the initial value of 70 to about 55 during the first 20 ns of simulations and then it fluctuates at around 55 during the rest of simulation period.

The trend of hydrogen bonding interaction is very similar to those of studied earlier. At higher temperature, the number of the PNIPAM intra-chain H-bonds increases whereas the numbers of the intermolecular hydrogen bonds between the polymer and water decrease accompanied by the LCST phase transition. At lower temperature, there exists an initial adjustment and then the number of hydrogen bonds remains more or less the same since the PNIPAM conformation remain extended.

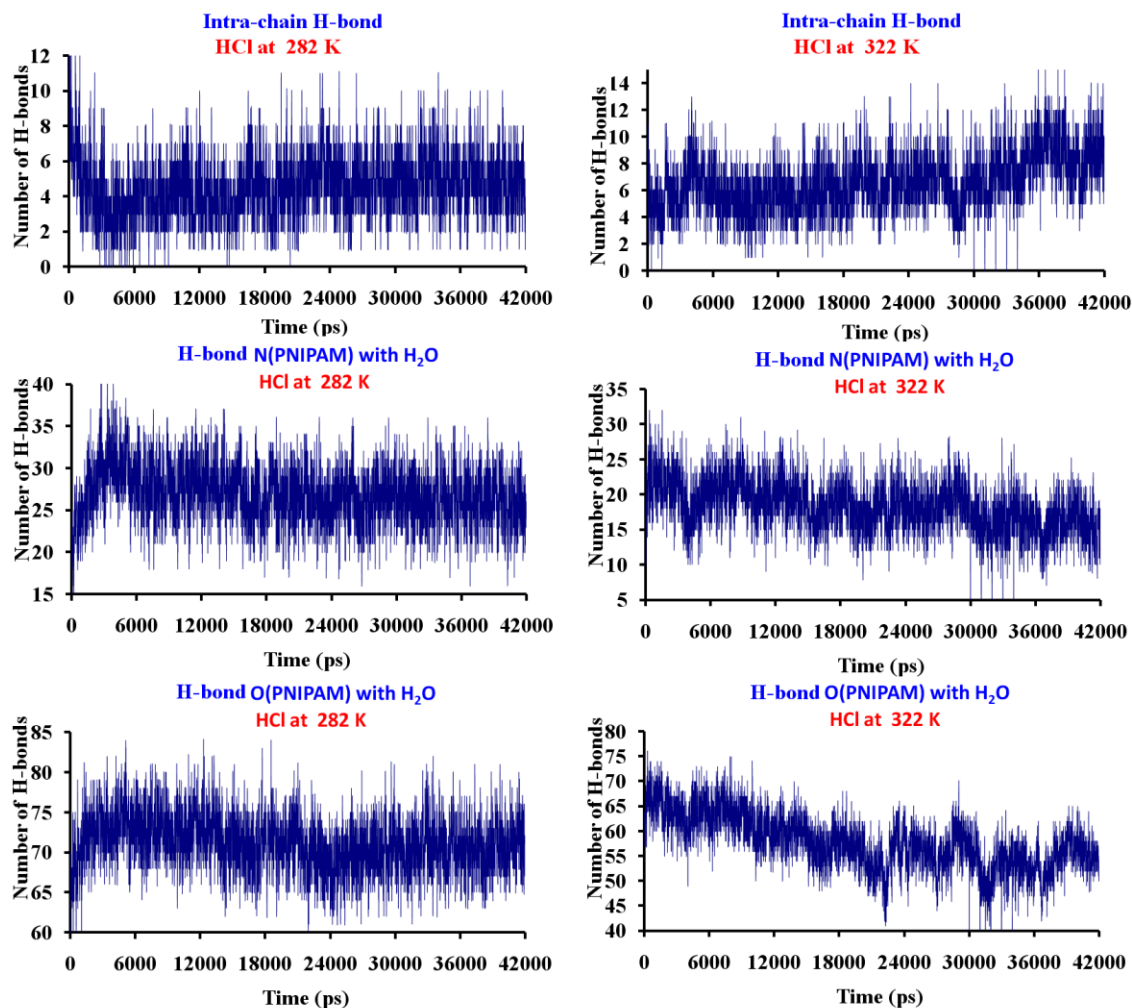


Figure 5-5 PNIPAM's intra-chain hydrogen bonds (top panel) and intermolecular hydrogen bonds between PNIPAM and water (middle and lower panels) during the course of simulations at higher and lower temperatures respectively.

Pair correlation functions ($g(r)$ factors) were evaluated based on the simulation period from 15 to 42 ns after the LCST phase transition of PNIPAM at the higher temperature occurred. Figure 5-6 shows the pair correlation functions between the O, N, C atoms on the amide group and H on H_3O^+ , Cl^- at temperatures above and below the estimated experimental LCST of PNIPAM in 1 M HCl solution. For the pair correlation

functions between the amide O and H (H_3O^+) as shown in Figure 5-6a, there are several peaks appearing along the distance from the amide O. The first peak is the lowest and located at 1.6 Å indicating the weak H-bonds formed between the amide O atoms and H_3O^+ ions. The interaction between the amid O atoms and H (H_3O^+) is slightly stronger at higher temperature than that at lower temperature when the correlation distance is less than 3 Å. However, at longer distance, the interaction appears to be stronger at lower temperature than at higher temperature. The first peak of the pair correlation function between the amide O and Cl^- is located at 4.6 Å with a very weak binding affinity. The interaction between the anion and the amide O appears to be similar to those observed earlier for PNIPAM in salt solutions. There is no direct binding between the amide O and Cl^- . Further, the interaction between the amide O and Cl^- is stronger at lower temperature than that at higher temperature. Compared to the pair correlation functions between the amide O and salt cations in different salt solutions, the proton ...amide O interaction is much weaker whereas the interaction between the amide O and Cl^- is similar in magnitude to those of the amide O and Cl^- in other Cl^- salt solutions. From the pair correlation functions between the amide N and H (H_3O^+) or Cl^- for both temperatures, we can see that there is no direct binding between the amide N and the hydronium ion or the Cl^- ion. The interactions between the amide N and H(H_3O^+) or Cl^- are weaker than those between the amide O and H(H_3O^+) or Cl^- . For the pair correlation functions between the amide C and H(H_3O^+) or Cl^- , the same trend as the pair correlation functions between the amide O and H(H_3O^+) or Cl^- was observed. Further, the strength of the interactions between the amide C and hydronium or Cl^- is weaker than that of the interactions between the amide O and hydronium or Cl^- at both temperatures.

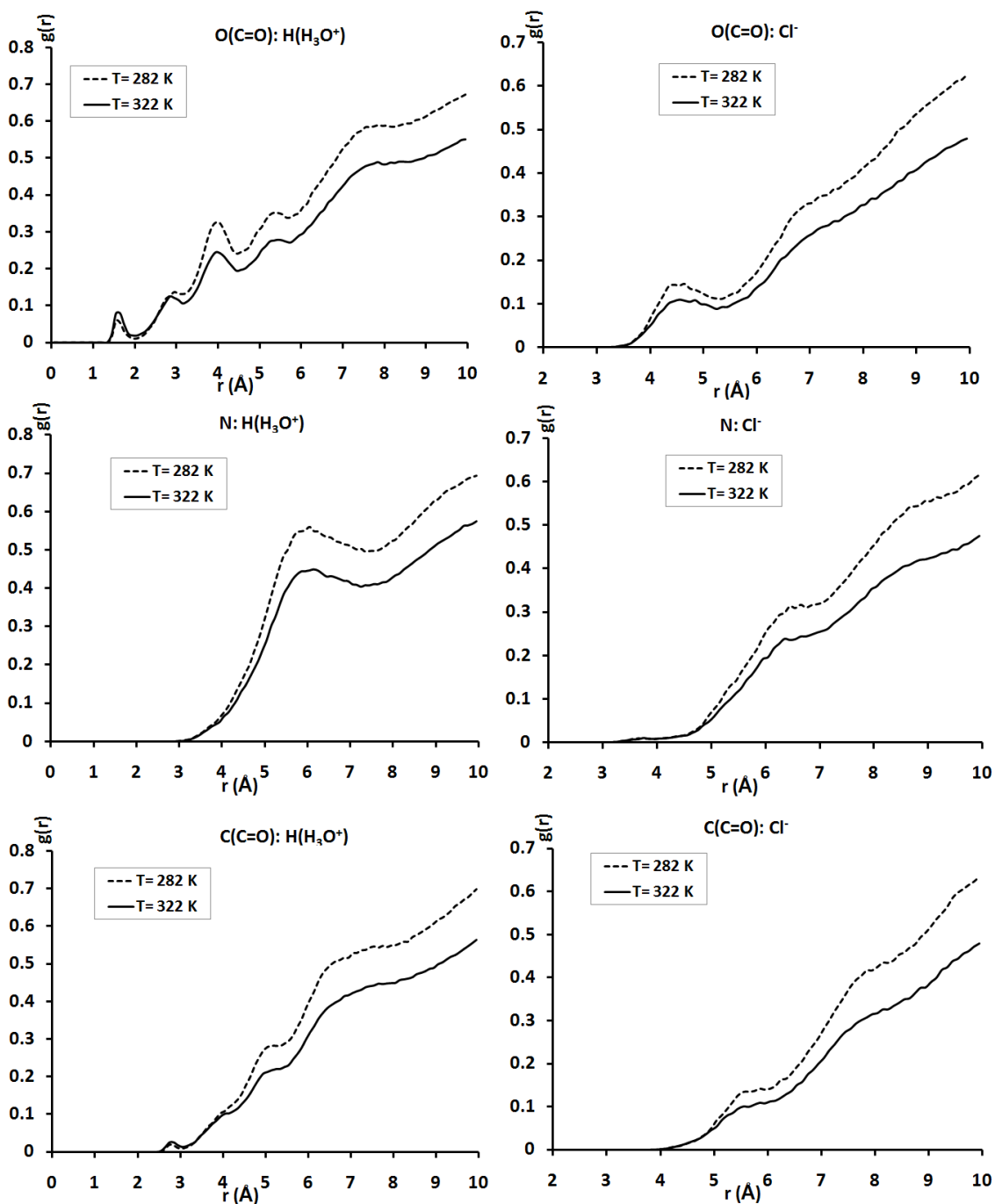


Figure 5-6 Pair correlation functions between the amide C, N or O on PNIPAM and the H atoms of the H_3O^+ or Cl^- ions

Figure 5-7 shows the pair correlation functions between the isopropyl C5, C6, C7 or the backbone C and H(H_3O^+) or Cl^- . The pair correlation functions between

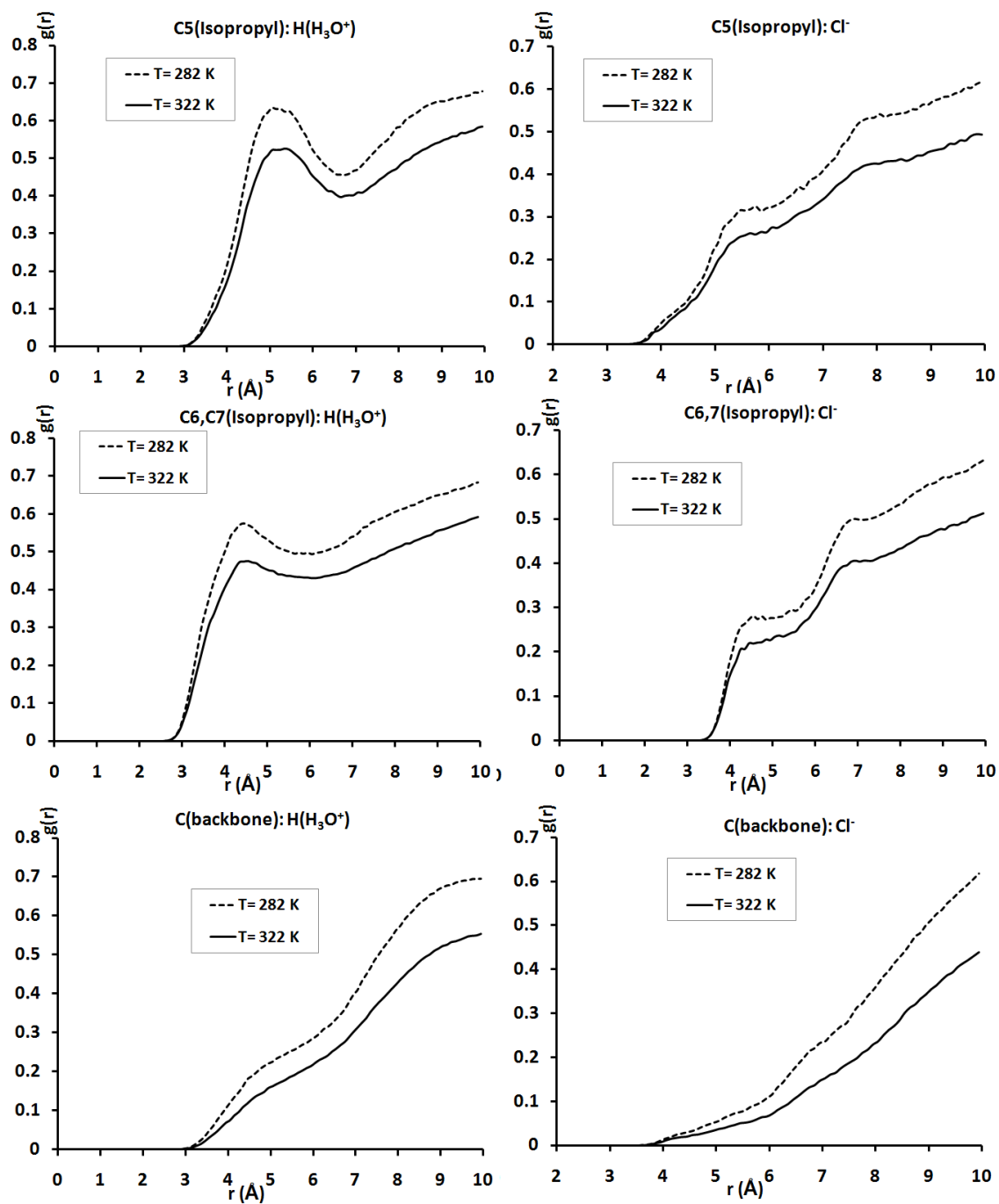


Figure 5-7 Pair correlation functions between the isopropyl C5, C6, C7 or backbone C on PNIPAM and the H_3O^+ or Cl^-

the $\text{H}(\text{H}_3\text{O}^+)$ and isopropyl C5 exhibit a peak at about 5 Å indicating indirect weak interaction between the atoms. The first peak on $g(r)$ between $\text{H}(\text{H}_3\text{O}^+)$ and isopropyl C6, C7 appears at around 4.2 Å. These correlations are similar to that between the amide N and $\text{H}(\text{H}_3\text{O}^+)$. The strength of the interactions decreases following the order with C6, C7 > C5 > amide N. The pair correlation functions between the backbone C and $\text{H}(\text{H}_3\text{O}^+)$ show that their correlation is much weaker than those between the isopropyl C atoms and $\text{H}(\text{H}_3\text{O}^+)$. The interactions between the C atoms and Cl^- is overall weaker than the corresponding interactions between the C atoms and $\text{H}(\text{H}_3\text{O}^+)$. Moreover, the correlations of these pairs are stronger at lower temperature than those at higher temperature.

Figure 5-8 shows the pair correlation functions between the amide O or N on the PNIPAM and the $\text{H}(\text{H}_2\text{O})$. The pair correlation functions between the amide O and $\text{H}(\text{H}_2\text{O})$ at both temperatures show that the affinity of the amide O to the $\text{H}(\text{H}_2\text{O})$ at about 1.8 Å, which is the hydrogen bonding distance between the amide O and hydrogen atoms on water molecules. The pair correlation functions between amide N and $\text{H}(\text{H}_2\text{O})$ show that there is no direct contact between amide N and $\text{H}(\text{H}_2\text{O})$ because the first peak is located at about 3.6 Å. The affinity of the amide O to the $\text{H}(\text{H}_2\text{O})$ is much higher than that of the amide N to the $\text{H}(\text{H}_2\text{O})$. When the surroundings of the amide N are checked, it can be observed that the hydrogen bonding between the amide N and water molecules is through the N-H (N-H bond) --- O (H_2O). The correlations of these pairs at lower temperature are also stronger than those at higher temperature due to temperature effects.

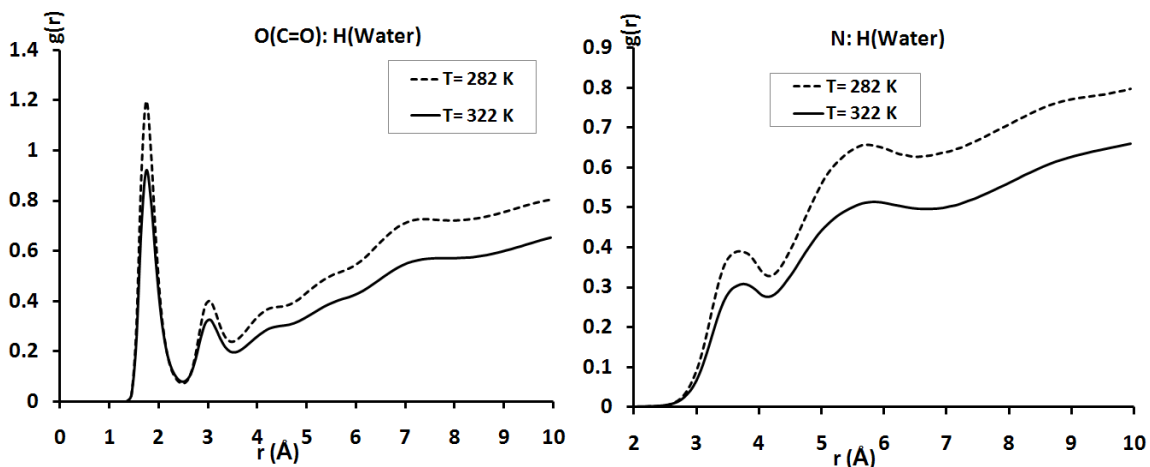


Figure 5-8 Pair correlation functions between the amide O or N and water H

After the surroundings of the NIPAM units of the PNIPAM chain in the HCl solutions were checked, It was found that there exists the hydrogen bonding between the amide O and $H(H_3O^+)$, and that the correlation of the amide C to the $H(H_3O^+)$ is induced from the interaction between the amide O and H_3O^+ . Compared to the corresponding pair correlation functions between PNIPAM and salt ions in different salt solutions, there are some differences between salt cation interactions and $H(H_3O^+)$ interactions with PNIPAM. There is weak hydrogen bonding between the $H(H_3O^+)$ and amide O on PNIPAM in the HCl solution. However, there exists higher affinity between salt cation and amide O on PNIPAM where salt cations directly contact the amide O in the different salt solutions. The correlation of the amide N or backbone C to the $H(H_3O^+)$ is also much weaker in HCl solution than that of the amide N or backbone C to salt cation in different salt solutions, which follows the similar trend of the affinity of the amide O to cation in salt solution. The interaction between PNIPAM and Cl^- in the HCl solution is similar to that between PNIPAM and Cl^- in NaCl or KCl solution. There is a problem, why is the affinity between H_3O^+ and amide group on PNIPAM much weaker than the affinity

between salt cation and amide group? There are maybe three reasons. The net +1 e charge of H_3O^+ equally distributes on three hydrogen atoms in the Urata model and the positive charge density is reduced compared to salt cation although the H_3O^+ and monovalent cation have the same +1 e charge. In addition, the size of H_3O^+ is much larger than the sizes of the salt cations and hinds the direct contact with the amide O on PNIPAM because the free space between the adjacent NIPAM units is too small sometimes during the simulations. Moreover, the diffusion of the hydronium ion is slower than that of salt cations in solution. Although the proton transfer in the HCl solution was ignored in the current simulations, it doesn't influence the interaction between hydronium and PNIPAM because there is no proton transfer between PNIPAM and hydronium, and proton only transfers between water molecules.

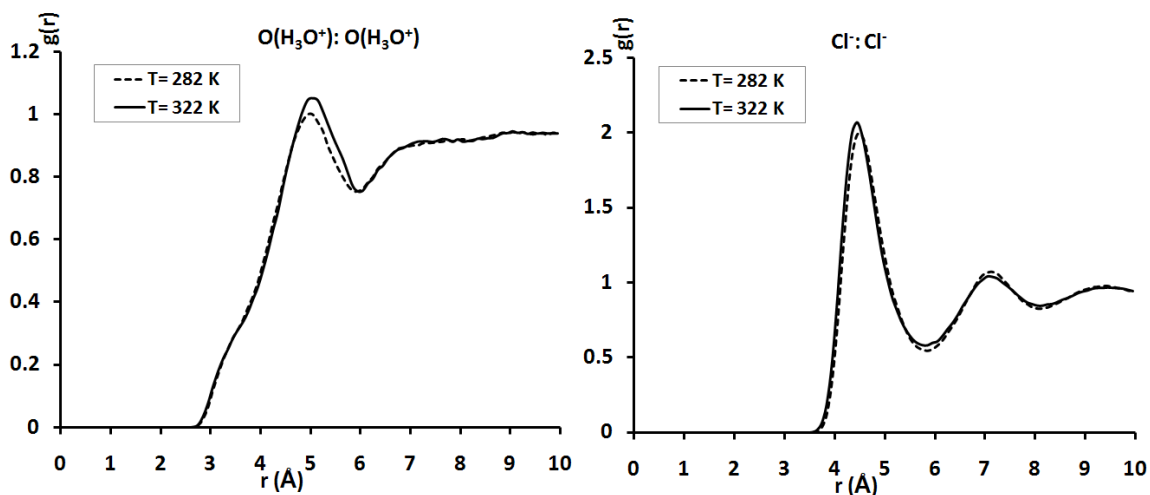


Figure 5-9 Pair correlation functions between $\text{O}(\text{H}_3\text{O}^+)$ and $\text{O}(\text{H}_3\text{O}^+)$ and between Cl^- and Cl^-

In order to further elucidate the interactions of the hydronium and Cl^- ions with PNIPAM, the pair correlation functions between $\text{O}(\text{H}_2\text{O})$ and $\text{O}(\text{H}_2\text{O})$, between Cl^- and

Cl^- and between $\text{H}(\text{H}_3\text{O}^+)$ and Cl^- were evaluated for both simulations at 282 and 322 K. Figure 9 shows the pair correlation functions between the atoms $\text{O}(\text{H}_3\text{O}^+)$ and $\text{O}(\text{H}_3\text{O}^+)$, between Cl^- and Cl^- for both simulations. Figure 5-10 shows the pair correlation functions between $\text{H}(\text{H}_3\text{O}^+)$ and Cl^- for both temperatures, which express the strong strength of ion pairing between $\text{H}(\text{H}_3\text{O}^+)$ and Cl^- . The results in Figures 9 and 10 don't agree well with the simulation results of the recent HCl solutions¹²¹. This is due to the not full-correct description of the real dilute HCl solution by using the current Urata model of the hydronium ion and the ionic parameters of Cl^- in the Amber force field.

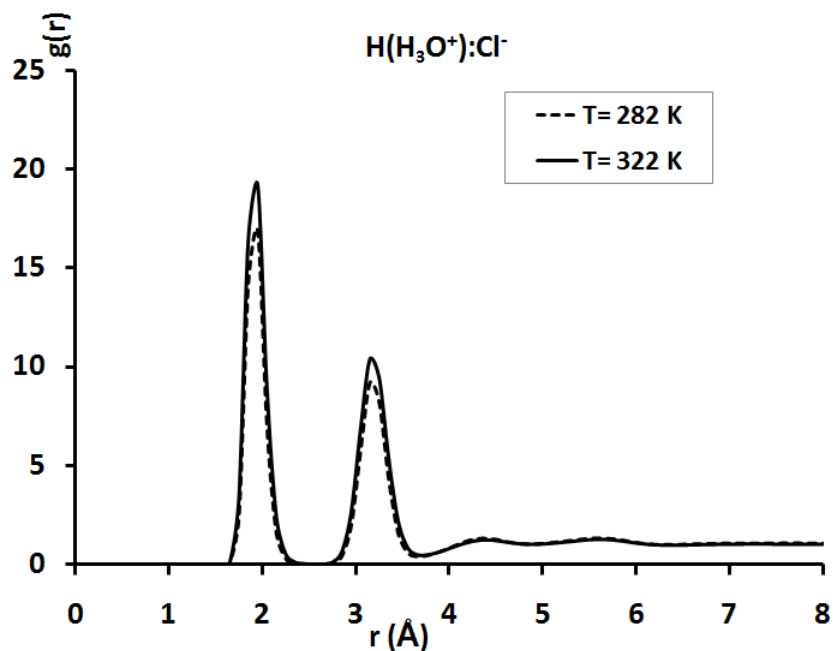


Figure 5-10 Pair correlation functions between $\text{H}(\text{H}_3\text{O}^+)$ and Cl^- at 282 and 322 K

Compared to the high affinity of the salt cations to the amide groups of PNIPAM in the different salt solutions, the affinity of hydronium ions to the amide groups is much weaker here. The interactions of Cl^- ions with PNIPAM in HCl solution are similar to the interactions of salt anions in the salt solutions. The weaker interaction of hydronium with

PNIPAM causes a small LCST shift of PNIPAM in HCl solution, e.g. the LCST decrease by 3 K in 1 M HCl from the 305 K in pure water.

5.4. CONCLUSION

MD simulations of PNIPAM were conducted in 1 M HCl solution at 282 and 322 K by using the Urata model of the hydronium ion and Amber force field for PNIPAM and Cl⁻. Along the higher temperature simulation, the PNIPAM chain undergoes the volume phase transition and changes into a folded structure. However, the polymer changes into a coil-like structure in the lower temperature simulation. Hydronium ions exhibit much weaker affinity to PNIPAM compared to the high affinity of salt cation to PNIPAM in different salt solution. However, the interactions between Cl⁻ and PNIPAM are similar to the interactions of salt anions with PNIPAM in different salt solutions. The lower affinity of hydronium to PNIPAM may cause the small LCST shift of PNIPAM in HCl solution from the LCST in water.

CHAPTER 6 CONCLUSIONS AND FUTURE WORK

6.1. CONCLUSIONS

PNIPAM is the most popular thermo-responsive polymer. The LCST of PNIPAM is 305 K (32 °C) in water. Its unique thermo-responsiveness originates from the presence of both a hydrophilic amide group in each side chain and the hydrophobicity of an isopropyl group in each side chain and its carbon backbone. The LCST is slightly influenced by molecular weight of PNIPAM, polymer concentration, and pH. However, salts have significant impacts on the LCST of PNIPAM and its copolymers. For some cases, the applications of PNIPAM in drug delivery and surface modifications are associated with salts and/or acids. Up to date, it is not clear how the salt ions interact with PNIPAM or its copolymers and how they affect the LCST. In order to elucidate the mechanisms of LCST shift of PNIPAM caused by the salt ions, various MD simulations of PNIPAM and its copolymer PNIPAM-co-PEGMA were carried out in different salt solutions.

Firstly the MD simulations of PNIPAM were successfully conducted in water at 295 and 310 K below and above the LCST to verify the LCST phase transition of PNIPAM in pure water. After that, the MD simulations of PNIPAM were subsequently

carried out in 1 M NaCl, NaBr, NaI and KCl solutions below and above their LCSTs respectively. Various methods were used to investigate the LCST phase transition of PNIPAM and the effects of salt on the LCST of PNIPAM, such as radius of gyration of PNIPAM, the number of water molecules in the first hydration shell of PNIPAM, the final conformation of PNIPAM, the numbers of three types of H-bonds and pair correlation function. During the MD simulations, PNIPAM undergoes the LCST phase transition and develops into a folded hydrophobic structure at higher temperatures; however, PNIPAM still keeps a hydrophobic coil-like structure at lower temperatures although it experiences some geometry adjustments. Salt cations have high affinity with the amide groups on PNIPAM, but salt anions exhibit no or very weak affinity with PNIPAM. The affinity of Na^+ to the amide groups (specifically amide O) of PNIPAM is much higher than that of K^+ . The strength of cation's interaction with the polymer is inversely correlated with the cation-anion contact pair association constant. The stronger the cation-anion interaction is, the weaker the cation binds to the polymer. Salt cation plays a critical role in the effects of salt on the LCST of PNIPAM. It was found that it is the cation which interacts strongly with PNIPAM, and more importantly, the interaction is modulated by the cation-anion pair interaction of salt in solution.

In order to investigate the effects of different salts on the LCST reduction in the same solution, the MD simulations of PNIPAM in the mixed NaCl-KBr solution were performed at 278 and 318 K below and above the LCST. The similar LCST phase transition to those at higher temperatures in different salt solutions was observed at 318 K, and it didn't at 278 K. It was still found that there exists the high affinity of salt cations to the amide groups and the weak affinity of salt anions. Na^+ also has the higher

affinity than K^+ . The results further validated the possible mechanisms of salt's interactions with PNIPAM proposed through the MD simulations in different salt solutions.

The LCSTs of some copolymers based on PNIPAM are also significantly reduced by some salts. The PNIPAM-co-PEGMA copolymer is more hydrophilic than PNIPAM due to the copolymerization with hydrophilic PEGMA and the copolymer is appropriate for surface modifications of bio-films and membranes to enhance surface antifouling. The LCST of the PNIPAM-co-PEGMA copolymer depends on the PEGMA content. The MD simulations of PNIPAM-co-PEGMA were conducted below and above the LCST in 1 M NaCl solution to investigate the interactions of salt ions with NIPAM and PEGMA units. The copolymer also develops into a folded dehydrated conformation after the LCST phase transition at higher temperature, whereas the copolymer remains extended and hydrated along the lower temperature simulation. The Na^+ exhibits high affinity to the copolymer too. At higher temperature, the Na^+ has higher affinity to NIPAM units, even higher affinity to one of the PEGMA chains. Moreover, one of the Na^+ ions forms a six O-coordinated complex with one of the PEGMA chain on the copolymer at higher temperature. The interactions between Cl^- and the copolymer are also weak at both temperatures.

The mechanism of acid effects on the LCST transition of PNIPAM is unclear although the reduction is smaller compared to the salt solution having the same ionic strength. The MD simulations of PNIPAM in 1 M HCl solution were tried to run above and below the LCST using one typical hydronium model of the Urata model. PNIPAM also undergoes the LCST phase transition at higher temperature, but it doesn't at lower

temperature. The interactions of hydronium with PNIPAM are much weaker than those of salt cations with PNIPAM in salt solution.

6.2. LIMITATIONS OF CURRENT WORK

Different from a real experiment, MD simulation can be easily used to investigate the interactions in polymer solution based on the molecular level. In the current work, classical MD simulations were carried out to investigate the effects of salt and pH on the LCST of PNIPAM and the LCST phase transition of the PNIPAM-co-PEGMA copolymer. Through MD simulations, it is possible to observe the conformations of the polymers at each time point and evaluate the pair distribution functions between ions and the polymers at the atomic level. However, due to the limitations of the current technology of classical MD simulation and the limited computing resources, there are some limitations on the current work. Non-polarized Amber 94 and 99 force fields were used in the current work, however, polarized force fields can represent the interactions between salt ions and hydrophobic alkyl groups more accurately. The current simulations are not applicable to mimic the interactions between different polymer chains grafted on the membrane surfaces in water treatment due to the limits of the sizes of the simulation cells and computing resources. For the modeling of PNIPAM simulation in HCl solution with TIP3P water model, the Urata model of hydronium ion and the ionic parameters of Cl⁻ in the Amber force field, the method used here didn't reflect the complications of dilute HCl solution, e.g. the different complexes of hydrated proton with several water molecules and proton transfer between different water molecules.

6.3. RECOMMENDATIONS FOR FUTURE WORK

One of the important applications of PNIPAM is potentially for water treatment by grafting the PNIPAM chains to modify membrane surfaces. With the temperature change, the grafted PNIPAM chains can change the conformations to shake off some colloids or particles deposited on the membrane surfaces^{141,142}. In the future work, the modeling of the grafted PNIPAM chains on the membrane can be achieved by fixing the terminal atoms of the PNIPAM chains on the membrane in MD simulation in aqueous solution and then the effects of grafting density and chain length may be investigated by adjusting the grafting density and chain length¹⁴³⁻¹⁴⁶. Further, the interactions of salt ions with multiple PNIPAM chains on the membrane should be studied by running MD simulations in salt solution. Because PEGMA is more hydrophilic than PNIPAM, the copolymerization of PNIPAM and PEGMA improves the hydrophilicity of the grafted chains, thus assisting the grafted chains to shake off the deposited colloids or particles. MD simulation of the membrane grafted with the PNIPAM-co-PEGMA copolymer in colloid solution may be carried out to investigate the effect of the copolymerization.

During the MD simulations of the PNIPAM-co-PEGMA copolymer in 1 M NaCl solution above and below the LCST, it is quite interesting that one of Na⁺ ions forms a complex with one of the PEGMA chain, but there is no complex developed at lower temperature. It seems that there exists a temperature selection of PEGMA side chain to salt cation. In order to clarify that, we recommend that MD simulations of the PNIPAM-co-PEGMA copolymer may be run in different salt solutions, such as KCl, LiCl, CsCl, and RbCl and NaBr solutions. Further, the complex developed at higher temperature is six O-coordinated in current simulation. We know that different cations have different

sizes. In the current MD simulations of the PNIPAM-co-PEGMA copolymer in 1 M NaCl solution, each PEGMA side chain has 4 PEG units. In order to further investigate the complex developed with different salt cations, the side chain length might be extended or shortened to check if the complex development depends on the side chain length and the size of the salt cation.

REFERENCES

- (1) Schmaljohann, D. *Advanced Drug Delivery Reviews* **2006**, *58*, 1655-1670.
- (2) Gant, R. M.; Hou, Y. P.; Grunlan, M. A.; Cote, G. L. *Journal of Biomedical Materials Research Part A* **2009**, *90A*, 695-701.
- (3) Kuckling, D. *Colloid and Polymer Science* **2009**, *287*, 881-891.
- (4) Alarcon, C. D. H.; Pennadam, S.; Alexander, C. *Chemical Society Reviews* **2005**, *34*, 276-285.
- (5) Rzaev, Z. M. O.; Dincer, S.; Piskin, E. *Progress in Polymer Science* **2007**, *32*, 534-595.
- (6) Gil, E. S.; Hudson, S. M. *Progress in Polymer Science* **2004**, *29*, 1173-1222.
- (7) Da Silva, R. M. P.; Mano, J. F.; Reis, R. L. *Trends in Biotechnology* **2007**, *25*, 577-583.
- (8) Guo, H. F.; Huang, J.; Wang, X. L. *Desalination* **2008**, *234*, 42-50.
- (9) Costa, R. O. R.; Freitas, R. F. S. *Polymer* **2002**, *43*, 5879-5885.
- (10) Zhang, Y. J.; Furyk, S.; Bergbreiter, D. E.; Cremer, P. S. *Journal of the American Chemical Society* **2005**, *127*, 14505-14510.
- (11) Zhang, Y.; Furyk, S.; Sagle, L. B.; Cho, Y.; Bergbreiter, D. E.; Cremer, P. S. *Journal of Physical Chemistry C* **2007**, *111*, 8916-8924.
- (12) Furyk, S.; Zhang, Y. J.; Ortiz-Acosta, D.; Cremer, P. S.; Bergbreiter, D. E. *Journal of Polymer Science Part a-Polymer Chemistry* **2006**, *44*, 1492-1501.
- (13) Sagle, L. B.; Zhang, Y. J.; Litosh, V. A.; Chen, X.; Cho, Y.; Cremer, P. S. *Journal of the American Chemical Society* **2009**, *131*, 9304-9310.
- (14) Gurau, M. C.; Lim, S. M.; Castellana, E. T.; Albertorio, F.; Kataoka, S.; Cremer, P. S. *Journal of the American Chemical Society* **2004**, *126*, 10522-10523.
- (15) LunaBarcenas, G.; Gromov, D. G.; Meredith, J. C.; Sanchez, I. C.; dePablo, J. J.; Johnston, K. P. *Chemical Physics Letters* **1997**, *278*, 302-306.
- (16) Ahmed, Z.; Gooding, E. A.; Pimenov, K. V.; Wang, L. L.; Asher, S. A. *Journal of Physical Chemistry B* **2009**, *113*, 4248-4256.
- (17) Meersman, F.; Wang, J.; Wu, Y. Q.; Heremans, K. *Macromolecules* **2005**, *38*, 8923-8928.
- (18) ten Wolde, P. R.; Chandler, D. *Proceedings of the National Academy of Sciences of the United States of America* **2002**, *99*, 6539-6543.
- (19) Paricaud, P.; Galindo, A.; Jackson, G. *Molecular Physics* **2003**, *101*, 2575-2600.
- (20) Smith, G. D.; Bedrov, D. *Journal of Physical Chemistry B* **2003**, *107*, 3095-3097.
- (21) Esteve, A.; Bail, A.; Landa, G.; Dkhissi, A.; Brut, M.; Rouhani, M. D.; Sudor, J.; Gue, A. M. *Chemical Physics* **2007**, *340*, 12-16.
- (22) Singh, D.; Kuckling, D.; Koul, V.; Choudhary, V.; Adler, H. J.; Dinda, A. K. *European Polymer Journal* **2008**, *44*, 2962-2970.
- (23) Okahata, Y.; Noguchi, H.; Seki, T. *Macromolecules* **1986**, *19*, 493-494.
- (24) You, Y. Z.; Oupicky, D. *Biomacromolecules* **2007**, *8*, 98-105.
- (25) Heath, F.; Haria, P.; Alexander, C. *Aaps Journal* **2007**, *9*, E235-E240.
- (26) Bae, Y. H.; Okano, T.; Kim, S. W. *Pharmaceutical Research* **1991**, *8*, 531-537.
- (27) Bae, Y. H.; Okano, T.; Kim, S. W. *Pharmaceutical Research* **1991**, *8*, 624-628.
- (28) Yoshida, R.; Uchida, K.; Kaneko, Y.; Sakai, K.; Kikuchi, A.; Sakurai, Y.; Okano, T. *Nature* **1995**, *374*, 240-242.
- (29) Schild, H. G.; Tirrell, D. A. *Journal of Physical Chemistry* **1990**, *94*, 4352-4356.
- (30) Fujishige, S.; Kubota, K.; Ando, I. *J. Phys. Chem.* **1989**, *93*, 3311-3313.

- (31) Pei, Y.; Chen, J.; Yang, L. M.; Shi, L. L.; Tao, Q.; Hui, B. J.; Li, R. *Journal of Biomaterials Science-Polymer Edition* **2004**, *15*, 585-594.
- (32) Eeckman, F.; Amighi, K.; Moes, A. J. *International Journal of Pharmaceutics* **2001**, *222*, 259-270.
- (33) Eeckman, F.; Moes, A. J.; Amighi, K. *International Journal of Pharmaceutics* **2002**, *241*, 113-125.
- (34) Vanzi, F.; Madan, B.; Sharp, K. *Journal of the American Chemical Society* **1998**, *120*, 10748-10753.
- (35) Zou, Q.; Bennion, B. J.; Daggett, V.; Murphy, K. P. *Journal of the American Chemical Society* **2002**, *124*, 1192-1202.
- (36) Omta, A. W.; Kropman, M. F.; Woutersen, S.; Bakker, H. J. *Science* **2003**, *301*, 347-349.
- (37) Batchelor, J. D.; Olteanu, A.; Tripathy, A.; Pielak, G. J. *Journal of the American Chemical Society* **2004**, *126*, 1958-1961.
- (38) Omta, A. W.; Kropman, M. F.; Woutersen, S.; Bakker, H. J. *Journal of Chemical Physics* **2003**, *119*, 12457-12461.
- (39) Collins, K. D. *Methods* **2004**, *34*, 300-311.
- (40) Kunz, W.; Henle, J.; Ninham, B. W. *Current Opinion in Colloid & Interface Science* **2004**, *9*, 19-37.
- (41) Kunz, W.; Lo Nostro, P.; Ninham, B. W. *Current Opinion in Colloid & Interface Science* **2004**, *9*, 1-18.
- (42) Zhang, Y. J.; Cremer, P. S. *Current Opinion in Chemical Biology* **2006**, *10*, 658-663.
- (43) Zhang, Y. J.; Cremer, P. S. *Proceedings of the National Academy of Sciences of the United States of America* **2009**, *106*, 15249-15253.
- (44) Cho, Y. H.; Zhang, Y. J.; Christensen, T.; Sagle, L. B.; Chilkoti, A.; Cremer, P. S. *Journal of Physical Chemistry B* **2008**, *112*, 13765-13771.
- (45) Heyda, J.; Vincent, J. C.; Tobias, D. J.; Dzubiella, J.; Jungwirth, P. *Journal of Physical Chemistry B*, *114*, 1213-1220.
- (46) Jagoda-Cwiklik, B.; Vacha, R.; Lund, M.; Srebro, M.; Jungwirth, P. *Journal of Physical Chemistry B* **2007**, *111*, 14077-14079.
- (47) Vrbka, L.; Vondrasek, J.; Jagoda-Cwiklik, B.; Vacha, R.; Jungwirth, P. *Proceedings of the National Academy of Sciences of the United States of America* **2006**, *103*, 15440-15444.
- (48) Collins, K. D. *Biophysical Journal* **1997**, *72*, 65-76.
- (49) Collins, K. D. *Biophysical Chemistry* **2006**, *119*, 271-281.
- (50) Lund, M.; Vacha, R.; Jungwirth, P. *Langmuir* **2008**, *24*, 3387-3391.
- (51) Longhi, G.; Lebon, F.; Abbate, S.; Fornili, S. L. *Chemical Physics Letters* **2004**, *386*, 123-127.
- (52) Wang, J. M.; Cieplak, P.; Kollman, P. A. *Journal of Computational Chemistry* **2000**, *21*, 1049-1074.
- (53) Cornell, W. D.; Cieplak, P.; Bayly, C. I.; Gould, I. R.; Merz, K. M.; Ferguson, D. M.; Spellmeyer, D. C.; Fox, T.; Caldwell, J. W.; Kollman, P. A. *Journal of the American Chemical Society* **1996**, *118*, 2309-2309.
- (54) Gangemi, F.; Longhi, G.; Abbate, S.; Lebon, F.; Cordone, R.; Ghilardi, G. P.; Fornili, S. L. *Journal of Physical Chemistry B* **2008**, *112*, 11896-11906.
- (55) Deshmukh, S.; Mooney, D. A.; McDermott, T.; Kulkarni, S.; MacElroy, J. M. D. *Soft Matter* **2009**, *5*, 1514-1521.
- (56) Tonsing, T.; Oldiges, C. *Physical Chemistry Chemical Physics* **2001**, *3*, 5542-5549.

- (57) Mendez, S.; Curro, J. G.; McCoy, J. D.; Lopez, G. P. *Macromolecules* **2005**, *38*, 174-181.
- (58) Francis, R.; Jijil, C. P.; Prabhu, C. A.; Suresh, C. H. *Polymer* **2007**, *48*, 6707-6718.
- (59) Gilson, M. K.; Zhou, H. X. *Annual Review of Biophysics and Biomolecular Structure* **2007**, *36*, 21-42.
- (60) Phillips, J. C.; Braun, R.; Wang, W.; Gumbart, J.; Tajkhorshid, E.; Villa, E.; Chipot, C.; Skeel, R. D.; Kale, L.; Schulten, K. *Journal of Computational Chemistry* **2005**, *26*, 1781-1802.
- (61) Humphrey, W.; Dalke, A.; Schulten, K. *Journal of Molecular Graphics* **1996**, *14*, 33-&.
- (62) Challacombe, M.; White, C.; HeadGordon, M. *Journal of Chemical Physics* **1997**, *107*, 10131-10140.
- (63) Darden, T.; York, D.; Pedersen, L. *Journal of Chemical Physics* **1993**, *98*, 10089-10092.
- (64) Phillips, J.; Isgro, T.; Sotomayor, M.; Villa, E., *NAMD tutorial unix/macOSX version*
- (65) Berendsen, H. J. C.; Postma, J. P. M.; Vangunsteren, W. F.; Dinola, A.; Haak, J. R. *Journal of Chemical Physics* **1984**, *81*, 3684-3690.
- (66) Feller, S. E.; Zhang, Y. H.; Pastor, R. W.; Brooks, B. R. *Journal of Chemical Physics* **1995**, *103*, 4613-4621.
- (67) Martyna, G. J.; Tobias, D. J.; Klein, M. L. *Journal of Chemical Physics* **1994**, *101*, 4177-4189.
- (68) CPMD 3.13, Copyrighted by IBM and Max-Planck Institute, 2009.
- (69) Frisch, M. J.; Trucks, G. W.; Schlegel, H. B.; Scuseria, G. E.; Robb, M. A.; Cheeseman, J. R.; Montgomery, J. A., Jr.; Vreven, T.; Kudin, K. N.; Burant, J. C.; Millam, J. M.; Iyengar, S. S.; Tomasi, J.; Barone, V.; Mennucci, B.; Cossi, M.; Scalmani, G.; Rega, N.; Petersson, G. A.; Nakatsuji, H.; Hada, M.; Ehara, M.; Toyota, K.; Fukuda, R.; Hasegawa, J.; Ishida, M.; Nakajima, T.; Honda, Y.; Kitao, O.; Nakai, H.; Klene, M.; Li, X.; Knox, J. E.; Hratchian, H. P.; Cross, J. B.; Bakken, V.; Adamo, C.; Jaramillo, J.; Gomperts, R.; Stratmann, R. E.; Yazyev, O.; Austin, A. J.; Cammi, R.; Pomelli, C.; Ochterski, J. W.; Ayala, P. Y.; Morokuma, K.; Voth, G. A.; Salvador, P.; Dannenberg, J. J.; Zakrzewski, V. G.; Dapprich, S.; Daniels, A. D.; Strain, M. C.; Farkas, O.; Malick, D. K.; Rabuck, A. D.; Raghavachari, K.; Foresman, J. B.; Ortiz, J. V.; Cui, Q.; Baboul, A. G.; Clifford, S.; Cioslowski, J.; Stefanov, B. B.; Liu, G.; Liashenko, A.; Piskorz, P.; Komaromi, I.; Martin, R. L.; Fox, D. J.; Keith, T.; Al-Laham, M. A.; Peng, C. Y.; Nanayakkara, A.; Challacombe, M.; Gill, P. M. W.; Johnson, B.; Chen, W.; Wong, M. W.; Gonzalez, C.; Pople, J. A. *Gaussian 03, revision C.02*; Gaussian, Inc.: Wallingford, CT, 2004.
- (70) Wang, J. M. *AmberTools Users' Manual 1.2*.
- (71) Zhang, W.; Hou, T. J.; Schafmeister, C.; Ross, W. S.; Case, D. A. *AmberTools Users' Manual 1.2*.
- (72) Martinez, L.; Andrade, R.; Birgin, E. G.; Martinez, J. M. *Journal of Computational Chemistry* **2009**, *30*, 2157-2164.
- (73) Gil, E. S.; Hudson, S. A. *Progress in Polymer Science* **2004**, *29*, 1173-1222.
- (74) Hofmeister, F. *Arch. Exp. Pathol. Pharmacol.* **1888**, *24*, 247-260.
- (75) Collins, K. D.; Washabaugh, M. W. *Q. Rev. Biophys.* **1985**, *18*, 323-422.
- (76) Cacace, M. G.; Landau, E. M.; Ramsden, J. J. *Q. Rev. Biophys.* **1997**, *30*, 241-277.
- (77) Jungwirth, P.; Tobias, D. J. *Journal of Physical Chemistry B* **2001**, *105*, 10468-10472.
- (78) Heyda, J.; Vincent, J. C.; Tobias, D. J.; Dzubiella, J.; Jungwirth, P. *Journal of Physical Chemistry B* **2010**, *114*, 1213-1220.

- (79) Hess, B.; van der Vegt, N. F. A. *Proceedings of the National Academy of Sciences of the United States of America* **2009**, *106*, 13296-13300.
- (80) Ikehata, A.; Hashimoto, C.; Mikami, Y.; Ozaki, Y. *Chemical Physics Letters* **2004**, *393*, 403-408.
- (81) Joung, I. S.; Cheatham, T. E. *The Journal of Physical Chemistry B* **2008**, *112*, 9020-9041.
- (82) Junmei, W.; Piotr, C.; Peter, A. K. *Journal of Computational Chemistry* **2000**, *21*, 1049-1074.
- (83) Conner, B. N.; Yoon, C.; Dickerson, J. L.; Dickerson, R. E. *Journal of Molecular Biology* **1984**, *174*, 663-695.
- (84) Pettersen, E. F.; Goddard, T. D.; Huang, C. C.; Couch, G. S.; Greenblatt, D. M.; Meng, E. C.; Ferrin, T. E. *Journal of Computational Chemistry* **2004**, *25*, 1605-1612.
- (85) D.C. Rapaport *Molecular Physics* **1983**, *50* 1151-1162.
- (86) Uejio, J. S.; Schwartz, C. P.; Duffin, A. M.; Drisdell, W. S.; Cohen, R. C.; Saykally, R. J. *Proceedings of the National Academy of Sciences of the United States of America* **2008**, *105*, 6809-6812.
- (87) Joung, I. S.; Cheatham, T. E. *The Journal of Physical Chemistry B* **2009**, *113*, 13279-13290.
- (88) Brodholt, J. P. *Chemical Geology* **1998**, *151*, 11-19.
- (89) Fedotova, M. V. *Journal of Molecular Liquids* **2010**, *153*, 9-14.
- (90) Bondarenko, G. V.; Gorbaty, Y. E.; Okhulkov, A. V.; Kalinichev, A. G. *The Journal of Physical Chemistry A* **2006**, *110*, 4042-4052.
- (91) Norberg, J.; Nilsson, L. *Biophysical Journal* **2000**, *79*, 1537-1553.
- (92) Horinek, D.; Mamatkulov, S. I.; Netz, R. R. *Journal of Chemical Physics* **2009**, *130*.
- (93) Fennell, C. J.; Bizjak, A.; Vlachy, V.; Dill, K. A. *Journal of Physical Chemistry B* **2009**, *113*, 6782-6791.
- (94) Chang, T. M.; Dang, L. X. *Journal of Physical Chemistry B* **1999**, *103*, 4714-4720.
- (95) General, I. J.; Ascianto, E. K.; Madura, J. D. *Journal of Physical Chemistry B* **2008**, *112*, 15417-15425.
- (96) Loncharich, R. J.; Brooks, B. R.; Pastor, R. W. *Biopolymers* **1992**, *32*, 523-535.
- (97) Lins, R. D.; Rothlisberger, U. *Journal of Chemical Theory and Computation* **2006**, *2*, 246-250.
- (98) Brown, M. A.; D'Auria, R.; Kuo, I. F. W.; Krisch, M. J.; Starr, D. E.; Bluhm, H.; Tobias, D. J.; Hemminger, J. C. *Physical Chemistry Chemical Physics* **2008**, *10*, 4778-4784.
- (99) Jorgensen, W. L.; Chandrasekhar, J.; Madura, J. D.; Impey, R. W.; Klein, M. L. *Journal of Chemical Physics* **1983**, *79*, 926-935.
- (100) Cheatham, T. E. *AmberTools Users' Manual 1.2*.
- (101) Lee, H.; Venable, R. M.; MacKerell, A. D.; Pastor, R. W. *Biophysical Journal* **2008**, *95*, 1590-1599.
- (102) Pal, S.; Milano, G.; Roccatano, D. *Journal of Physical Chemistry B* **2006**, *110*, 26170-26179.
- (103) Han, S.; Hagiwara, M.; Ishizone, T. *Macromolecules* **2003**, *36*, 8312-8319.
- (104) Schild, H. G. *Progress in Polymer Science* **1992**, *17*, 163-249.
- (105) Galaev, I. Y.; Mattiason, B. *Smart polymers for bioseparation and bioprocessing. 2002.: Taylor and Francis*.
- (106) Lu, T.; Vesterinen, E.; Tenhu, H. *Polymer* **1998**, *39*, 641-650.
- (107) Vesterinen, E.; Tenhu, H.; Dobrodumov, A. *Polymer* **1994**, *35*, 4852-4856.
- (108) Liu, X. M.; Wang, L. S.; Wang, L.; Huang, J. C.; He, C. B. *Biomaterials* **2004**, *25*, 5659-5666.

- (109) Cheng, V.; Lee, B. H.; Pauken, C.; Vernon, B. L. *Journal of Applied Polymer Science* **2007**, *106*, 1201-1207.
- (110) Cruickshank, J.; Hubbard, H. V. S.; Boden, N.; Ward, I. M. *Polymer* **1995**, *36*, 3779-3781.
- (111) Mohsen-Nia, M.; Rasa, H.; Modarress, H. *Journal of Chemical and Engineering Data* **2006**, *51*, 1316-1320.
- (112) Nozary, S.; Modarress, H.; Eliassi, A. *Journal of Applied Polymer Science* **2003**, *89*, 1983-1990.
- (113) Auffinger, P.; Cheatham, T. E.; Vaiana, A. C. *Journal of Chemical Theory and Computation* **2007**, *3*, 1851-1859.
- (114) Joung, I. S.; Cheatham, T. E. *Journal of Physical Chemistry B* **2008**, *112*, 9020-9041.
- (115) Rapaport, D. C. *Molecular Physics* **1983**, *50*, 1151-1162.
- (116) Vonhelden, G.; Wyttenbach, T.; Bowers, M. T. *Science* **1995**, *267*, 1483-1485.
- (117) Gidden, J.; Wyttenbach, T.; Jackson, A. T.; Scrivens, J. H.; Bowers, M. T. *Journal of the American Chemical Society* **2000**, *122*, 4692-4699.
- (118) Yokoyama, Y.; Hirajima, R.; Morigaki, K.; Yamaguchi, Y.; Ueda, K. *Journal of the American Society for Mass Spectrometry* **2007**, *18*, 1914-1920.
- (119) Dzubiella, J. *Journal of the American Chemical Society* **2008**, *130*, 14000-14007.
- (120) Xantheas, S. S. *Nature* **2009**, *457*, 673-674.
- (121) Xu, J. Q.; Izvekov, S.; Voth, G. A. *Journal of Physical Chemistry B*, *114*, 9555-9562.
- (122) Fulton, J. L.; Balasubramanian, M. *Journal of the American Chemical Society*, *132*, 12597-12604.
- (123) Wang, F.; Izvekov, S.; Voth, G. A. *Journal of the American Chemical Society* **2008**, *130*, 3120-3126.
- (124) Buch, V.; Dubrovskiy, A.; Mohamed, F.; Parrinello, M.; Sadlej, J.; Hammerich, A. D.; Devlin, J. P. *Journal of Physical Chemistry A* **2008**, *112*, 2144-2161.
- (125) Cavalleri, M.; Naslund, L. A.; Edwards, D. C.; Wernet, P.; Ogasawara, H.; Myneni, S.; Ojamae, L.; Odelius, M.; Nilsson, A.; Pettersson, L. G. M. *Journal of Chemical Physics* **2006**, *124*.
- (126) Selvan, M. E.; Keffer, D. J.; Cui, S. T.; Paddison, S. J. *Journal of Physical Chemistry C*, *114*, 11965-11976.
- (127) Schmitt, U. W.; Voth, G. A. *Journal of Chemical Physics* **1999**, *111*, 9361-9381.
- (128) Vuilleumier, R.; Borgis, D. *Journal of Chemical Physics* **1999**, *111*, 4251-4266.
- (129) Lill, M. A.; Helms, V. *Journal of Chemical Physics* **2001**, *115*, 7993-8005.
- (130) Case, D. A.; Cheatham, T. E.; Darden, T.; Gohlke, H.; Luo, R.; Merz, K. M.; Onufriev, A.; Simmerling, C.; Wang, B.; Woods, R. J. *Journal of Computational Chemistry* **2005**, *26*, 1668-1688.
- (131) Hess, B.; Kutzner, C.; van der Spoel, D.; Lindahl, E. *Journal of Chemical Theory and Computation* **2008**, *4*, 435-447.
- (132) Laurs, N.; Bopp, P. *Berichte Der Bunsen-Gesellschaft-Physical Chemistry Chemical Physics* **1993**, *97*, 982-996.
- (133) Baaden, M.; Burgard, M.; Wipff, G. *Journal of Physical Chemistry B* **2001**, *105*, 11131-11141.
- (134) Chialvo, A. A.; Ho, P. C.; Palmer, D. A.; Gruszkiewicz, M. S.; Cummings, P. T.; Simonson, J. M. *Journal of Physical Chemistry B* **2002**, *106*, 2041-2046.
- (135) Chialvo, A. A.; Simonson, J. M. *Journal of Physical Chemistry C* **2007**, *111*, 15569-15574.
- (136) Hofmann, D. W. M.; Kuleshova, L.; D'Aguzzo, B.; Di Noto, V.; Negro, E.; Conti, F.; Vittadello, M. *Journal of Physical Chemistry B* **2009**, *113*, 632-639.

- (137) Urata, S.; Irisawa, J.; Takada, A.; Shinoda, W.; Tsuzuki, S.; Mikami, M. *Journal of Physical Chemistry B* **2005**, *109*, 4269-4278.
- (138) Devanathan, R.; Venkatnathan, A.; Dupuis, M. *Journal of Physical Chemistry B* **2007**, *111*, 13006-13013.
- (139) Cui, S. T.; Liu, J. W.; Selvan, M. E.; Keffer, D. J.; Edwards, B. J.; Steele, W. V. *Journal of Physical Chemistry B* **2007**, *111*, 2208-2218.
- (140) <http://comporgchem.com/blog/?p=784>.
- (141) Synytska, A.; Svetushkina, E.; Puretskiy, N.; Stoychev, G.; Berger, S.; Ionov, L.; Bellmann, C.; Eichhorn, K. J.; Stamm, M. *Soft Matter* **2010**, *6*, 5907-5914.
- (142) Cooperstein, M. A.; Canavan, H. E. *Langmuir* **2010**, *26*, 7695-7707.
- (143) Ishida, N.; Biggs, S. *Macromolecules* **2009**, *43*, 7269-7276.
- (144) Li, P. F.; Xie, R.; Jiang, J. C.; Meng, T.; Yang, M.; Ju, X. J.; Yang, L. H.; Chu, L. *Y. J. Membr. Sci.* **2009**, *337*, 310-317.
- (145) Yim, H.; Kent, M. S.; Mendez, S.; Lopez, G. P.; Satija, S.; Seo, Y. *Macromolecules* **2006**, *39*, 3420-3426.
- (146) Plunkett, K. N.; Zhu, X.; Moore, J. S.; Leckband, D. E. *Langmuir* **2006**, *22*, 4259-4266.

APPENDIX A - PERL PROGRAM 1

```

#!/usr/bin/perl
#
#put PNIPAM in the water box
#
$row=0;
$column=0;
$ncal=0;
$norganic=955;
$water=$norganic+69954;
$nw=0;
$total=0;
open(OUTPUT, ">test.pdbtxt");
open(INPUT, "<solvate.pdbtxt");
while (<INPUT>) {
    chomp;
    if(substr($_,0,4) eq "ATOM")
    {
        @tmp=split(/ * /,$_);
        for($column=0;$column<=11;$column++)
        {$data[$row][$column]=$tmp[$column];
        $middle[$row][$column]=$tmp[$column];}
#    print OUTPUT $data[$row][$column];
    }
    $row++;
#    print OUTPUT "\n";
}

}

for($ncalA=0;$ncalA<=($norganic-1);$ncalA++)
{
    for($ncalB=$norganic;$ncalB<=$water;$ncalB++)
    {$seperation=($data[$ncalA][5]-$data[$ncalB][5])**2+
    ($data[$ncalA][6]-$data[$ncalB][6])**2+
    ($data[$ncalA][7]-$data[$ncalB][7])**2;
    if($seperation<=4)
    { $data[$ncalB][3]=R;}
}

}

$increase=955;
$residue=50;
for($nw=0;$nw<=23317;$nw++)
#23318 water molecules in the water box
{ $tmpatmw=$norganic+$nw*3;

```

```

if(($data[$tmpatmwt][3]eq"R") or ($data[$tmpatmwt+1][3]eq"R") or
($data[$tmpatmwt+2][3]eq"R"))
{;}
else {$nresidue++; print OUTPUT "TER\n";print STDOUT "TER\n";
for ($i=0;$i<=2;$i++)
{
$increase++;
$middle[$increase-1][0]=$data[$tmpatmwt+$i][0];
$middle[$increase-1][1]=$increase;
$middle[$increase-1][2]=$data[$tmpatmwt+$i][2];
$middle[$increase-1][3]=$data[$tmpatmwt+$i][3];
$middle[$increase-1][4]=$nresidue;
$middle[$increase-1][5]=$data[$tmpatmwt+$i][5];
$middle[$increase-1][6]=$data[$tmpatmwt+$i][6];
$middle[$increase-1][7]=$data[$tmpatmwt+$i][7];
$middle[$increase-1][8]=$data[$tmpatmwt+$i][8];
$middle[$increase-1][9]=$data[$tmpatmwt+$i][9];
printf OUTPUT "%4s%7d %-4s%-3s%6d%12.3f%8.3f%8.3f%6.2f%6.2f\n",
$middle[$increase-1][0],$middle[$increase-1][1],$middle[$increase-
1][2],$middle[$increase-1][3],$middle[$increase-1][4],
$middle[$increase-1][5],$middle[$increase-1][6],$middle[$increase-
1][7],$middle[$increase-1][8],$middle[$increase-1][9];
}
}
}
print OUTPUT "TER\n";

exit 0;

```

APPENDIX B - PERL PROGRAM 2

```

#!/usr/bin/perl
#
#put PNIPAM in the NaCl-water box and keep the charge of O
#
$row=0;
$column=0;
$ncalA=0;
$ncalB=0;
$norganic=955;
$nnatotal=400;
$ncltotal=400;
$nwater=23000;
$na=0;
$nc1=0;
$nw=0;
$total=$norganic+$na+$nc1+$nwater*3;
open(OUTPUT, ">orgnaclwater.pdb");
open(INPUT, "<naclwater.pdb");
while (<INPUT>) {
    chomp;
    if(substr($_,0,4) eq "ATOM")
    {
        if($row<$norganic) {print OUTPUT $_,"\n";}
        @tmp=split(/ * /,$_);
        for($column=0;$column<=11;$column++)
        {$data[$row][$column]=$tmp[$column];
        $middle[$row][$column]=$tmp[$column];
        #    print OUTPUT $data[$row][$column];
        }

        $row++;
        #    print OUTPUT "\n";
        }
    }
for($ncalA=0;$ncalA<=($norganic-1);$ncalA++)
{
    for($ncalB=$norganic;$ncalB<=$total;$ncalB++)
    {$seperation=($data[$ncalA][5]-$data[$ncalB][5])**2+
        ($data[$ncalA][6]-$data[$ncalB][6])**2+
        ($data[$ncalA][7]-$data[$ncalB][7])**2;
        if($seperation<=4)
        { $data[$ncalB][3]=R;}
    }
}

```

```

}
$increase=955;
$residue=50;

for($nwt=0;$nwt<=$nwater-1;$nwt++)
# water molecules in the nacl-water box
{ $tmpatmwt=$norganic+$nntotal*2+$nwt*3;
  if(($data[$tmpatmwt][3]eq"R") or ($data[$tmpatmwt+1][3]eq"R") or
($data[$tmpatmwt+2][3]eq"R") )
  {;}
  else {$residue++; print OUTPUT "TER\n";
    for ($i=0;$i<=2;$i++)
    {
      $increase++;
      $middle[$increase-1][0]=$data[$tmpatmwt+$i][0];
      $middle[$increase-1][1]=$increase;
      $middle[$increase-1][2]=$data[$tmpatmwt+$i][2];
      $middle[$increase-1][3]=$data[$tmpatmwt+$i][3];
      $middle[$increase-1][4]=$residue;
      $middle[$increase-1][5]=$data[$tmpatmwt+$i][5];
      $middle[$increase-1][6]=$data[$tmpatmwt+$i][6];
      $middle[$increase-1][7]=$data[$tmpatmwt+$i][7];
      $middle[$increase-1][8]=$data[$tmpatmwt+$i][8];
      $middle[$increase-1][9]=$data[$tmpatmwt+$i][9];
      printf OUTPUT "%4s%7d %-4s%-3s%6d%12.3f%8.3f%8.3f%6.2f%6.2f\n",
      $middle[$increase-1][0],$middle[$increase-1][1],$middle[$increase-
1][2],$middle[$increase-1][3],$middle[$increase-1][4],
      $middle[$increase-1][5],$middle[$increase-1][6],$middle[$increase-
1][7],$middle[$increase-1][8],$middle[$increase-1][9];
    }
  }
}

for($nna=0;$nna<=$nntotal-1;$nna++)
#400 Na+ in the NaCl-water box
{ $tmpatmna=$norganic+$nna;
  if($data[$tmpatmna][3]eq"R")
  {;}
  else {$residue++; print OUTPUT "TER\n";
    $increase++;
    $middle[$increase-1][0]=$data[$tmpatmna+$i][0];
    $middle[$increase-1][1]=$increase;
    $middle[$increase-1][2]=$data[$tmpatmna+$i][2];
    $middle[$increase-1][3]=$data[$tmpatmna+$i][3];
    $middle[$increase-1][4]=$residue;
    $middle[$increase-1][5]=$data[$tmpatmna+$i][5];
  }
}

```

```

    $middle[$increase-1][6]=$data[$tmpatmna+$i][6];
    $middle[$increase-1][7]=$data[$tmpatmna+$i][7];
    $middle[$increase-1][8]=$data[$tmpatmna+$i][8];
    $middle[$increase-1][9]=$data[$tmpatmna+$i][9];
    printf OUTPUT "%4s%7d %-4s%-3s%6d%12.3f%8.3f%8.3f%6.2f%6.2f\n",
    $middle[$increase-1][0],$middle[$increase-1][1],$middle[$increase-
1][2],$middle[$increase-1][3],$middle[$increase-1][4],
    $middle[$increase-1][5],$middle[$increase-1][6],$middle[$increase-
1][7],$middle[$increase-1][8],$middle[$increase-1][9];

    }
}

for($ncl=0;$ncl<=$ncltotal-1;$ncl++)
#400 Cl- in the naCl-water box
{ $tmpatmcl=$norganic+$nнатotal*4+$ncl;
  if($data[$tmpatmcl][3]eq"R")
  {;}
  else {$nresidue++; print OUTPUT "TER\n";
    $increase++;
    $middle[$increase-1][0]=$data[$tmpatmcl][0];
    $middle[$increase-1][1]=$increase;
    $middle[$increase-1][2]=$data[$tmpatmcl][2];
    $middle[$increase-1][3]=$data[$tmpatmcl][3];
    $middle[$increase-1][4]=$nresidue;
    $middle[$increase-1][5]=$data[$tmpatmcl][5];
    $middle[$increase-1][6]=$data[$tmpatmcl][6];
    $middle[$increase-1][7]=$data[$tmpatmcl][7];
    $middle[$increase-1][8]=$data[$tmpatmcl][8];
    $middle[$increase-1][9]=$data[$tmpatmcl][9];
    printf OUTPUT "%4s%7d %-4s%-3s%6d%12.3f%8.3f%8.3f%6.2f%6.2f\n",
    $middle[$increase-1][0],$middle[$increase-1][1],$middle[$increase-
1][2],$middle[$increase-1][3],$middle[$increase-1][4],
    $middle[$increase-1][5],$middle[$increase-1][6],$middle[$increase-
1][7],$middle[$increase-1][8],$middle[$increase-1][9];
  }
}

print OUTPUT "TER\nEND\n";

exit 0;

```

APPENDIX C - PERL PROGRAM 3

```

#!/usr/bin/perl
#
#put NaCl in the water box, where the water box is taken from the copolymer in water
#
$row=0;
$column=0;
$ncal=0;
$nNa=400;
$nCl=400;
$nwater=22965;
$nwt=0;
$total=0;
open(OUTPUT, ">conacl.pdb");
open(INPUT, "<cowtr.pdb");
  while (<INPUT>) {
    chomp;
    if(substr($_,0,4) eq "ATOM")
      {
        @tmp=split(/ * /,$_);
        for($column=0;$column<=9;$column++)
          {$data[$row][$column]=$tmp[$column];
           $middle[$row][$column]=$tmp[$column];
#    print OUTPUT $data[$row][$column];
          }
        $row++;
#    print OUTPUT "\n";
      }
  }
}
$increase=0;
$residue=48;
$tmp1=0;
$tmp2=0;
for($nwtr=0;$nwtr<=$nwater-1;$nwtr++)
  #20492 water molecules in the water cell with NaCl
  { if (($nwtr%56==0) and ($nwtr>=54))
    { $tmp1++;
      if ($tmp1<=$nNa)
        { $increase++;
          $residue++;
          $middle[$increase-1][0]=$data[$nwtr*3][0];
          $middle[$increase-1][1]=$increase+807;
          $middle[$increase-1][2]="Na+";
          $middle[$increase-1][3]="Na+";

```

```

$middle[$increase-1][4]=$nresidue;
$middle[$increase-1][5]=$data[$nwtr*3][5];
$middle[$increase-1][6]=$data[$nwtr*3][6];
$middle[$increase-1][7]=$data[$nwtr*3][7];
$middle[$increase-1][8]=$data[$nwtr*3][8];
$middle[$increase-1][9]=$data[$nwtr*3][9];}
else {$nresidue++;
for ($i=0;$i<=2;$i++)
{
    $increase++;
$middle[$increase-1][0]=$data[$nwtr*3+$i][0];
$middle[$increase-1][1]=$increase+807;
$middle[$increase-1][2]=$data[$nwtr*3+$i][2];
$middle[$increase-1][3]=$data[$nwtr*3+$i][3];
$middle[$increase-1][4]=$nresidue;
$middle[$increase-1][5]=$data[$nwtr*3+$i][5];
$middle[$increase-1][6]=$data[$nwtr*3+$i][6];
$middle[$increase-1][7]=$data[$nwtr*3+$i][7];
$middle[$increase-1][8]=$data[$nwtr*3+$i][8];
$middle[$increase-1][9]=$data[$nwtr*3+$i][9];
}
}
}
elseif (($nwtr%56==28) and ($nwtr>=55))
{$tmp2++;
if ($tmp2<=$nCl)
{ $increase++;
$nresidue++;
$middle[$increase-1][0]=$data[$nwtr*3][0];
$middle[$increase-1][1]=$increase+807;
$middle[$increase-1][2]="Cl-";
$middle[$increase-1][3]="Cl-";
$middle[$increase-1][4]=$nresidue;
$middle[$increase-1][5]=$data[$nwtr*3][5];
$middle[$increase-1][6]=$data[$nwtr*3][6];
$middle[$increase-1][7]=$data[$nwtr*3][7];
$middle[$increase-1][8]=$data[$nwtr*3][8];
$middle[$increase-1][9]=$data[$nwtr*3][9];}
else {$nresidue++;
for ($i=0;$i<=2;$i++)
{
    $increase++;
$middle[$increase-1][0]=$data[$nwtr*3+$i][0];
$middle[$increase-1][1]=$increase+807;
$middle[$increase-1][2]=$data[$nwtr*3+$i][2];
$middle[$increase-1][3]=$data[$nwtr*3+$i][3];

```

```

    $middle[$increase-1][4]=$nresidue;
    $middle[$increase-1][5]=$data[$nwtr*3+$i][5];
    $middle[$increase-1][6]=$data[$nwtr*3+$i][6];
    $middle[$increase-1][7]=$data[$nwtr*3+$i][7];
    $middle[$increase-1][8]=$data[$nwtr*3+$i][8];
    $middle[$increase-1][9]=$data[$nwtr*3+$i][9];
    }
  }
}
else{ $nresidue++;
  for ($i=0;$i<=2;$i++)
  {
    $increase++;
    $middle[$increase-1][0]=$data[$nwtr*3+$i][0];
    $middle[$increase-1][1]=$increase+807;
    $middle[$increase-1][2]=$data[$nwtr*3+$i][2];
    $middle[$increase-1][3]=$data[$nwtr*3+$i][3];
    $middle[$increase-1][4]=$nresidue;
    $middle[$increase-1][5]=$data[$nwtr*3+$i][5];
    $middle[$increase-1][6]=$data[$nwtr*3+$i][6];
    $middle[$increase-1][7]=$data[$nwtr*3+$i][7];
    $middle[$increase-1][8]=$data[$nwtr*3+$i][8];
    $middle[$increase-1][9]=$data[$nwtr*3+$i][9];
  }
}
print STDOUT "tmp1=", $tmp1, "tmp2=", $tmp2, "\n";
}
print STDOUT $increase;
for($n=0;$n<=$increase-1;$n++)
{if (($middle[$n][4]-$middle[$n-1][4]==1) and ($n>1))
  {print OUTPUT "TER\n";}
printf OUTPUT "%4s%7d %-4s%-3s%6d%12.3f%8.3f%8.3f%6.2f%6.2f\n",
  $middle[$n][0],$middle[$n][1],$middle[$n][2],$middle[$n][3],$middle[$n][4],
  $middle[$n][5],$middle[$n][6],$middle[$n][7],$middle[$n][8],$middle[$n][9];
}
print OUTPUT "TER\nEND";
exit 0;

```

APPENDIX D - PERL PROGRAM 4

```
#!/usr/bin/perl
# divide *.dcd file for g(r) calculations
#
print STDOUT "Please input the dcd file name:";
chomp ($dcdfile=<STDIN>);
open(OUTPUT,">grcatdcd.sh");
print STDOUT "Please input the starting time:";
chomp ($starting=<STDIN>);
print STDOUT "Please input the end time:";
chomp ($end=<STDIN>);
$startingnum=$starting*1;
$endnum=$end*1;
for($m=$startingnum;$m<$endnum;$m++)
{print $m,"\n";
$first=($m-$starting)*1000+1;
$last=($m-$starting+1)*1000;
printf OUTPUT "catdcd -o %2dns.dcd -first %4d -last %4d -stride 1
%20s\n", $m+1,$first,$last,$dcdfile;
print OUTPUT "wait\n";
}
close(OUTPUT);
exit 0;
```

APPENDIX E - PERL PROGRAM 5

```
#!/usr/bin/perl
# generate inputfiles for g(r) calculations for the copolymer
#
print STDOUT "Please input the starting time:";
chomp ($starting=<STDIN>);
print STDOUT "Please input the end time:";
chomp ($end=<STDIN>);
$startingnum=$starting;
$endnum=$end;
$after="ns.in";
$alpha="@";
for($i=$startingnum+1;$i<=$endnum;$i++)
{
$before1="gr";
$before2=$i;
  $gr=$before1.$before2.$after;
  open(OUTPUT,">$gr");
  print OUTPUT "trajin ",$i,"ns.dcd\n";
  print OUTPUT "radial conacl318",$i,"nsona 0.1 10 :Na+",$alpha,"Na+ :1-14,20-33,39-48",$alpha,"O1\n";
  print OUTPUT "radial conacl318",$i,"nsocl 0.1 10 :Cl-",$alpha,"Cl- :1-14,20-33,39-48",$alpha,"O1\n";
  print OUTPUT "radial conacl318",$i,"nsnna 0.1 10 :Na+",$alpha,"Na+ :1-14,20-33,39-48",$alpha,"N1\n";
  print OUTPUT "radial conacl318",$i,"nsncl 0.1 10 :Cl-",$alpha,"Cl- :1-14,20-33,39-48",$alpha,"N1\n";
  print OUTPUT "radial conacl318",$i,"nsh8cl 0.1 10 :Cl-",$alpha,"Cl- :1-14,20-33,39-48",$alpha,"H8\n";
  print OUTPUT "radial conacl318",$i,"nsowtrna 0.1 10 :WAT",$alpha,"O :Na+",$alpha,"Na+\n";
  print OUTPUT "radial conacl318",$i,"nsowtrcl 0.1 10 :WAT",$alpha,"O :Cl-",$alpha,"Cl-\n";
  print OUTPUT "radial conacl318",$i,"nsoc3hwtr 0.1 10 :WAT",$alpha,"H1,H2 :1-14,20-33,39-48",$alpha,"C3\n";
  print OUTPUT "radial conacl318",$i,"nsnhwtr 0.1 10 :WAT",$alpha,"H1,H2 :1-14,20-33,39-48",$alpha,"N1\n";
  print OUTPUT "radial conacl318",$i,"nsc3na 0.1 10 :Na+",$alpha,"Na+ :1-14,20-33,39-48",$alpha,"C3\n";
  print OUTPUT "radial conacl318",$i,"nsc3cl 0.1 10 :Cl-",$alpha,"Cl- :1-14,20-33,39-48",$alpha,"C3\n";
  print OUTPUT "radial conacl318",$i,"nsc5na 0.1 10 :Na+",$alpha,"Na+ :1-14,20-33,39-48",$alpha,"C5\n";
  print OUTPUT "radial conacl318",$i,"nsc5cl 0.1 10 :Cl-",$alpha,"Cl- :1-14,20-33,39-48",$alpha,"C5\n";
}
```

```

print OUTPUT "radial conacl318",$i,"nsc67na 0.1 10 :Na+",$alpha,"Na+ :1-14,20-33,39-48",$alpha,"C6, C7\n";
print OUTPUT "radial conacl318",$i,"nsc67cl 0.1 10 :Cl-",$alpha,"Cl- :1-14,20-33,39-48",$alpha,"C6, C7\n";
print OUTPUT "radial conacl318",$i,"nsbcna 0.1 10 :Na+",$alpha,"Na+ :1-14,20-33,39-48",$alpha,"C1,C2,C4\n";
print OUTPUT "radial conacl318",$i,"nsbccl 0.1 10 :Cl-",$alpha,"Cl- :1-14,20-33,39-48",$alpha,"C1,C2,C4\n";
print OUTPUT "radial conacl318",$i,"nsnacl 0.1 10 :Na+",$alpha,"Na+ :Cl-",$alpha,"Cl-\n";
print OUTPUT "radial conacl318",$i,"nspgsdo1na 0.1 10 :Na+",$alpha,"Na+ :16,35",$alpha,"O1\n";
print OUTPUT "radial conacl318",$i,"nspgsdo1cl 0.1 10 :Cl-",$alpha,"Cl- :16,35",$alpha,"O1\n";
print OUTPUT "radial conacl318",$i,"nspgso2na 0.1 10 :Na+",$alpha,"Na+ :16,35",$alpha,"O2\n";
print OUTPUT "radial conacl318",$i,"nspgso2cl 0.1 10 :Cl-",$alpha,"Cl- :16,35",$alpha,"O2\n";
print OUTPUT "radial conacl318",$i,"nsetherona 0.1 10 :Na+",$alpha,"Na+ :17,18,36,37",$alpha,"O2,O3,O4\n";
print OUTPUT "radial conacl318",$i,"nsetherocl 0.1 10 :Cl-",$alpha,"Cl- :17,18,36,37",$alpha,"O2,O3,O4\n";
print OUTPUT "radial conacl318",$i,"nsetherohwtr 0.1 10 :WAT",$alpha,"H1,H2 :17,18,36,37",$alpha,"O2,O3,O4\n";
print OUTPUT "radial conacl318",$i,"nspgpfiona 0.1 10 :Na+",$alpha,"Na+ :19,38",$alpha,"O2\n";
print OUTPUT "radial conacl318",$i,"nspfiocl 0.1 10 :Cl-",$alpha,"Cl- :19,38",$alpha,"O2\n";

close (OUTPUT);
}

```

```

exit 0;

```

APPENDIX F - PERL PROGRAM 6

```
#!/usr/bin/perl
# generate input files for g(r) in mixed salt solution
print STDOUT "Please input the starting time:";
chomp ($starting=<STDIN>);
print STDOUT "Please input the end time:";
chomp ($end=<STDIN>);
$startingnum=$starting;
$endnum=$end;
$after="ns.in";$alpha="@";
for($i=$startingnum+1;$i<=$endnum;$i++)
{ $before1="gr";$before2=$i;
  $gr=$before1.$before2.$after;
  open(OUTPUT,">$gr");
  print OUTPUT "trajin ",$i,"ns.dcd\n";
  print OUTPUT "radial nabrkc1318",$i,"nsona 0.1 10 :Na+",$alpha,"Na+ :1-50",$alpha,"O1\n";
  print OUTPUT "radial nabrkc1318",$i,"nsok 0.1 10 :K+",$alpha,"K+ :1-50",$alpha,"O1\n";
  print OUTPUT "radial nabrkc1318",$i,"nsocl 0.1 10 :Cl-",$alpha,"Cl- :1-50",$alpha,"O1\n";
  print OUTPUT "radial nabrkc1318",$i,"nsobr 0.1 10 :Br-",$alpha,"Br- :1-50",$alpha,"O1\n";
  print OUTPUT "radial nabrkc1318",$i,"nsna 0.1 10 :Na+",$alpha,"Na+ :1-50",$alpha,"N1\n";
  print OUTPUT "radial nabrkc1318",$i,"nsnk 0.1 10 :K+",$alpha,"K+ :1-50",$alpha,"N1\n";
  print OUTPUT "radial nabrkc1318",$i,"nsncl 0.1 10 :Cl-",$alpha,"Cl- :1-50",$alpha,"N1\n";
  print OUTPUT "radial nabrkc1318",$i,"nsnbr 0.1 10 :Br-",$alpha,"Br- :1-50",$alpha,"N1\n";
  print OUTPUT "radial nabrkc1318",$i,"nsc3na 0.1 10 :Na+",$alpha,"Na+ :1-50",$alpha,"C3\n";
  print OUTPUT "radial nabrkc1318",$i,"nsc3k 0.1 10 :K+",$alpha,"K+ :1-50",$alpha,"C3\n";
  print OUTPUT "radial nabrkc1318",$i,"nsc3cl 0.1 10 :Cl-",$alpha,"Cl- :1-50",$alpha,"C3\n";
  print OUTPUT "radial nabrkc1318",$i,"nsc3br 0.1 10 :Br-",$alpha,"Br- :1-50",$alpha,"C3\n";
  print OUTPUT "radial nabrkc1318",$i,"nsc5na 0.1 10 :Na+",$alpha,"Na+ :1-50",$alpha,"C5\n";
  print OUTPUT "radial nabrkc1318",$i,"nsc5k 0.1 10 :K+",$alpha,"K+ :1-50",$alpha,"C5\n";
  print OUTPUT "radial nabrkc1318",$i,"nsc5cl 0.1 10 :Cl-",$alpha,"Cl- :1-50",$alpha,"C5\n";
```

```

print OUTPUT "radial nabrkl318",$,i,"nsc5br 0.1 10 :Br-",$alpha,"Br- :1-50",$,alpha,"C5\n";
print OUTPUT "radial nabrkl318",$,i,"nsc67na 0.1 10 :Na+",$alpha,"Na+ :1-50",$,alpha,"C6, C7\n";
print OUTPUT "radial nabrkl318",$,i,"nsc67k 0.1 10 :K+",$alpha,"K+ :1-50",$,alpha,"C6, C7\n";
print OUTPUT "radial nabrkl318",$,i,"nsc67cl 0.1 10 :Cl-",$alpha,"Cl- :1-50",$,alpha,"C6, C7\n";
print OUTPUT "radial nabrkl318",$,i,"nsc67br 0.1 10 :Br-",$alpha,"Br- :1-50",$,alpha,"C6, C7\n";
print OUTPUT "radial nabrkl318",$,i,"nsbcna 0.1 10 :Na+",$alpha,"Na+ :1-50",$,alpha,"C1,C2,C4\n";
print OUTPUT "radial nabrkl318",$,i,"nsbck 0.1 10 :K+",$alpha,"K+ :1-50",$,alpha,"C1,C2,C4\n";
print OUTPUT "radial nabrkl318",$,i,"nsbccl 0.1 10 :Cl-",$alpha,"Cl- :1-50",$,alpha,"C1,C2,C4\n";
print OUTPUT "radial nabrkl318",$,i,"nsbcbr 0.1 10 :Br-",$alpha,"Br- :1-50",$,alpha,"C1,C2,C4\n";
print OUTPUT "radial nabrkl318",$,i,"nsnacl 0.1 10 :Na+",$alpha,"Na+ :Cl-",$alpha,"Cl-\n";
print OUTPUT "radial nabrkl318",$,i,"nsnabr 0.1 10 :Na+",$alpha,"Na+ :Br-",$alpha,"Br-\n";
print OUTPUT "radial nabrkl318",$,i,"nskcl 0.1 10 :K+",$alpha,"K+ :Cl-",$alpha,"Cl-\n";
print OUTPUT "radial nabrkl318",$,i,"nskbr 0.1 10 :K+",$alpha,"K+ :Br-",$alpha,"Br-\n";
print OUTPUT "radial nabrkl318",$,i,"nsh8br 0.1 10 :Br-",$alpha,"Br- :1-50",$,alpha,"H8\n";
print OUTPUT "radial nabrkl318",$,i,"nsh8cl 0.1 10 :Cl-",$alpha,"Cl- :1-50",$,alpha,"H8\n";
print OUTPUT "radial nabrkl318",$,i,"nsowtrcl 0.1 10 :WAT",$alpha,"O :Cl-",$alpha,"Cl-\n";
print OUTPUT "radial nabrkl318",$,i,"nsowtrbr 0.1 10 :WAT",$alpha,"O :Br-",$alpha,"Br-\n";
print OUTPUT "radial nabrkl318",$,i,"nsowtrna 0.1 10 :WAT",$alpha,"O :Na+",$alpha,"Na+\n";
print OUTPUT "radial nabrkl318",$,i,"nsowtrk 0.1 10 :WAT",$alpha,"O :K+",$alpha,"K+\n";
print OUTPUT "radial nabrkl318",$,i,"nsc3hwtr 0.1 10 :WAT",$alpha,"H1,H2 :1-50",$,alpha,"C3\n";
print OUTPUT "radial nabrkl318",$,i,"nsnhwtr 0.1 10 :WAT",$alpha,"H1,H2 :1-50",$,alpha,"N1\n";
close (OUTPUT);
}
exit 0;

```

APPENDIX G - PERL PROGRAM 7

```
#!/usr/bin/perl
# batch process for g(r) calculations
#
print STDOUT "Please input the prmtop file name:";
chomp ($prmtop=<STDIN>);
open(OUTPUT,">grinput.sh");
print STDOUT "Please input the starting time:";
chomp ($starting=<STDIN>);
print STDOUT "Please input the end time:";
chomp ($end=<STDIN>);
$startingnum=$starting;
$endnum=$end;
for($i=$startingnum+1;$i<=$endnum;$i++)
{
print OUTPUT "ptraj ",$prmtop," gr",$i,"ns.in", ">gr",$i,"ns.out & \n";
}

exit 0;
```

APPENDIX H - PERL PROGRAM 8

```

#!/usr/bin/perl
#average g(r) based on a long time period
#
#
print STDOUT "Please input the temperature:";
chomp ($temperature=<STDIN>);

for($row=0;$row<=99;$row++)
{
    for($column=0;$column<=15;$column++)
        {$data[$row][$column]=0;}
}
$outfile="saltmix2454ns".$temperature."ona.xmgr";
open(OUTPUT, ">$outfile");

$startpoint=25;
for($i=0;$i<=29;$i++)
{
    $row=0;
    $before="nabrkl";
    $middle=$i+$startpoint;
    $after="nsona_volume.xmgr";
    $inputfile=$before.$temperature.$middle.$after;
# print $inputfile,"\n";
open(INPUT, "<$inputfile");
while (<INPUT>) {
    chomp;
    @tmp=split(/ * /,$_);
    $data[$row][0]=($row)*0.1+0.050;
    $data[$row][$i+2]=$tmp[2];
# print $data[$row][1];
    $row++;
# print $tmp[2];

# print OUTPUT "\n";
}
close(INPUT);
}

for($total=0;$total<=$row-1;$total++)
{
    printf OUTPUT "%8.3f", $data[$total][0];
}

```

```

$data[Total][1]=($data[Total][2]+$data[Total][3]+$data[Total][4]+$data[Total][5]+$data[Total][6]
+$data[Total][7]+$data[Total][8]+$data[Total][9]+$data[Total][10]+$data[Total][11]
+$data[Total][12]+$data[Total][13]+$data[Total][14]+$data[Total][15]+$data[Total][16]
+$data[Total][17]+$data[Total][18]+$data[Total][19]+$data[Total][20]+$data[Total][21]
+$data[Total][22]+$data[Total][23]+$data[Total][24]+$data[Total][25]+$data[Total][26]
+$data[Total][27]+$data[Total][28]+$data[Total][29]+$data[Total][30]+$data[Total][31])/30;
# print $data[Total][1],"\n";
for($i=0;$i<=30;$i++)
    {printf OUTPUT "% 14.8f",$data[Total][$i+1]; }
print OUTPUT "\n";
}

exit 0;

```

APPENDIX I - PERL PROGRAM 9

```
#!/usr/bin/perl
# Divide *.dcd file for H-bond analysis
#
print STDOUT "Please input the dcd file name:";
chomp ($dcdfile=<STDIN>);
open(OUTPUT,">catdcd.sh");
print STDOUT "Please input the starting time:";
chomp ($starting=<STDIN>);
print STDOUT "Please input the end time:";
chomp ($end=<STDIN>);
$startingnum=$starting*500+1;
$endnum=$end*500;
#printf OUTPUT "catdcd -o 0.dcd -first 1 -last 1 -stride 1 %20s \nwait\n",$dcdfile;
for($i=$startingnum;$i<=$endnum;$i++)
{
#$first=$i*2-$starting*1000+30;
$first=$i*2-$starting*1000; #start from the *ns
printf OUTPUT "catdcd -o %5d.dcd -first %4d -last %4d -stride 1
%20s\n",$i,$first,$first,$dcdfile;
print OUTPUT "wait\n";
}

exit 0;
```

APPENDIX J - PERL PROGRAM 10

```
#!/usr/bin/perl
#
# generated input files for hydrogen bonding analyses
print STDOUT "Please input the starting time:";
chomp ($starting=<STDIN>);
print STDOUT "Please input the end time:";
chomp ($end=<STDIN>);
$startingnum=$starting*500;
#$startingnum=$starting*500+1; #start from the #ns.
$endnum=$end*500;
$after=".in";
for($i=$startingnum;$i<=$endnum;$i++)
{
    $before=$i;
    $hbondinput=$before.$after;
    open(OUTPUT,">$hbondinput");
    printf OUTPUT "trajin %5d.dcd\n",$i;
    print OUTPUT "donor IPA O1
donor NIP O1
donor PPA O1
donor IPA N1
donor NIP N1
donor PPA N1
donor PGS O1
donor PGS O2
donor PGT O3
donor PGT O4
donor PFO O2
donor PFI O2
acceptor IPA N1 H8
acceptor NIP N1 H8
acceptor PPA N1 H8
acceptor PFI O2 H10
hbond distance 3.5 angle 130.0 solventneighbor 6 solventdonor WAT O solventacceptor
WAT O H1 solventacceptor WAT O H2\n";
    close (OUTPUT);
}

exit 0;
```

APPENDIX K - PERL PROGRAM 11

```
#!/usr/bin/perl
# generate batch processing file for hydrogen bonding analysis
#
print STDOUT "Please input the prmtop file name:";
chomp ($prmtop=<STDIN>);
open(OUTPUT,">run.sh");
print STDOUT "Please input the starting time:";
chomp ($starting=<STDIN>);
print STDOUT "Please input the end time:";
chomp ($end=<STDIN>);
$startingnum=$starting*500+1;
$endnum=$end*500;
print OUTPUT "ptraj $prmtop <0.in>0.out\nwait\n";
for($i=$startingnum;$i<=$endnum;$i++)
{
  printf OUTPUT "ptraj % 16s<$i.in>$i.out\n",$prmtop,$i,$i;
  print OUTPUT "wait\n";
}

exit 0;
```

APPENDIX L - PERL PROGRAM 12

```

#!/usr/bin/perl
# Calculate H-bonds for PNIPAM
#
print STDOUT "Please input the output file name:";
chomp ($outfile=<STDIN>);
open(OUTPUT,">$outfile");
print STDOUT "Please input the temperature:";
chomp ($temperature=<STDIN>);
print STDOUT "Please input the angle:";
chomp ($angle=<STDIN>);
printf OUTPUT "temperature=%5s ,angle=%5d\n",$temperature,$angle;
print OUTPUT "  intra  waterN  waterO\n";

print STDOUT "Please input the starting time:";
chomp ($starting=<STDIN>);
print STDOUT "Please input the end time:";
chomp ($end=<STDIN>);
#first one
$startingnum=$starting*500;
$endnum=$end*500;
for($i=$startingnum;$i<=$endnum;$i++)
{
  $hbondOHN=0;
  $hbondwtrN=0;
  $hbondwtrO=0;
  $hbondNIPH3O=0;
  $row=0;
  chomp ($before=$i);
  $after=".out";
  $infile=$before.$after;
  open(INPUT, "< $infile");
  while (<INPUT>) {
    chomp;
    @tmp = split(' ', $_);
    for($column=0;$column<=20;$column++)
      { $data[$row][$column]=$tmp[$column];
        }
    # print OUTPUT $data[$row][$column];
    $row++;
  }

for ($nout=1;$nout<=$row-1;$nout++)
{

```

```

if (($data[$nout][0] eq "|")and ($data[$nout][3] eq "|"))
{ #printf OUTPUT "% 8d% 8s% 8d% 8s% 8d% 8s% 8.3f% 8.2f\n",
  # $data[$nout][1],$data[$nout][2],$data[$nout][4],$data[$nout][5],$data[$nout][6],
  # $data[$nout][7],$data[$nout][10],$data[$nout][13]+120;
  if (((($data[$nout][2] =~ "O1") or ($data[$nout][2] =~ "N1")) and
($data[$nout][7] =~ "N1") and ($data[$nout][9] =~ "100"))
    { $hbondOHN++;}
  elseif (((($data[$nout][2] =~ "O1") or ($data[$nout][2] =~ "N1")) and
($data[$nout][7] =~ "O") and ($data[$nout][9] =~ "100"))
    { $hbondNIPH3O++;}
  elseif (($data[$nout][2] =~ "donor") and ($data[$nout][7] =~ "N1") and
($data[$nout][9] =~ "300"))
    { $hbondwtrN=$hbondwtrN+3;}
  elseif (($data[$nout][2] =~ "donor") and ($data[$nout][7] =~ "N1") and
($data[$nout][9] =~ "200"))
    { $hbondwtrN=$hbondwtrN+2;}
  elseif (($data[$nout][2] =~ "donor") and ($data[$nout][7] =~ "N1") and
($data[$nout][9] =~ "100"))
    { $hbondwtrN=$hbondwtrN+1;}
  elseif (($data[$nout][2] =~ "N1") and ($data[$nout][5] =~ "acceptor") and
($data[$nout][7] =~ "300"))
    { $hbondwtrN=$hbondwtrN+3;}
  elseif (($data[$nout][2] =~ "N1") and ($data[$nout][5] =~ "acceptor") and
($data[$nout][7] =~ "200"))
    { $hbondwtrN=$hbondwtrN+2;}
  elseif (($data[$nout][2] =~ "N1") and ($data[$nout][5] =~ "acceptor") and
($data[$nout][7] =~ "100"))
    { $hbondwtrN=$hbondwtrN+1;}
  elseif (($data[$nout][2] =~ "O1") and ($data[$nout][5] =~ "acceptor") and
($data[$nout][7] =~ "300"))
    { $hbondwtrO=$hbondwtrO+3;}
  elseif (($data[$nout][2] =~ "O1") and ($data[$nout][5] =~ "acceptor") and
($data[$nout][7] =~ "200"))
    { $hbondwtrO=$hbondwtrO+2;}
  elseif (($data[$nout][2] =~ "O1") and ($data[$nout][5] =~ "acceptor") and
($data[$nout][7] =~ "100"))
    { $hbondwtrO=$hbondwtrO+1;}
  }
}
printf OUTPUT
"% 10d% 10d% 10d% 10d\n", $hbondOHN, $hbondNIPH3O, $hbondwtrN, $hbondwtrO;
close(INPUT);
}
exit 0;

```

APPENDIX M - PERL PROGRAM 13

```
#!/usr/bin/perl
# Calculate H-bonds for the copolymer
#
print STDOUT "Please input the output file name:";
chomp ($outfile=<STDIN>);
open(OUTPUT,">$outfile");
print STDOUT "Please input the temperature:";
chomp ($temperature=<STDIN>);
print STDOUT "Please input the angle:";
chomp ($angle=<STDIN>);
printf OUTPUT "temperature=%5s ,angle=%5d\n",$temperature,$angle;
print OUTPUT "  intra  waterN  waterO\n";

print STDOUT "Please input the starting time:";
chomp ($starting=<STDIN>);
print STDOUT "Please input the end time:";
chomp ($end=<STDIN>);
#first one
$startingnum=$starting*500;
$endnum=$end*500;
for($i=$startingnum;$i<=$endnum;$i++)
{
  $intra=0;
  $hbondwtrN=0;
  $hbondwtrO=0;
  $hbondwtrpegma=0;
  $row=0;
  chomp ($before=$i);
  $after=".out";
  $infile=$before.$after;
  open(INPUT, "< $infile");
  while (<INPUT>) {
    chomp;
    @tmp = split(' ', $_);
    for($column=0;$column<=20;$column++)
      { $data[$row][$column]=$tmp[$column];
        }
    # print OUTPUT $data[$row][$column];
    $row++;
  }

  for ($nout=1;$nout<=$row-1;$nout++)
  {
```

```

if (($data[$nout][0] eq "|")and ($data[$nout][3] eq"|"))
{ #printf OUTPUT "% 8d% 8s% 8d% 8s% 8d% 8s% 8.3f% 8.2f\n",
  #data[$nout][1],$data[$nout][2],$data[$nout][4],$data[$nout][5],$data[$nout][6],
  #data[$nout][7],$data[$nout][10],$data[$nout][13]+120;
  #intra-chain hbonds
  if (((data[$nout][2]=~"O1") or (data[$nout][2]=~"N1") or (data[$nout][2]=~"O2")
  or (data[$nout][2]=~"O3") or (data[$nout][2]=~"O4" ))
  and ((data[$nout][7]=~"N1") or (data[$nout][7]=~"O2"))) and
(data[$nout][9]=~"100"))
  { $intra++;}

  #Honds between -OH of PEGMA and water due to water donor
  elseif ((data[$nout][2]=~"donor") and (data[$nout][7]=~"O2") and
(data[$nout][9]=~"300"))
    { $hbondwtrpegma=$hbondwtrpegma+3;}
  elseif ((data[$nout][2]=~"donor") and (data[$nout][7]=~"O2") and
(data[$nout][9]=~"200"))
    { $hbondwtrpegma=$hbondwtrpegma+2;}
  elseif ((data[$nout][2]=~"donor") and (data[$nout][7]=~"O2") and
(data[$nout][9]=~"100"))
    { $hbondwtrpegma=$hbondwtrpegma+1;}

  #Honds between N of NIPAAm and water due to water donor
  elseif ((data[$nout][2]=~"donor") and (data[$nout][7]=~"N1") and
(data[$nout][9]=~"300"))
    { $hbondwtrN=$hbondwtrN+3;}
  elseif ((data[$nout][2]=~"donor") and (data[$nout][7]=~"N1") and
(data[$nout][9]=~"200"))
    { $hbondwtrN=$hbondwtrN+2;}
  elseif ((data[$nout][2]=~"donor") and (data[$nout][7]=~"N1") and
(data[$nout][9]=~"100"))
    { $hbondwtrN=$hbondwtrN+1;}

  #Honds between PEGMA(except -OH) and water due to water donor
  elseif (((data[$nout][2]=~"16@O1") or (data[$nout][2]=~ "16@O2") or
(data[$nout][2]=~"18@O2")
  or (data[$nout][2]=~"19@O2") or (data[$nout][2]=~"O3") or
(data[$nout][2]=~"O4")
  or (data[$nout][2]=~"35@O1") or (data[$nout][2]=~"35@O2") or
(data[$nout][2]=~"37@O2")
  or (data[$nout][2]=~"38@O2"))) and (data[$nout][5]=~"acceptor") and
(data[$nout][7]=~"300"))
    { $hbondwtrpegma=$hbondwtrpegma+3;}
  elseif (((data[$nout][2]=~"16@O1") or (data[$nout][2]=~ "16@O2") or
(data[$nout][2]=~"18@O2")

```

```

        or ($data[$nout][2]=~"19@O2") or ($data[$nout][2]=~"O3") or
($data[$nout][2]=~"O4")
        or ($data[$nout][2]=~"35@O1") or ($data[$nout][2]=~"35@O2") or
($data[$nout][2]=~"37@O2")
        or ($data[$nout][2]=~"38@O2")) and ($data[$nout][5]=~"acceptor") and
($data[$nout][7]=~"200")
        { $hbondwtrpegma=$hbondwtrpegma+2;}
        elseif (((($data[$nout][2]=~"16@O1") or ($data[$nout][2]=~ "16@O2") or
($data[$nout][2]=~"18@O2")
        or ($data[$nout][2]=~"19@O2") or ($data[$nout][2]=~"O3") or
($data[$nout][2]=~"O4")
        or ($data[$nout][2]=~"35@O1") or ($data[$nout][2]=~"35@O2") or
($data[$nout][2]=~"37@O2")
        or ($data[$nout][2]=~"38@O2")) and ($data[$nout][5]=~"acceptor") and
($data[$nout][7]=~"100")
        { $hbondwtrpegma=$hbondwtrpegma+1;}

#Honds between NIPAAm and water due to water acceptor
elseif (($data[$nout][2]=~"N1") and ($data[$nout][5]=~"acceptor") and
($data[$nout][7]=~"300"))
{ $hbondwtrN=$hbondwtrN+3;}
elseif (($data[$nout][2]=~"N1") and ($data[$nout][5]=~"acceptor") and
($data[$nout][7]=~"200"))
{ $hbondwtrN=$hbondwtrN+2;}
elseif (($data[$nout][2]=~"N1") and ($data[$nout][5]=~"acceptor") and
($data[$nout][7]=~"100"))
{ $hbondwtrN=$hbondwtrN+1;}
elseif (($data[$nout][2]=~"O1") and ($data[$nout][5]=~"acceptor") and
($data[$nout][7]=~"300"))
{ $hbondwtrO=$hbondwtrO+3;}
elseif (($data[$nout][2]=~"O1") and ($data[$nout][5]=~"acceptor") and
($data[$nout][7]=~"200"))
{ $hbondwtrO=$hbondwtrO+2;}
elseif (($data[$nout][2]=~"O1") and ($data[$nout][5]=~"acceptor") and
($data[$nout][7]=~"100"))
{ $hbondwtrO=$hbondwtrO+1;}
}
}
printf OUTPUT
"% 10d% 10d% 10d% 10d\n",$sintra,$hbondwtrN,$hbondwtrO,$hbondwtrpegma;
close(INPUT);
}
exit 0;

```

APPENDIX N - PERL PROGRAM 14

```
#!/usr/bin/perl
#cut off for PNIPAM in HCl solution
#cut water cells into small cell; remove "X" in the pdb file.
#
$row=0;
$column=0;
$norganic=955;
$nh3ocl=296;
$nwttotal=15845;
$totalatom=49970;
$total=0;
$index=0;
print STDOUT "Please input the input pdb file name:";
chomp ($infile=<STDIN>);
open(OUTPUT, ">$outfile");
print STDOUT "Please input the output pdb file name:";
chomp ($outfile=<STDIN>);
print STDOUT "Please input the cutoff:";
chomp ($cutoff=<STDIN>);
$squire=$cutoff*$cutoff;
open(OUTPUT, ">$outfile");
open(INPUT, "<$infile");
  while (<INPUT>) {
    chomp;
    if(substr($_,0,4) eq "ATOM")
      {
        @tmp=split(/ * /,$_);
        for($column=0;$column<=11;$column++)
          {$data[$row][$column]=$tmp[$column];
#      print OUTPUT $data[$row][$column];
          }
        $row++;
#      print OUTPUT "\n";
      }
  }

for($ncalA=0;$ncalA<=($norganic-1);$ncalA++)
{
  for($ncalB=$norganic;$ncalB<=$totalatom-1;$ncalB++)
  {$seperation=($data[$ncalA][5]-$data[$ncalB][5])**2+
    ($data[$ncalA][6]-$data[$ncalB][6])**2+
    ($data[$ncalA][7]-$data[$ncalB][7])**2;
  if($seperation<=$squire)
    { $data[$ncalB][9]=K;}
}
```

```

    }
  }
  for($nh3o=0;$nh3o<=$nh3ocl-1;$nh3o++)
  { $tmpatmh3o=$norganic+$nh3o*4;
    if(($data[$tmpatmh3o][9]eq"K") or ($data[$tmpatmh3o+1][9]eq"K") or
($data[$tmpatmh3o+2][9]eq"K")or ($data[$tmpatmh3o+3][9]eq"K"))

{ $data[$tmpatmh3o][9]=K;$data[$tmpatmh3o+1][9]=K;$data[$tmpatmh3o+2][9]=K;$da
ta[$tmpatmh3o+3][9]=K;}
}
for($nwt=0;$nwt<=$nwttotal-1;$nwt++)
#22075 water molecules in the water cell with NaCl
{
  $tmpatmwt=$norganic+$nh3ocl*5+$nwt*3;
  if(($data[$tmpatmwt][9]eq"K") or ($data[$tmpatmwt+1][9]eq"K") or
($data[$tmpatmwt+2][9]eq"K"))
  { $data[$tmpatmwt][9]=K;$data[$tmpatmwt+1][9]=K;$data[$tmpatmwt+2][9]=K;}
}

for($total=0;$total<=$norganic-1;$total++)
{
  $index++;
  printf OUTPUT "%4s%7d%5s%4s%6s", $data[$total][0], $data[$total][1],
  $data[$total][2], $data[$total][3], $data[$total][4];
  printf OUTPUT "%12.3f%8.3f%8.3f%6.2f 0.00\n",
  $data[$total][5], $data[$total][6], $data[$total][7], $data[$total][8];
}

for($total=$norganic;$total<=$totalatom-1;$total++)
{
  if ($data[$total][9] eq "K")
  {
    $index++;
    printf OUTPUT "%4s%7d%5s%4s%6s", $data[$total][0], $index,
    $data[$total][2], $data[$total][3], $data[$total][4];
    printf OUTPUT "%12.3f%8.3f%8.3f%6.2f 0.00\n",
    $data[$total][5], $data[$total][6], $data[$total][7], $data[$total][8];
  }
}

exit 0;

```

APPENDIX O - PERL PROGRAM 15

```
#!/usr/bin/perl
#
#
$atom1=O1;
$atom2=Na;
print STDOUT "Please input the dcd file name:";
chomp ($dcdfile=<STDIN>);
open(OUTPUT,">distance.in");
print OUTPUT "trajin ",$dcdfile,"\n";
for($m=0;$m<=49;$m++)
{ $tmp1=$m+1;
  for ($n=0;$n<=399;$n++)
  { $tmp2=51+2*$n;
    print OUTPUT "distance ","o",$tmp1,"cation",$tmp2,
      " :",$tmp1,"@","O1 :",$tmp2,"@",$atom2,
      "+ out o",$tmp1,"cation",$tmp2,".dat\n";
  }
}
exit 0;
```

APPENDIX P - PERL PROGRAM 16

```

#!/usr/bin/perl
# Find the minimal distance of cation to O on NIPAM
#
$outfile="minnabr278ona.txt";
open(OUTPUT,">$outfile");
$mindistance=50;
$datalength=32000;
$minposition=0;
$numaion=0;
$timeps=0;
$countlimt=0;
$before="o";
$time="time(ps)";
$anion="cation";
$after=".dat";
for($m=0;$m<=49;$m++)
{
    $row=0;
    $middle=$m+1;
    print OUTPUT $middle,"\n";
    $infile=$before.$middle.$after;
    open(INPUT, "< $infile");
    while (<INPUT>) {
        chomp;
        @tmp = split(' ', $_);
        for($column=0;$column<=1;$column++)
        {
            $data[0][$column]=$tmp[$column];
        }
        $row++;
        if($data[0][1]<2.2)
        {
            $numaion=($row/$datalength-($row%$datalength)/$datalength)+1;
            $markanion=49+$numaion*2;
            $timeps=$row-($numaion-1)*$datalength;
            $countlimt++;
            print OUTPUT
            $data[0][1],$before,$middle,$anion,$markanion,$time,$timeps,"\n";
        }
        if($data[0][1]<$mindistance)
        {
            $mindistance=$data[0][1];
            $numaion=($row/$datalength-($row%$datalength)/$datalength)+1;
            $markanion=49+$numaion*2;
            $timeps=$row-($numaion-1)*$datalength;
            $minposition=$before.$middle.$anion.$markanion.$time.$timeps;
        }
    }
}
close (INPUT);

```

```
}  
print OUTPUT "coutlimt ", $countlimt, " ", $mindistance, " ", $minposition;  
exit 0;
```

APPENDIX Q - PERL PROGRAM 17

```
#!/usr/bin/perl
#genrate input files for end-to-end distance calculations
#
$atom1=C1;
$atom2=C2;
$startframe=1;
print STDOUT "Please input the number of total frames:";
chomp ($endframe=<STDIN>);
print STDOUT "Please input the number of interval:";
chomp ($interval=<STDIN>);
print STDOUT "Please input the dcd file name:";
chomp ($dcdfile=<STDIN>);
open(OUTPUT,">distance.in");
print OUTPUT "trajin ",$dcdfile," ",$startframe," ",$endframe," ",$interval,"\n";
for($m=0;$m<=49;$m++)
{
  $tmp1=$m+1;
  for ($n=0;$n<=49;$n++)
  {
    $tmp2=$n+1;
    print OUTPUT "distance ","A",$tmp1,"A",$tmp2,
      " :",$tmp1,"@",$atom1," :",$tmp2,"@",$atom1,
      " out ee1t",$tmp1,"to",$tmp2,".dat noimage\n";#1t means AA
    print OUTPUT "distance ","A",$tmp1,"B",$tmp2,
      " :",$tmp1,"@",$atom1," :",$tmp2,"@",$atom2,
      " out ee2t",$tmp1,"to",$tmp2,".dat noimage\n";#2t means AB
    print OUTPUT "distance ","B",$tmp1,"B",$tmp2,
      " :",$tmp1,"@",$atom2," :",$tmp2,"@",$atom2,
      " out ee3t",$tmp1,"to",$tmp2,".dat noimage\n";#3t means BB
  }
}
}
exit 0;
```

APPENDIX R - PERL PROGRAM 18

```
#!/usr/bin/perl
# combine output files of endtoend distance calculation
#
$outfile="cat.sh";
open(OUTPUT,">$outfile");
for($m=0;$m<=49;$m++)
{
    print OUTPUT "cat ";
    for($n=0;$n<=49;$n++)
        {for($i=0;$i<=2;$i++)
            {print OUTPUT "ee",$i+1,"t",$m+1,"to",$n+1,".dat "};}
    }
    print OUTPUT ">sumfrom",$m+1,".dat &\n wait\n"
}
print OUTPUT "cat ";
for($m=0;$m<=49;$m++)
{
    print OUTPUT "sumfrom",$m+1,".dat ";}
print OUTPUT ">sum.dat\n";
exit(0);
```

APPENDIX S - PERL PROGRAM 19

```
#!/usr/bin/perl
#Calculations of end-to-end distance
#
print STDOUT "Please input the outfile name for endtoend:";
chomp ($outfile=<STDIN>);
open(OUTPUT,">$outfile");
print STDOUT "Please input the total lines in outfile:";
chomp ($totalline=<STDIN>);
for($row=0;$row<$totalline;$row++)
{
    for($column=0;$column<=1;$column++)
    {
        $etoe[$row][$column]=1;
#        print $etoe[$row][1];
    }
}
$row=0;
$count=0;
open(INPUT, "<sum.dat");
while (<INPUT>) {
    chomp;
    @tmp=split(/ * /,$_);
    $tmp1=$row%$totalline;
#    if($tmp1 eq 1) {print $count++,"\n";}
    if($etoe[$tmp1][1]<=$tmp[2])
        {$etoe[$tmp1][1]=$tmp[2];}
    $row++;
#    print $row;
}
close(INPUT);

for($total=0;$total<$totalline;$total++)
{
    $tmp4=$total+1;
    printf OUTPUT "% 8d% 14.8f\n",$tmp4,$etoe[$total][1];
}
}
```

APPENDIX T - PUBLICATIONS

- (1) Dong, H. T.; Du, H. B.; Qian, X. H. Theoretical Prediction of pK(a) Values for Methacrylic Acid Oligomers Using Combined Quantum Mechanical and Continuum Solvation Methods. *Journal of Physical Chemistry A*, 112, 2008, p.12687-12694;
- (2) Dong, H. T.; Du, H. B.; Qian, X. H. Prediction of pK(a) Values for Oligo-methacrylic Acids Using Combined Classical and Quantum Approaches. *Journal of Physical Chemistry B*. 113, 2009, p.12857-12859;
- (3) Dong, H. T.; Du, H. B.; Wickramasinghe, S. R.; Qian, X. H. The Effects of Chemical Substitution and Polymerization on the pK(a) Values of Sulfonic Acids. *the Journal of Physical Chemistry B* 113, 2009, p. 14094-14101;
- (4) Zhang, Y. T.; Du, H. B.; Qian, X. H.; Chen, E. Y. X. Ionic Liquid-Water Mixtures: Enhanced K_w for Efficient Cellulosic Biomass Conversion. *Energy & Fuels*, 24, 2010, p. 2410-2417;
- (5) Du, H. B.; Wickramasinghe, S. R.; Qian, X. H. Effects of Salt on the Lower Critical Solution Temperature of Poly(N-Isopropylacrylamide). *Journal of Physical Chemistry B*. 2010, 114, 16594–16604.
- (6) Du, H. B.; Qian, X. H. Molecular Dynamics Simulations of Copolymer PNIPAM-co-PEGMA Phase Transition at Lower Critical Solution Temperature in NaCl Solution. *Journal of Polymer Science Part B: Polymer Physics* (submitted).